NASA CONTRACTOR
REPORT

NASA CR-61263

February, 1969

NASA CR-61263

STUDIES OF VERTICAL WIND PROFILES AT CAPE KENNEDY, FLORIDA

Prepared under Contract No. NAS 8-21148 by
R. M. Endlich, R. C. Singleton, K. A. Drexhage, and
R. L. Mancuso

STANFORD RESEARCH INSTITUTE

APR 1969
RECEIVED
NASA STI FACILITY
INPUT BRANCH

For

NASA-GEORGE C. MARSHALL SPACE FLIGHT CENTER
Marshall Space Flight Center, Alabama

N 69-21148
(ACCESSION NUMBER)
94
(PAGES)
NASA-CR-61263
(NASA CR OR TMX OR AD NUMBER)
(THRU)
(CODE)
20
(CATEGORY)
FACILITY FORM 602

February 1969 Final Report NASA CR-61263

STUDIES OF VERTICAL WIND PROFILES AT CAPE KENNEDY, FLORIDA

By

R. M. Endlich, R. C. Singleton, K. A. Drexhage and
R. L. Mancuso

Prepared under Contract No. NAS 8-21148 by

STANFORD RESEARCH INSTITUTE

For

Aero-Astrodynamics Laboratory

Distribution of this report is provided in the interest of information exchange. Responsibility for the contents resides in the author or organization that prepared it.

NASA-GEORGE C. MARSHALL SPACE FLIGHT CENTER

FOREWORD

One of the major goals in the study of wind profiles is to develop a technique to predict the detail characteristics several hours in advance. This report is a contribution to this goal. The work was performed by the Stanford Research Institute, Menlo Park, California under NASA-Marshall Space Flight Center contract NAS8-21148. The NASA contract monitor was Mr. John Kaufman of the Aerospace Environment Division, Aero-Astrodynamics Laboratory, Marshall Space Flight Center, Alabama.

ABSTRACT

This study is concerned with methods of forecasting vertical wind profiles for NASA operations in launching missiles and spacecraft. The first subject considered is the structure, persistence, and predictability of details of vertical wind profiles. This portion of the investigation is based on sequences of wind profiles measured at Cape Kennedy, Florida, using the FPS-16 radar/Jimsphere technique. The details of the flow are shown by wind measurements at 25 m intervals between the surface and the lower stratosphere. The main analytical tool used is spectrum analysis. Spectra were computed using the "fast Fourier transform" rather than the more common but less efficient "lagged product" method. The spectra have the general characteristic that power is proportional to frequency to the -3 power. There are no clear minima in them that would indicate natural separations between predominant scales of motion as suggested by terminology such as large scale, mesoscale, and microscale. If these terms are to be used in reference to speed variations along a vertical axis, they must be defined on some other basis than the existence of clearly demarked spectral regions.

Spectra were also computed for deviations from mean speed profiles, and for speed changes between successive wind profiles. These deviations and changes show predominantly the smaller, transitory features of the flow. To a large extent, the behavior of these features appears to be random. At frequencies above approximately 0.3 cycles km^{-1}, their spectra have a slope near -2.5. If short-range forecasts are made from previous profiles, the errors of the forecasts can be expected to have spectral distributions similar to these spectra. The spectra of vertical profiles are compared with previous ones computed from winds measured by aircraft in horizontal flights across jet streams. Horizontal and vertical wavelengths having equal spectral density are shown.

In the second portion of the study, numerical methods of forecasting the general wind profile for periods twelve to twenty-four hours in advance are described. These methods are based on objective analyses of

standard wind observations. The forecast is made by advection of fields of wind components, vorticity, and divergence. Winds are matched to the forecast vorticity by a direct method. Test results indicate that the technique can be applied rapidly and is at least as accurate as other methods presently in use.

CONTENTS

ABSTRACT iii

LIST OF ILLUSTRATIONS vii

I INTRODUCTION AND SUMMARY 1

II SPECTRAL ANALYSIS OF WIND PROFILES 7

A. Introduction. 7

B. Computations. 8

C. Data. 13

D. The Sequence of Wind Speed Profiles on 8 April 1966 14

E. Wind Speed Profiles on 5 July 1966. 32

F. Wind Speed Profiles on 10 November 1965 47

G. Discussion. 59

H. Forecasting Implications. 67

III NUMERICAL WIND FORECASTS 69

ACKNOWLEDGMENTS 85

REFERENCES. 87

DD Form 1473

PRECEDING PAGE BLANK NOT FILMED.

ILLUSTRATIONS

Fig. 1 Schematic Diagram of the Investigation. 2

Fig. 2 Schematic Diagram Showing Time-Frequency Relations in Digital Spectral Analysis 10

Fig. 3 Wind Speed Profiles Measured at Cape Kennedy, Florida by the FPS-16 Jimsphere Technique on 8 April 1966. The Speed Scale is Shown only for Profiles a and g. . 18

Fig. 4 Spectra of Wind Speed Profiles of Fig. 3. 19

Fig. 5 Deviations of Individual Wind Speed Profiles from the Mean Profile, 8 April 1966. 23

Fig. 6 Spectra of the Profiles of Deviations from the Mean Shown in Fig. 5 24

Fig. 7 Speed Changes Between Successive Profiles, 8 April 1966. 27

Fig. 8 Spectra of the Speed Change Profiles of Fig. 7. . . . 28

Fig. 9 Summary of Spectra of Wind Speed Profiles on 8 April 1966. 31

Fig. 10 Wind Speed Profiles Measured at Cape Kennedy, Florida by the FPS-16 Jimsphere Technique on 4-5 July 1966. . 34

Fig. 11 Spectra of Wind Speed Profiles of Fig. 10 35

Fig. 12 Deviations of Individual Wind Speed Profiles from the Mean Profile, 5 July 1966 39

Fig. 13 Spectra of the Profiles of Deviations from the Mean Shown in Fig. 12. 40

Fig. 14 Speed Changes Between Successive Vertical Profiles, 5 July 1966 43

Fig. 15 Spectra of the Speed Change Profiles of Fig. 14 . . . 44

Fig. 16 Summary of Spectra of Wind Speed Profiles on 5 July 1966. 46

Fig. 17 Wind Speed Profiles Measured at Cape Kennedy, Florida by the FPS-16 Jimsphere Technique on 10 November 1965 48

Fig. 18 Spectra of Wind Speed Profiles of Fig. 17 49

Fig. 19 Deviations of Individual Wind Speed Profiles from the Mean Profile, 10 November 1965. 52

Fig. 20 Spectra of the Profiles of Deviations from the Mean Shown in Fig. 19. 53

Fig. 21 Speed Changes Between Successive Vertical Profiles, 10 November 1965. 55

Fig. 22 Spectra of the Speed Change Profiles of Fig. 21 . . . 56

Fig. 23 Summary of Spectra of Wind Speed Profiles on 10 November 1965 58

Fig. 24 Smoothed Spectra for the Sequences of Wind Profiles on 8 April 1966, 5 July 1966, and 10 November 1965. . 62

Fig. 25 Comparison of Vertical and Horizontal Eddy Scales that have the same Power Spectral Density in the Mesoscale Region. 66

Fig. 26 Observed Winds in Layers as Plotted on a Computer-Controlled Cathode Ray Tube for 0000 GMT, 28 March 1966. 71

Fig. 27 Objective Analyses of the Winds of Fig. 26 and Wind Shears using the CRT Display. 74

Fig. 28 Objective Wind Analysis for the 300-250 mb Layer at 1200 GMT, 11 March 1965 80

Fig. 29 Forecast 24-Hour Changes in Wind Vectors made from Fig. 28 82

Fig. 30 Observed 24-Hour Changes in Wind Vectors. Compare with Fig. 29. 83

I INTRODUCTION AND SUMMARY

This report describes an analysis of the scales of motion shown in sequences of vertical wind profiles measured by the FPS-16 radar/Jimsphere technique and an investigation of methods of forecasting the different scales for application in launching vehicles and spacecraft. Normally, it assumed that the total (observed) wind profile is the composite of certain predominant patterns of motion identified by terms such as synoptic- or large-scale, mesoscale (intermediate size), and microscale. If this is true, these predominant scales should appear as relative maxima in power spectral analyses of the winds. Moreover, a natural separation of scales would permit consideration of forecasting methods to deal with the different scales in a quasi-independent manner, at least in the first approximation. On the contrary, we found that the spectra of wind profiles show a wide mixture of eddy sizes without predominant modes. Therefore the forecasting problem may be separated into scales on nonspectral grounds such as operational requirements or the accuracy and detail of available input data.

The different subjects considered in this study are shown in block form in Fig. 1. On the left side, studies of FPS-16 radar/Jimsphere wind profiles are represented. These were concerned with the problem of forecasting details of wind profiles for periods of a few hours. On the right side of the figure, objective analyses and numerical forecasts of winds for twelve to twenty-four hour periods, based on standard upper-air soundings, are indicated.

In the first portion of the work (Sec. II of this report), digital spectral analysis was used to determine the distribution of the power (or energy) of the wind speed variations along a vertical axis. The computational method uses the direct Fourier transform of the wind data. These data are processed at each 25 meter height over a layer 50 meters in depth; therefore the highest frequency they contain is 10 cycles km^{-1}, corresponding to a 100-meter wavelength. Three sequences of wind speed

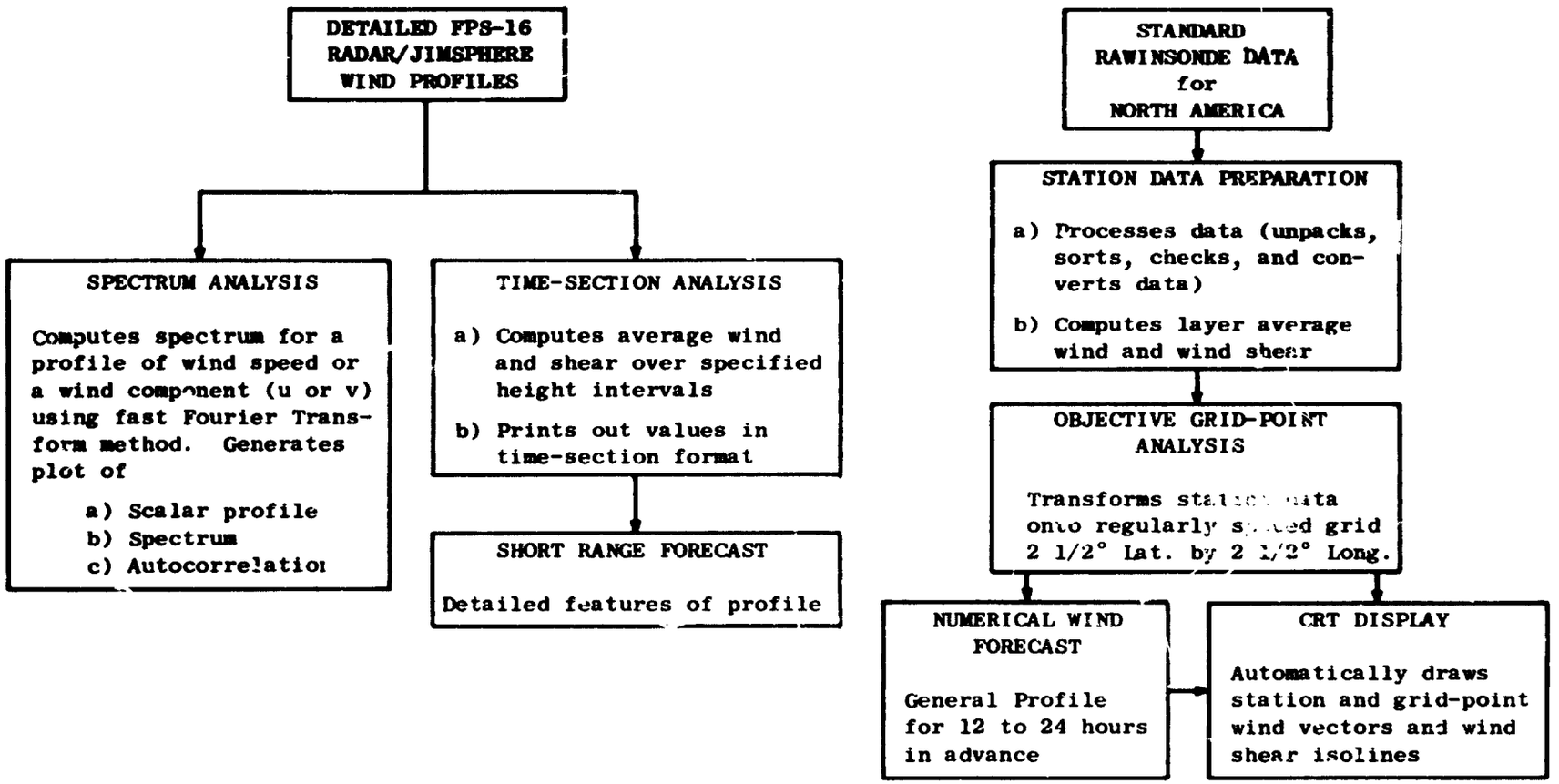

FIG. 1 SCHEMATIC DIAGRAM OF THE INVESTIGATION

profiles from Cape Kennedy, Florida were examined in detail. Each sequence contains four or more profiles measured at one to two hour intervals. One sequence (on 8 April 1966) shows a typical jet stream profile, the second (on 5 July 1966) appears typical of weak summer-time flow, and the third (on 10 November 1965) has intermediate speeds with a considerable amount of jaggedness suggesting prevalent mesoscale features. These profiles are shown in Figs. 3, 10, and 17 (pages 18, 34, and 48). (Those figures which contribute most directly to this summary are mentioned here; the others are discussed in Sec. II and III.) Since the wind speeds are at 25-m intervals from the surface to approximately 20 km in altitude, the frequency range of the spectral analysis of the profiles is from 0.05 to 20 cycles km^{-1} (corresponding to wavelengths of 50 m to 20 km). The spectra of all of the profiles show that energy decreases rapidly with frequency; on an overall basis it is approximately proportional to frequency to the -3 power. If only the higher-frequency end of the spectrum is considered, then the exponent is approximately -2.5. Spectra of individual profiles of a given sequence differ somewhat in minor features, but there are no consistent or well-defined maxima or minima that indicate natural separations between scales of motion. The spectrum plots are summarized in Fig. 24(a) (page 62). The main difference between them is that the higher-speed profiles (for April and November) have greater energy at low frequencies. Also, the jagged profiles of the November sequence have slightly higher energy in the so-called mesoscale portion of the spectrum (wavelengths of approximately 1 to 3 km) than do the other two cases. This indicates that the intuitive interpretation of jaggedness as a measure of energy content in this portion of the spectrum is partially correct.

To study the spectral properties more completely, each sequence of profiles was treated as follows. A mean-speed profile was computed by averaging the individual speeds at each height level, and deviation profiles (the difference between the individual profiles and the mean) were computed. Inspection of a sequence of deviation profiles (Figs. 5, 12, and 19 on pages 23, 39, and 52) will indicate the extent to which anomalies in speed tend to persist over periods of a few hours. While some maxima and minima of deviations appear in successive profiles, many other

features have little persistence, and therefore must be considered random, for practical purposes. Spectra of the mean profile and of each deviation profile were calculated. The former contain most of the low-frequency energy; the latter contain the higher frequencies. Neither spectra indicate natural separations between scales of motion. These spectra of means and deviations are summarized in Figs. 24(b) and 24(c) (pages 63 and 64). If a persistence-type forecast is made (i.e., assuming that the mean profile will remain for a few hours), then the forecast errors will have the spectral breakdown of Fig. 24(c). The spectra of deviations are very similar for the three different sequences considered, indicating that seasonal and synoptic influences on them are not large.

Another way to examine the behavior of sequences of wind speed profiles is by computing differences between successive pairs. If these speed-difference profiles show similarities to each other as time progresses, there is an implication that changes in the recent past can be used to predict future changes. Speed-change profiles for the three data sequences are shown in Figs. 7, 14, and 21 (pages 27, 43, and 55). As with the deviation profiles, these do not have regular behavior when viewed as a time sequence. Their spectra are summarized in Fig. 24(d) (page 65). They do not indicate any predominant frequencies, and are quite similar to 24(c). If the last available measured profile is used as a short-range forecast for launch time, the spectra of errors will be similar to those of Fig. 24(d).

We consider it significant that the spectra for the three cases investigated are quite similar. Contrary to intuitive expectations, there are no consistent concentrations of energy at scales corresponding to the terminology <u>large scale</u>, <u>mesoscale</u>, and <u>microscale</u>. This does not imply that certain phenomena (such as fronts, sea breezes, mountain waves, sharp troughs, and jet fingers) do not have large variability over mesoscale distances, or that inertial waves and shear-gravity waves are not present in the atmosphere. However, in regard to their appearance in vertical wind profiles, such phenomena are evidently only part of a large population of variations of all sizes; therefore they do not stand out in the overall statistics.

The problem of forecasting small, short-term features of the wind profiles, of the sort that are critical in rocket launching, appears to be very difficult because of the lack of natural separations between scales of motion and because of the considerable degree of randomness in the growth and decay of relative speed maxima and minima. In view of the importance of our space effort, the large costs involved, and the possibly hazardous effects of small, unanticipated wind features, further study of detailed profiles is needed. It is a relatively unexplored field of meteorology. One avenue of investigation concerns the vertical air motions (recently deduced by NASA from variations in balloon-ascent rates) and their use in forecasting changes in relative maxima and minima in the horizontal speeds. Detailed temperature soundings will also be of value in such a study. Another avenue would require a fairly dense network of stations (say four to six in number) upwind of Cape Kennedy, to take wind soundings every few hours as a launch approaches. Standard GMD-1 equipment would probably suffice for such measurements provided that data reduction is done by computer to obtain the required accuracy and timeliness of winds. With such data, which is now unavailable, methods of forecasting detailed wind features could be investigated through study of the formation, movement, and dissipation of the smaller features. Also a network of this sort could easily detect the approach of major wind changes due to fronts, troughs, etc., and would prevent their unexpected arrival at Cape Kennedy. Exploration of these two approaches toward more accurate wind forecasting appears very desirable.

The portion of this study concerned with standard upper-air data is described in Sec. III. The purpose is to obtain numerical forecasts of the general wind profile (based on winds at height intervals of approximately 1 km) for periods 12 to 24 hours in advance. Such forecasts are intended to show whether major changes in winds would occur during such periods at localities such as Cape Kennedy. No attempt was made to forecast the details of wind profiles for 12 hours or more, for reasons given earlier. The investigation applied techniques of objective analysis to represent standard wind observations for the southern United States, Mexico, and the Caribbean on a regular latitude-longitude mesh. An area

of this rather large size must be considered in order to encompass winds that can reach Cape Kennedy in less than a day under jet stream conditions. Analyses were made for layers 1 to 2 km in depth. These analyzed winds were portrayed as vectors and plotted on a cathode ray tube by the computer. Examples are shown in Fig. 27 (page 74). Numerical forecasts of changes in the wind field were made for each layer based primarily on the equation for conservation of vorticity; however, the finite difference analogues and methods of relating winds and vorticity were different from those ordinarily used. The differences were intended to emphasize winds, the factor of interest, without resort to intermediate quantities such as pressure heights or stream functions. Forecasts can be made by this technique quite quickly; also, the technique might be adapted to smaller-scale features if detailed initial data were available. The accuracy of the test forecasts was somewhat better than that of other methods presently being used, and further improvements appear possible. An example is shown in Figs. 28-30 (pages 80 to 83). We believe that such numerical products would be a valuable and timely aid to the forecasters responsible for predicting the launch winds.

The principal recommendations of the study are that

1. The predictability of small-scale features of wind profiles be studied further; first, by considering the effects of vertical motions in altering these features, and second, by using a network of wind-measuring stations upwind of Cape Kennedy to document wind changes and the movements of smaller-scale features across Florida.

2. Consideration be given to the desirability of establishing a computer system for making and displaying operational forecasts of larger-scale wind features and profiles for periods 12 to 24 hours in advance. At the same time, further improvements of forecasting methods should be made. This can be done by elaboration of numerical methods used so far.

II SPECTRAL ANALYSIS OF WIND PROFILES

A. Introduction

The vertical wind profile that exists when a missile or spacecraft is launched affects its trajectory. Therefore, a forecast of the general shape of the profile is needed as preflight input to the guidance and control system. In addition, detailed features of the wind profile are of concern because they produce effects such as bending of the structure and fuel sloshing. Vaughan (1962) states that winds in the 10 to 15 km altitude range, associated with maximum dynamic pressure on the rising vehicle, are of most importance. Jet streams, having high speeds and large vertical shears, are found at these critical altitudes. It is also true that standard measurements are least reliable under high-wind conditions. Therefore, NASA has used a special wind-measuring technique at Cape Kennedy, Florida. The basic tools are an FPS-16 tracking radar and a rising balloon, the Jimsphere, designed to follow the atmospheric motions with minimal wobbling due to aerodynamic forces (Scoggins, 1964). Studies of wind profiles measured with this technique have been made by Reiter and Lester (1967), DeMandel and Scoggins (1967), and Endlich and Davies (1967). These papers have been concerned primarily with so-called mesoscale features (e.g., relative speed maxima and minima, and large shears) shown by sequences of profiles measured at one to two-hour intervals. The present report describes the statistical properties of FPS-16 radar/Jimsphere wind profiles as shown by spectral analysis. The information is desired for the light it may shed on questions of possible natural separations between scales of motion, and for implications in regard to forecasting the wind profiles down to the smallest details that can be considered deterministic. Furthermore, even if the instantaneous details of a profile cannot be predicted, it may still be possible to specify their power spectrum.

Much previous work has been done using spectral analysis of detailed meteorological data, particularly those obtained on towers (see Lumley and Panofsky, 1966). In the free atmosphere, spectrum computations have

been applied to aircraft measurements of small-scale, three-dimensional turbulence in the inertial subrange. At this scale, it is well known that turbulent eddy energy decreases with frequency according to the -5/3 power law. Here, turbulence is used in the meteorological sense and refers to erratic, small-scale wind variations in time at a fixed altitude, or in a small moving volume of air. In the free atmosphere, such turbulence exists only in regions associated with storms (fronts, thunderstorms, etc.) and in patches of clear air turbulence.

The present study is concerned with the spectral distribution of wind variations measured along paths that, for purposes of interpretation, are considered to be essentially vertical. The time difference of approximately one hour between the beginning and end of a Jimsphere balloon flight is ignored. The present spectra relate to wind speed fluctuations over the total vertical profile and do not pertain to turbulence as defined above, since such turbulence would occur only in certain restricted layers. From the rocket standpoint, the wind variations in space encountered by the moving vehicle give an effect analogous to turbulence. However, it is desirable to distinguish between meteorological turbulence and the accelerations experienced by a rapidly rising body in passing through a variable wind field.

The wind profiles generally cover heights from approximately 0.5 to 15 km. Within this distance the winds may increase to jet-stream speeds at 10-12 km and then decrease again to low speeds in the stratosphere. The same variation of winds occurs only in much greater horizontal distances, on the order of several hundreds of kilometers across a jet stream, or of a thousand kilometers or so along a jet. This difference in scale makes it interesting to compare spectra of winds from rising balloons to previous spectra along horizontal lines, as given for example by Pinus (1963) and Kao and Woods (1964).

B. Computations*

The computational method used in this study was developed as a general purpose routine by the Mathematical Sciences Department of SRI. Power spectral density function estimates were calculated by the "direct transform," rather than the "lagged product," method. Since this method

*By R. C. Singleton

has been little used in meteorological studies, a brief description follows.

We start with a sequence $\{x_j\}$ of wind velocity measurements, taken at equally spaced heights; in the present case, height assumes the role of "time" in spectral analysis. We estimate the power spectral density function by computing the smoothed power spectrum of these measurements, following one of the possible paths from the upper left to the lower right corner of Fig. 2. In the lagged product method, (Blackman and Tukey, 1958) the usual sequence of steps is to compute the sample autocovariance function,

$$\psi_\tau = \frac{1}{n} \sum_{j=0}^{n-1-\tau} x_j x_{j+\tau} \tag{1}$$

for $\tau = 0, 1, \ldots T$, with the maximum lag T typically in the range of 10 to 30 percent of n, and then to compute the estimated power spectrum with a Fourier cosine transform

$$p_k = \frac{1}{T} \left\{ w_0 \psi_0 + 2 \sum_{\tau=1}^{T-1} w_\tau \psi_\tau \cos(\pi k \tau / T) + w_T \psi_T \cos(\pi_k) \right\}$$

for $k = 0, 1, \ldots T$, where w_τ is a window function for the purpose of reducing interactions of spectral estimates.

In the direct transform method (Bingham et al, 1967; Singleton and Poulter, 1967; Larson and Singleton, 1967), we transform from the time to the frequency domain at the first step, obtaining the Fourier cosine and sine coefficients

$$a_k = \frac{2}{n} \sum_{j=0}^{n-1} x_j \cos(2\pi jk/n)$$

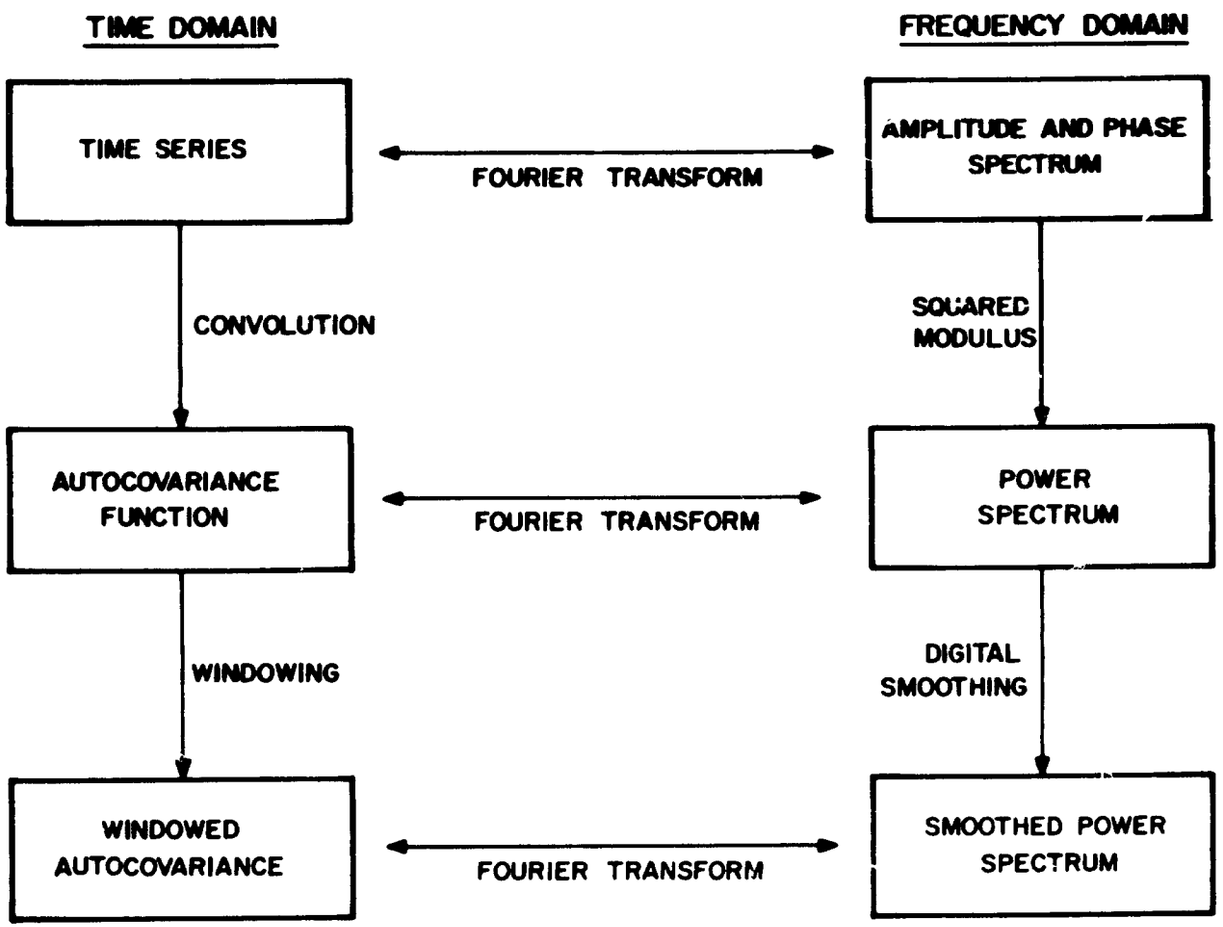

FIG. 2 SCHEMATIC DIAGRAM SHOWING TIME-FREQUENCY RELATIONS IN DIGITAL SPECTRAL ANALYSIS

and

$$b_k = \frac{2}{n} \sum_{j=0}^{n-1} x_j \sin(2\pi jk/n)$$

for k = 0, 1, ... n/2. We then compute the raw power spectrum estimates

$$P_k = \frac{1}{2} [(a_k)^2 + (b_k)^2] \tag{2}$$

for k = 0, 1, ... n/2. These values sum to the average squared value of x_j, denoted S, in the following way:

$$S = \frac{P_o}{2} + \sum_{k=1}^{n/2-1} P_k + \frac{P_{n/2}}{2} \tag{3}$$

An autocorrelation function estimate

$$C_\tau = \frac{1}{n} \sum_{j=0}^{n-1} x_j x_{(j+\tau) \bmod n} \tag{4}$$

for τ = 0, 1, ... n/2 can be computed by transforming back to the time domain (Stockham, 1966); this result differs from Eq. (1) but is logically consistent with the assumption that the data sequence $\{x_j\}$ is periodic with period n.

In the absence of noise we could stop with the raw spectrum estimates (2). With noise we smooth the power spectrum estimates, reducing the resolution in exchange for a gain in statistical stability. A convenient weighting for this purpose is

$$P'_k = \frac{1}{4} (P_{k-1} + 2P_k + P_{k+1})$$

using at the ends the property that P is an even function with period n. In the time domain this smoothing is equivalent to truncating the autocovariance function (Singleton and Poulter, 1967) with the window

$$C'_\tau = \cos^2 (\pi\tau/n) C_\tau$$

for $\tau = 0, 1, \ldots n/2$. In computing the results included in this report, the power spectrum was averaged three times with this weighting, equivalent to multiplying the autocovariance by the window function

$$\cos^6 (\pi\tau/n).$$

This function decreases from one at zero lag to zero at maximum lag $\tau = n/2$, and has the value 1/8 at 50 percent lag. With an autocovariance truncation of this or similar form, the difference between Eq. (1) and Eq. (4) at large lags becomes relatively unimportant.

The direct transform method is rapidly replacing the lagged products method as the standard technique of spectral analysis, since the introduction of the fast Fourier transform algorithm (Cooley and Tukey, 1965). With this algorithm, the direct transform method is much faster and more accurate than the lagged products method. The computational time is proportional to $n \cdot \log n$ for the fast transform, and to n^2 for the older method. Thus the relative advantage of the former increases for long records. As noted above, we now find it advantageous to compute the autocovariance function from the power spectrum, rather than the other way around.

We mention in passing that the practice of "prewhitening" the data, i.e., high-pass filtering by partial first differencing, then correcting the power spectrum to compensate for this filtering, is seldom used with the direct transform method. The improved accuracy of the fast Fourier transform gives high dynamic range in the power spectrum without resort to the device of prewhitening.

An area of increasing interest within spectral analysis is that of model-fitting, the decomposition of the data sequence into component parts. In examining wind profile data, for example, we have in some of the calculations separated the data into a trend function of average wind speed as a function of altitude, and a noise-like function representing the fluctuations about this trend. With this decomposition, we can study separately the problems of predicting the trend function and of predicting the shape of the power spectrum of the fluctuations about the trend. While we cannot predict the instantaneous fluctuations in wind speed, we should be able to characterize the shape of the power spectrum that can be expected under various atmospheric conditions.

C. Data

The data processing method that produces the wind data used in this report has been described by Scoggins and Susko (1965). The zonal and meridional components of wind are averages over a layer approximately 50 m in depth, and are given at 25 m height intervals. Thus, the aerodynamic balloon motions and any atmospheric eddies smaller than approximately 100 m have been eliminated to a large degree. However, a few spurious points, mostly false speed maxima or minima, were encountered in the wind profiles. These were eliminated by a subprogram that tested the difference between successive points. If this difference (in either speed component) was larger than a critical value, an interpolated point was substituted for the erroneous one. The critical value was taken as 4 m sec^{-1} for strong wind profiles, and as low as 2.5 m sec^{-1} for cases of weak winds. Even so, a few small, spurious-looking features remain in some profiles shown later. Experimentation showed that the high-frequency end of a spectrum plot was significantly raised if even a few spurious spikes were included; thus the matter is of practical importance.

The wind data generally began approximately 500 m above sea level and terminated at an altitude between 15 and 18 km. In studying a given sequence of FPS-16 Jimsphere runs, all were terminated at the lowest upper limit, so that each profile of the sequence would cover exactly the same altitude range.

A basic assumption in spectral analysis is that the data sample spans one period of a periodic function, i.e., that the final point of the sounding is followed by the first point, and then by the rest of the record, ad infinitum. If the values of the first and last points are nearly the same, only a small discontinuity in shape is implied if they are effectively made adjacent to each other. However, in the present data, the differences between the speeds of the first and last points were sometimes large. To avoid a discontinuity in shape and the concommitant effects of added high-frequency power in the spectrum, a smooth, cosine-shaped connection was inserted between the last measured point and the first point. The first point of the profile was assumed to occur again at 20.5 km, and the cosine connection was made between the last point (say at 16 km) and this repeated value. (An example is shown later in the smooth, upper portion of curve g in Fig. 3.) Comparisons between actual spectra computed with and without the cosine connection show its effectiveness in accurately portraying the higher frequencies. Computations were made using SRI's Burroughs 5500 computer. Wind profiles and spectra were plotted using a California Computer Company automatic plotter.

D. The Sequence of Wind Speed Profiles on 8 April 1966

Wind profiles measured at 0835, 0955, 1215, 1455, 1607, and 1723 GMT are shown in Fig. 3, and are designated by the letters a to f. The profiles were measured in a uniform westerly, upper-air flow. All have maximum speeds slightly greater than 60 m sec^{-1}. Their shapes are similar, but rather large changes can be noted in detailed features; these will be discussed later.

The spectra of the speed profiles are shown in Fig. 4 in the same order as in Fig. 3. The graphs are the customary log-log plot with the abscissa as frequency (or inverse wave number) in cycles km^{-1}. As stated in Sec. II-B, P was computed so that the estimates sum to the total power in $m^2 sec^{-2}$. To convert to the usual meteorological units of $m^2 sec^{-2}/(cycles\ km^{-1})$, the original power estimates were multiplied by $1/\Delta f = 20$; these converted values are used as the ordinate in the spectral plots.

The power spectral density in the plots of Fig. 4(a-f) drops off rapidly with increasing frequency, as expected. The steepest decline is at a frequency of approximately 0.2 cycles km^{-1}; here the slope is nearly -8. At frequencies above approximately 0.5 cycles km^{-1}, the slope is close to -2.5. Differences between the spectra of Fig. 4 appear to be rather random, and are of course due to differences in the features of Fig. 3(a-f). It is interesting that a line with a slope of -5/3 (which applies to turbulence in the inertial subrange) is not nearly steep enough to fit any portion of the spectra. Spectra were computed also for meridional and zonal wind components, treated separately. These were very similar to the spectra of speeds in Fig. 4, except that the meridional components had less energy at low frequencies, due to their relatively small magnitudes in this case of westerly winds.

Another way to investigate the scales of variability of these wind profiles is to compute an average profile and the deviation of each individual profile from the average. The average speed at each 25-m height increment is determined simply as the mean of the six speed values there. The profile of these averages is shown as curve g in Fig. 3. This curve is smoother than the individual profiles but otherwise resembles them closely since the large-scale patterns were not changing rapidly. Its spectrum is shown in Fig. 4(g). This graph then may be considered to be a spectrum of the larger-scale, vertical wind profile on this particular occasion of high wind speeds.

The profiles of the deviations from the mean are shown in Fig. 5. Each has some similarities and some differences from its neighbors. Some features, such as the relative maximum at 3 km elevation in the last four profiles, persist almost unchanged for several hours; others, such as the speed maximum at 8.5 km altitude at 1215 GMT, do not persist. Spectra of the deviation profiles should give some information on any predominant frequencies of small-scale motions. The computed values [Fig. 6(a-f)] clearly tend to flatten at frequencies less than approximately 0.5 cycles km^{-1}, since the longer wavelengths have been largely relegated to the mean profile, removed by subtraction. The frequencies

higher than approximately 1 cycle km^{-1} have a slope near -2.5, with no consistent gaps. Differences between the several spectra of deviations of Fig. 6 are largest at frequencies from 0.3 to 1.0 cycle km^{-1}.

A further interesting comparison of the wind profiles comes from the differences between them. We may inquire whether changes to be expected in a few hours are similar to those changes that have occurred in previous hours. Differences between successive profiles are shown in Fig. 7(a-e). (Note that the time intervals are not uniform but vary from 1 hour 20 minutes to 2 hours 40 minutes.) The change profiles have similar general characteristics to the deviation profiles of Fig. 5. Consistency of appearance between the change profiles is not very great. Of course, a relatively high speed in one profile of Fig. 3 at a given altitude will appear as a maximum at that altitude in one speed-change profile, and as a minimum point in the following speed-change profile. Spectra of the five profiles of speed changes are shown in Fig. 8(a-e). Their general shapes are similar to the spectra of deviations of Fig. 6.

In order to compare the different types of spectra, those of Fig. 4(a-f) were drawn on a single graph, and a smooth curve was fitted to them by graphical averaging. This curve is identified as the "smoothed spectrum of individual wind speed profiles" in Fig. 9. Two other smoothed curves were prepared from Fig. 6(a-f), and Fig. 8(a-f); these are denoted as the "smoothed spectrum of speed deviations," and "smoothed spectrum of speed changes" in Fig. 9. Also, a smoothed version of Fig. 4(g) is called the "smoothed spectrum of the mean speed profile."

Curve A in Fig. 9, the "smoothed spectrum of individual speed profiles," has a relative minimum (in terms of deviation from the -5 line) at vertical wavelengths between approximately 1 and 3 km. This was mentioned earlier in regard to Fig. 4. Since this region is often referred to as mesoscale, there seems to be considerable doubt that mesoscale eddies in these vertical profiles are particularly significant. Although one can certainly identify maxima and minima in layers 1 to 3 km deep in the profiles of Fig. 3, such features are evidently the combined effects of a variety of wavelengths in the spectrum rather

than the result of a predominant scale. This result may be taken as a warning against making interpretations of scales of motion by simple visual inspection of complex wind profiles.

The "smoothed spectrum of the mean profile" (curve B in Fig. 9) departs from curve A at a wavelength of approximately 4 km, and then conforms roughly to a -3 slope with some rather minor deviations. Curve C, the "smoothed spectrum of speed deviations," lies between the two spectra discussed above and has a smooth shape with only small high and low points. If it were possible to forecast the mean wind speed profile (curve g in Fig. 3) but not the deviations (Fig. 5), then curve C would represent the spectral distribution of errors. Note that curve C intersects curve B at a wavelength of approximately 2 km; here the mean and deviation profiles contribute equally to the variance. The "smoothed spectrum of speed changes," curve D in Fig. 9, lies slightly above the other spectra at the high-frequency end of the spectrum. This implies that the smaller-scale features of successive profiles are basically uncorrelated. Also note that curve D intersects curve C at a wavelength of approximately 3 km; at longer wavelengths it has slightly lower power than curve C. Curve D can be interpreted as the spectrum of the errors of a pure persistence forecast of the wind profile; i.e., if a detailed wind profile measured an hour or two before launch is input to the guidance system, then the changes therefrom will be errors having the statistical properties of curve D.

These spectral relationships apply only to the particular synoptic situation of 8 April 1966, and therefore other cases must be investigated to examine the generality of these findings. Two of these are discussed below.

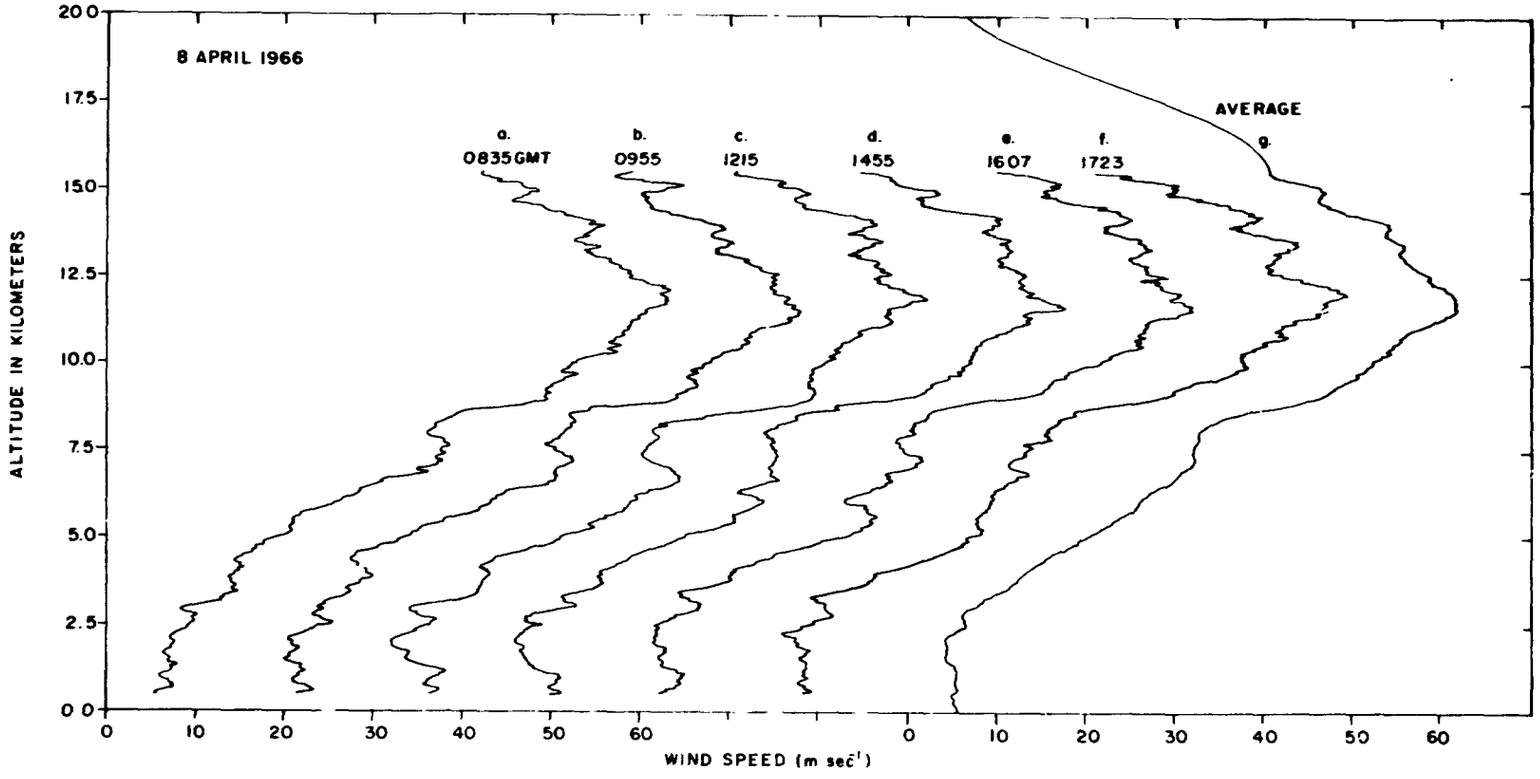

FIG. 3 WIND SPEED PROFILES MEASURED AT CAPE KENNEDY, FLORIDA BY THE FPS -16 JIMSPHERE TECHNIQUE ON APRIL 8, 1966. The speed scale is shown only for profiles a and g.

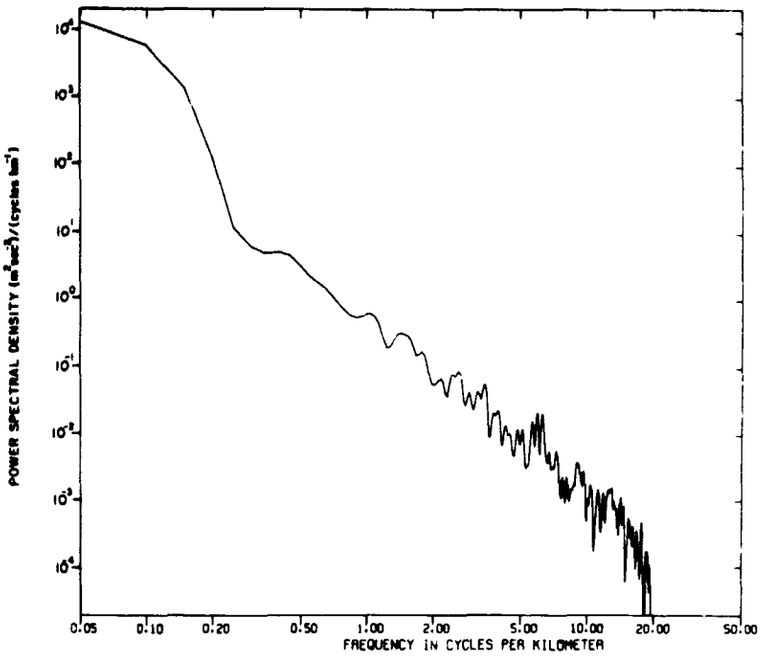

FIG. 4 SPECTRA OF WIND SPEED PROFILES OF FIG. 3
(a) At 0835 GMT

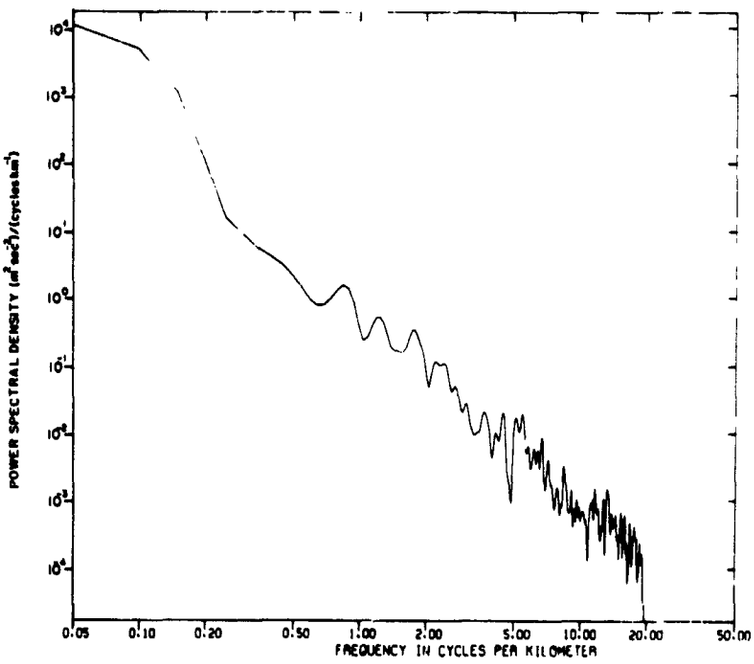

FIG. 4 – (b) At 0955 GMT

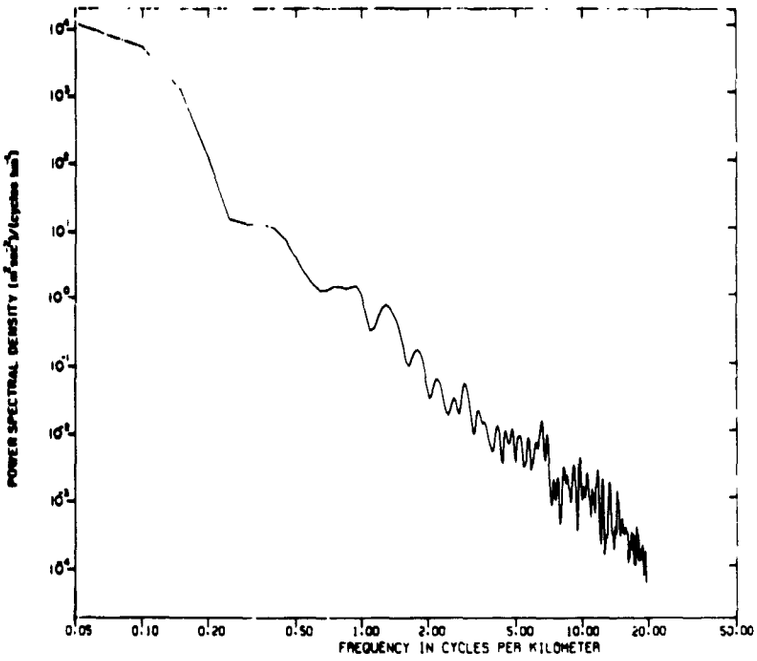

FIG. 4 – (c) At 1215 GMT

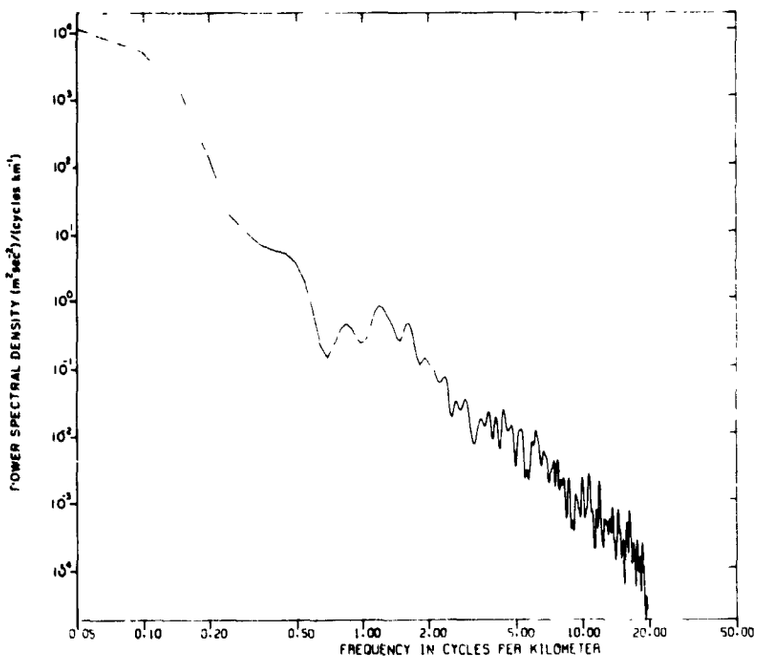

FIG. 4 – (d) At 1455 GMT

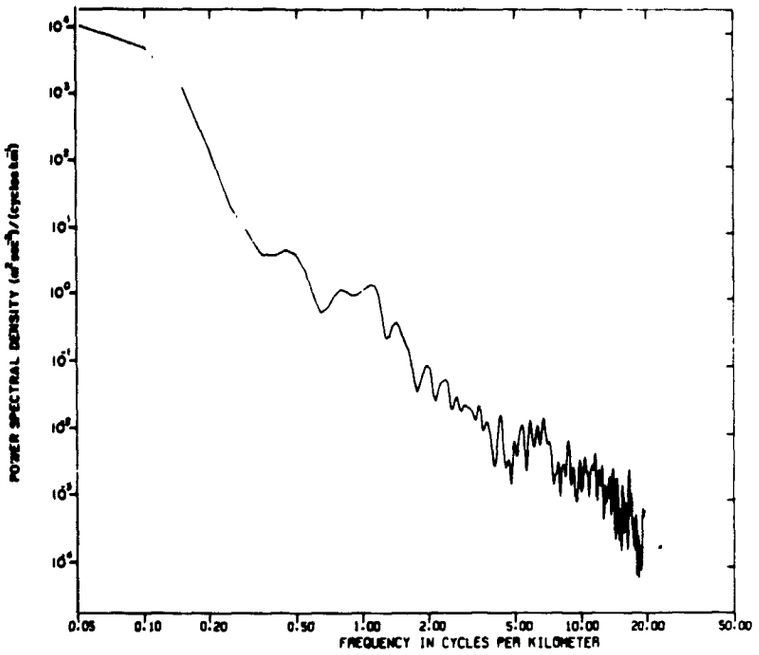

FIG. 4 – (e) At 1607 GMT

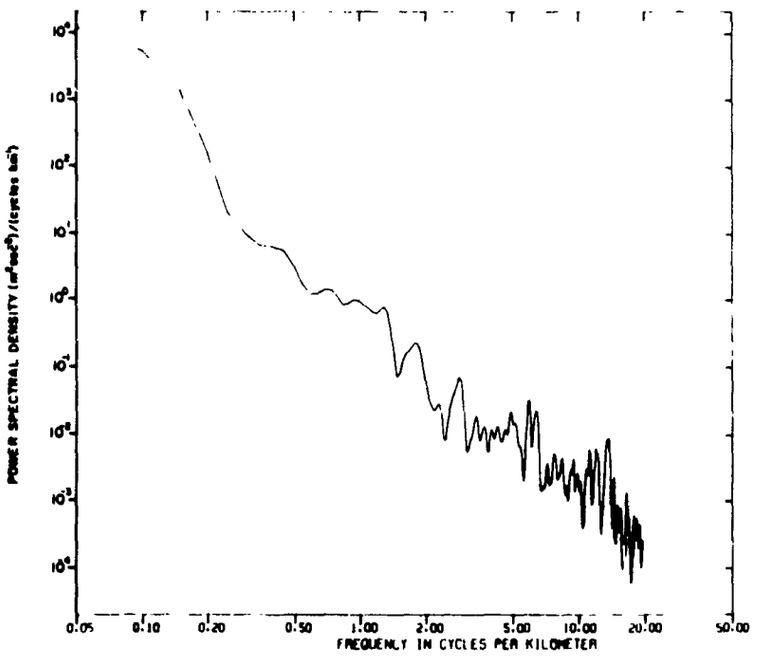

FIG. 4 – (f) At 1723 GMT

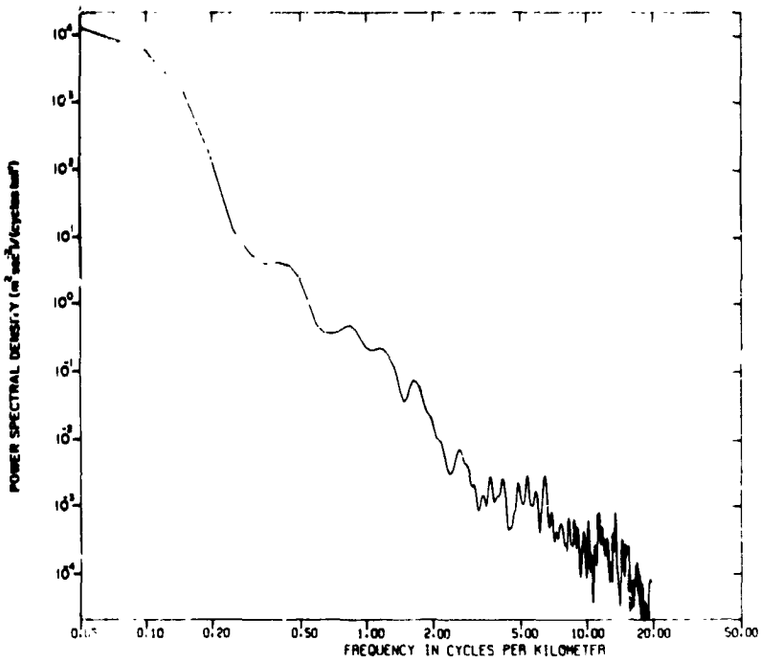

FIG. 4 – (g) Mean speed profile

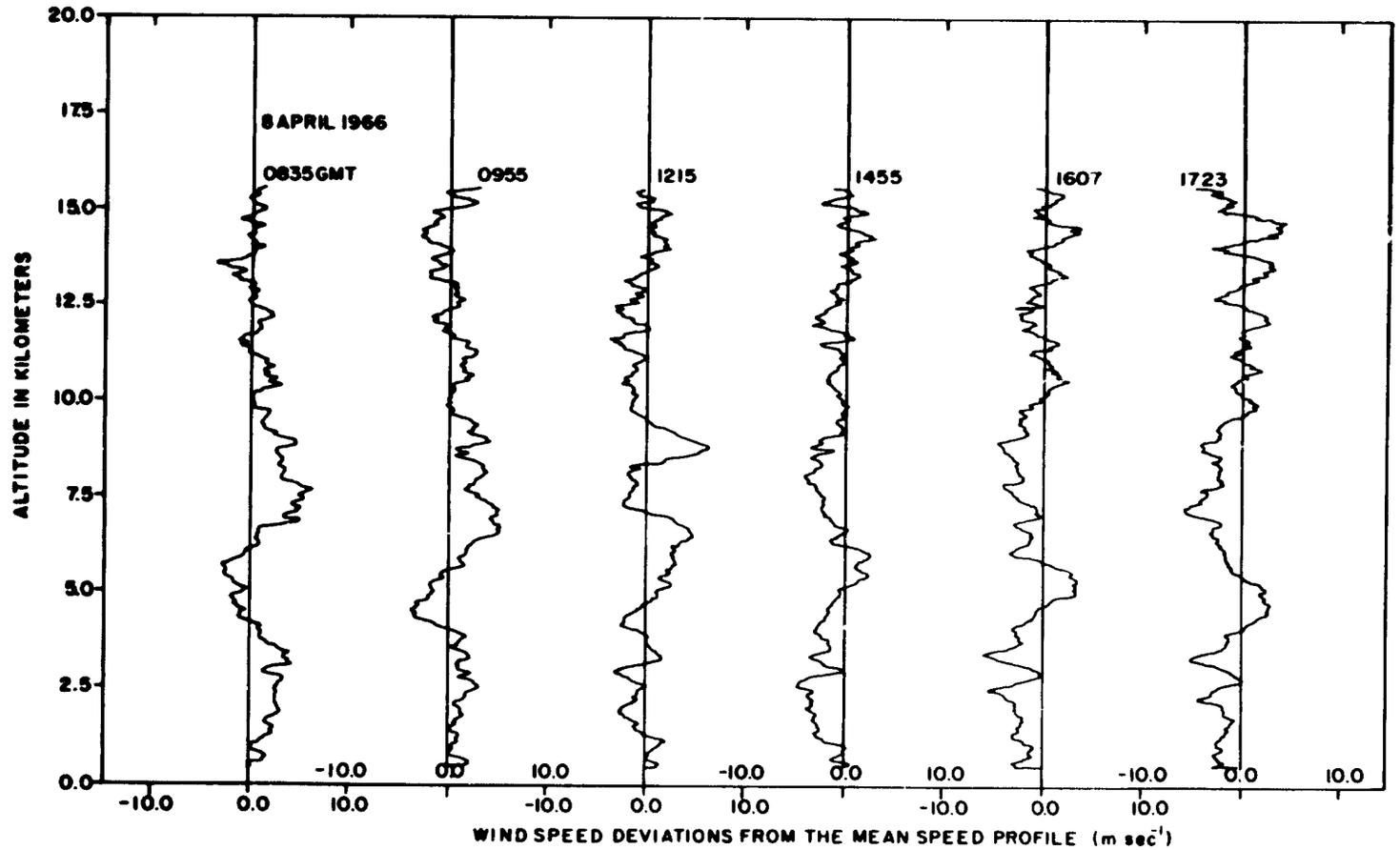

FIG. 5 DEVIATIONS OF INDIVIDUAL WIND SPEED PROFILES FROM THE MEAN PROFILE, APRIL 8, 1966

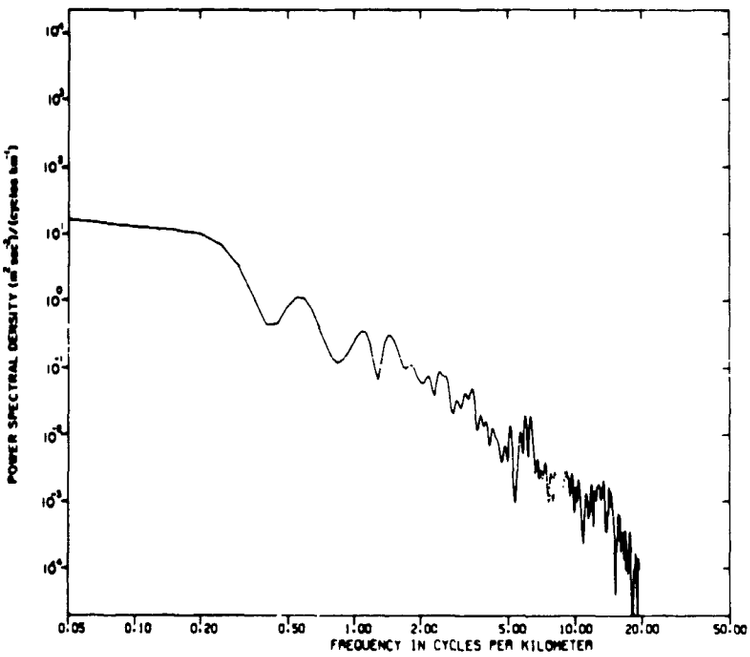

FIG. 6 SPECTRA OF THE PROFILES OF DEVIATIONS FROM THE MEAN SHOWN IN FIG. 5 (a) At 0835 GMT

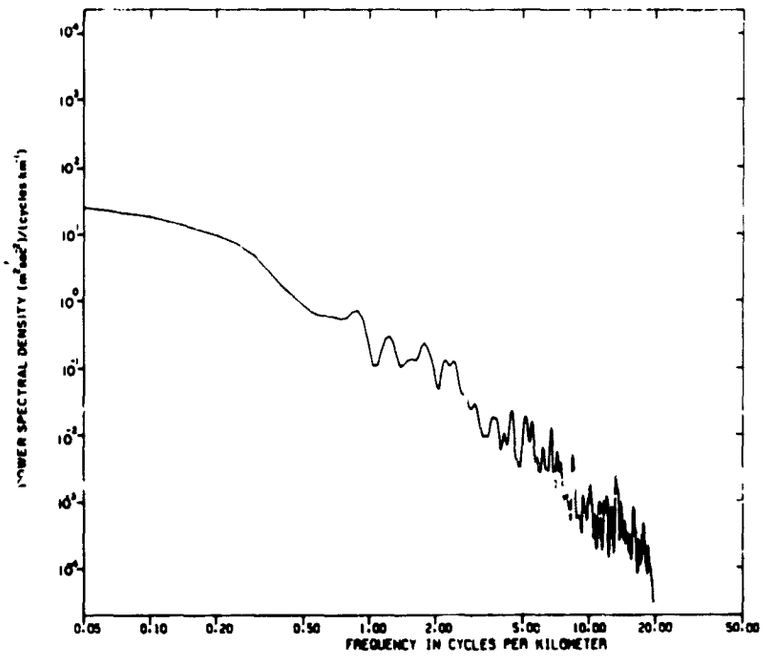

FIG. 6 – (b) At 0955 GMT

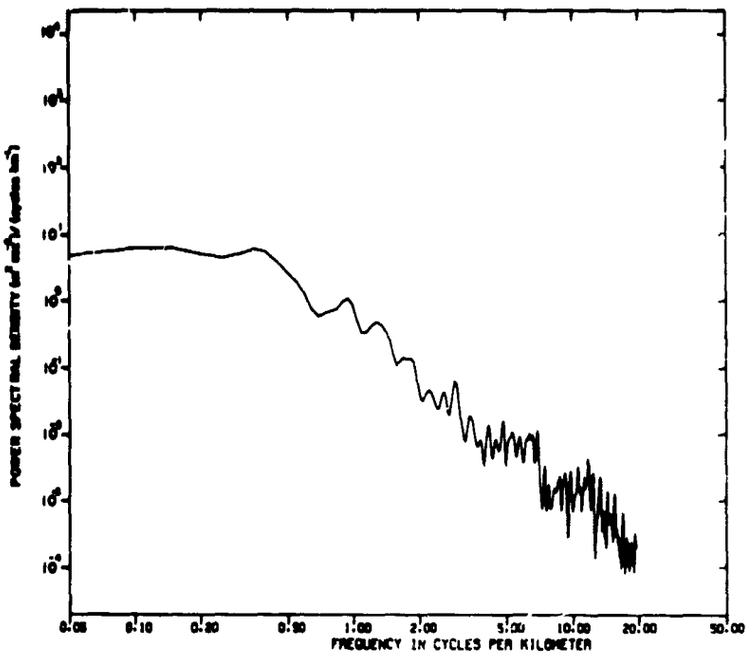

FIG. 6 – (c) At 1214 GMT

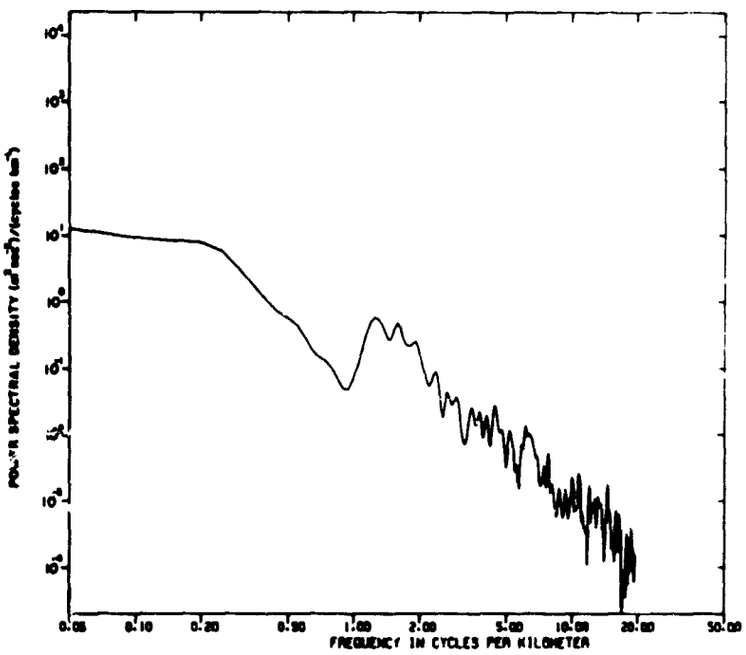

FIG. 6 – (d) At 1455 GMT

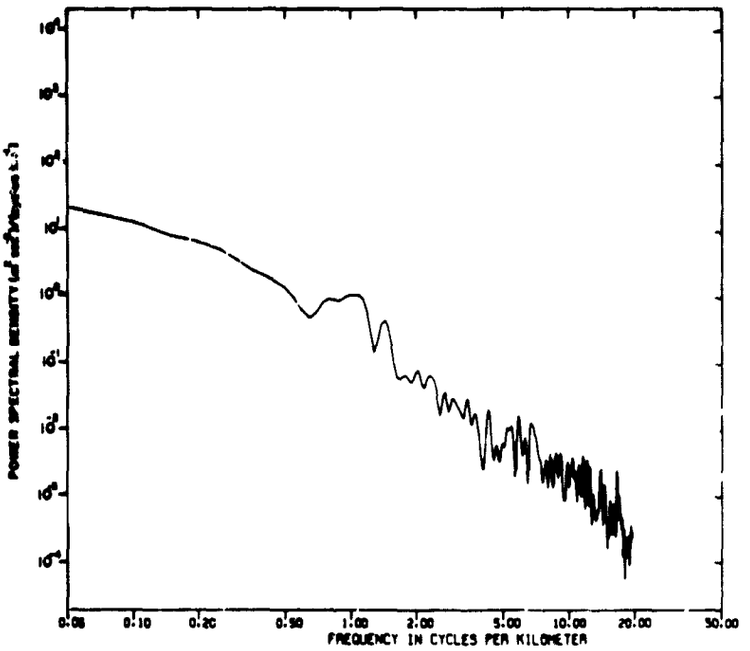

FIG. 6 – (e) At 1707 GMT

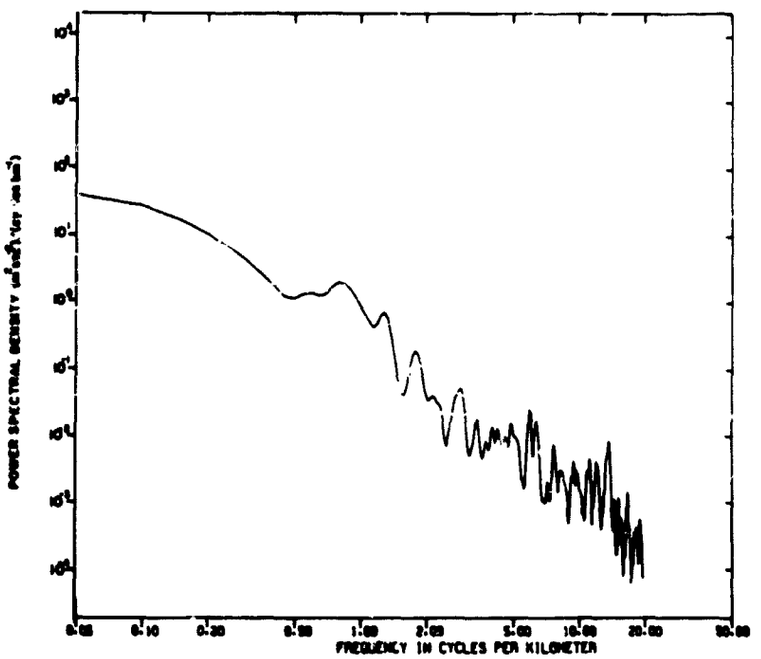

FIG. 6 – (f) At 1723 GMT

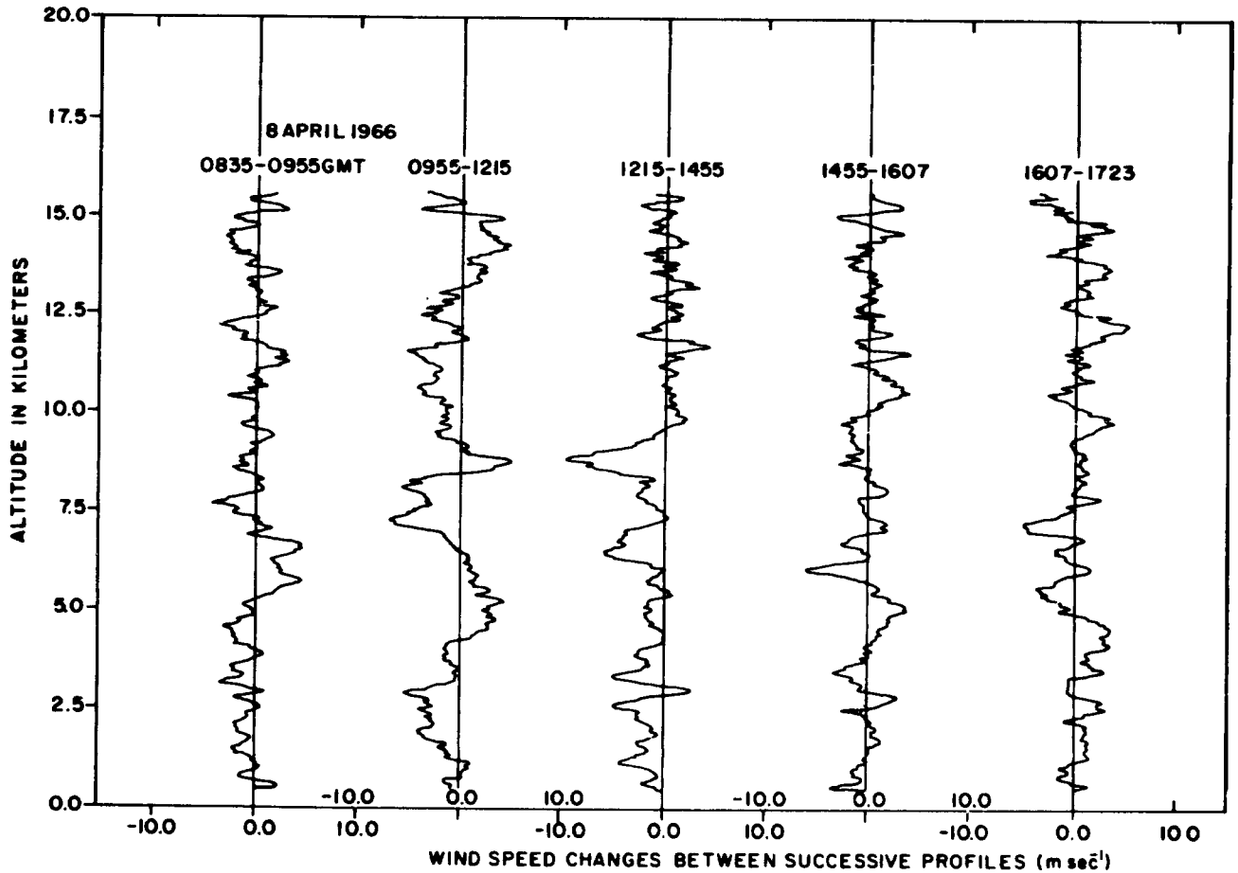

FIG. 7 SPEED CHANGES BETWEEN SUCCESSIVE PROFILES, APRIL 8, 1966

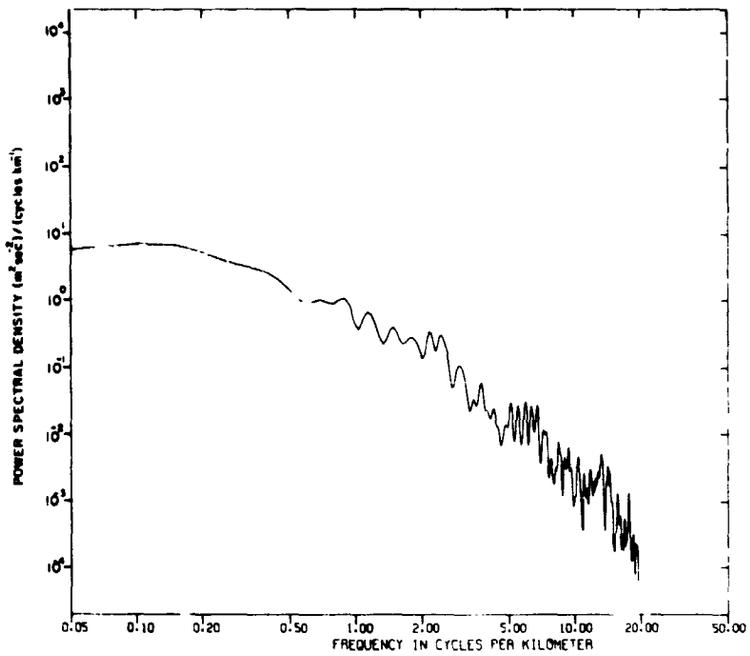

FIG. 8 SPECTRA OF THE SPEED CHANGE PROFILES OF FIG. 7 (a) From 0835 to 0955 GMT

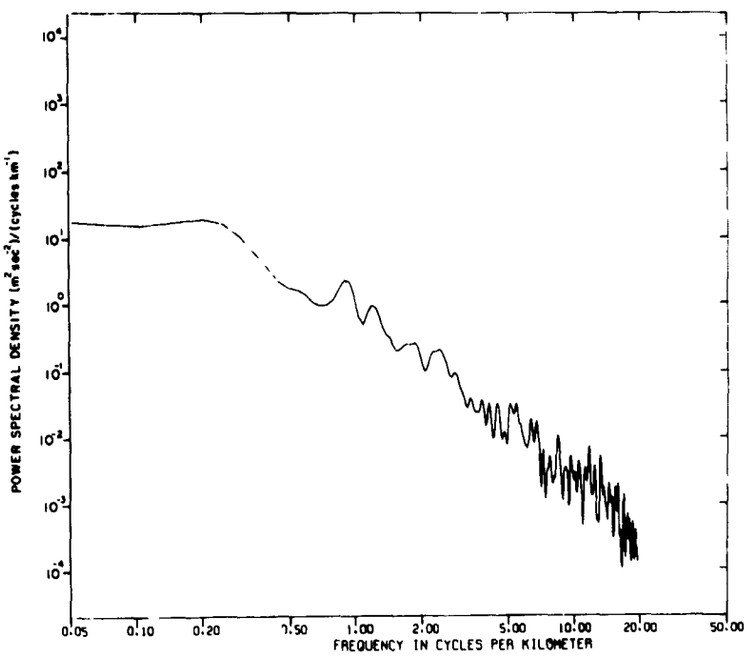

FIG. 8 – (b) From 0955 to 1215 GMT

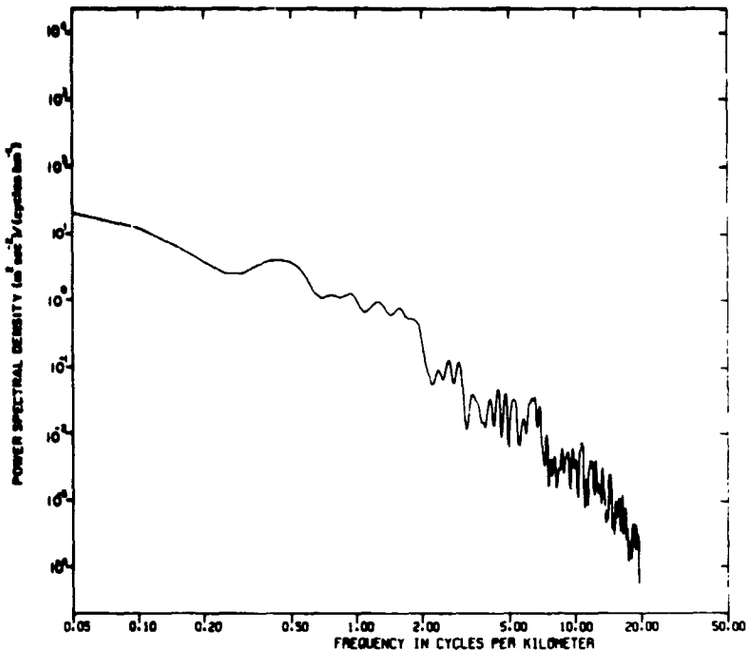

FIG. 8 – (c) From 1215 to 1455 GMT

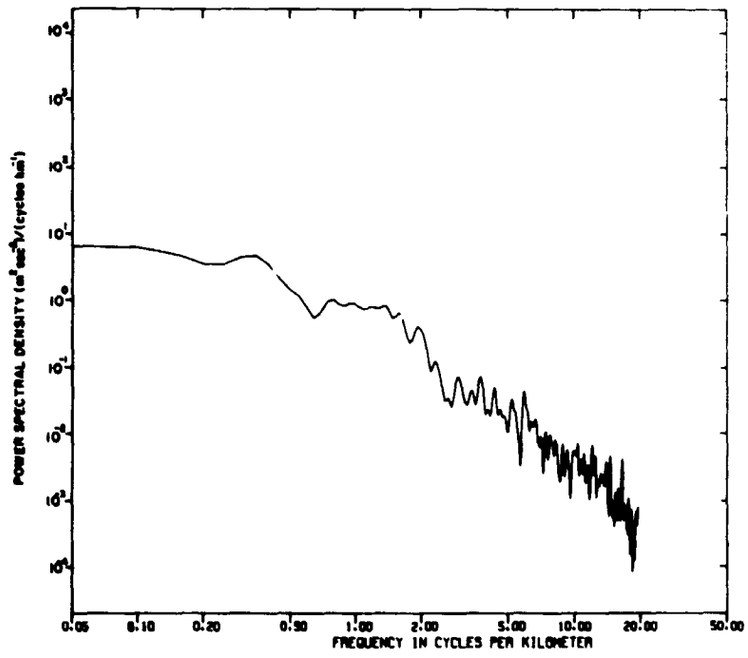

FIG. 8 – (d) From 1455 to 1607 GMT

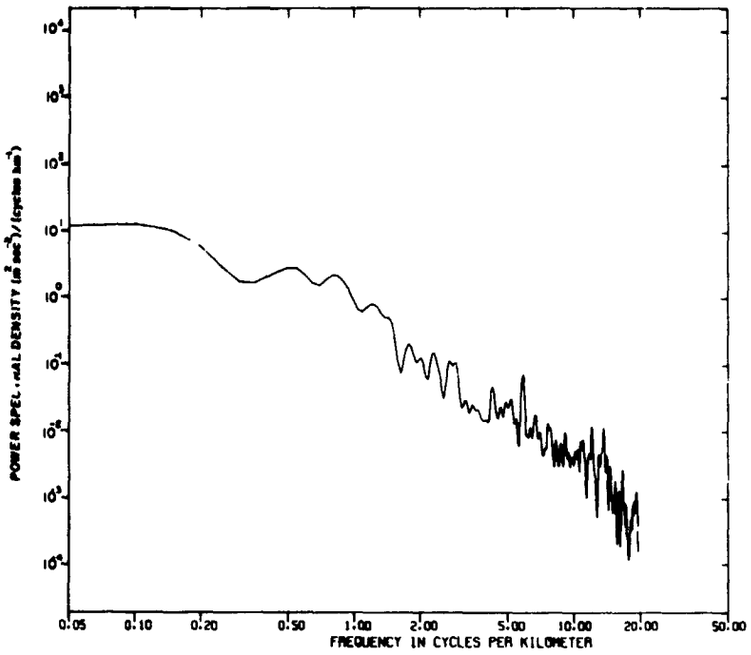

FIG. 8 – (e) From 1607 to 1723 GMT

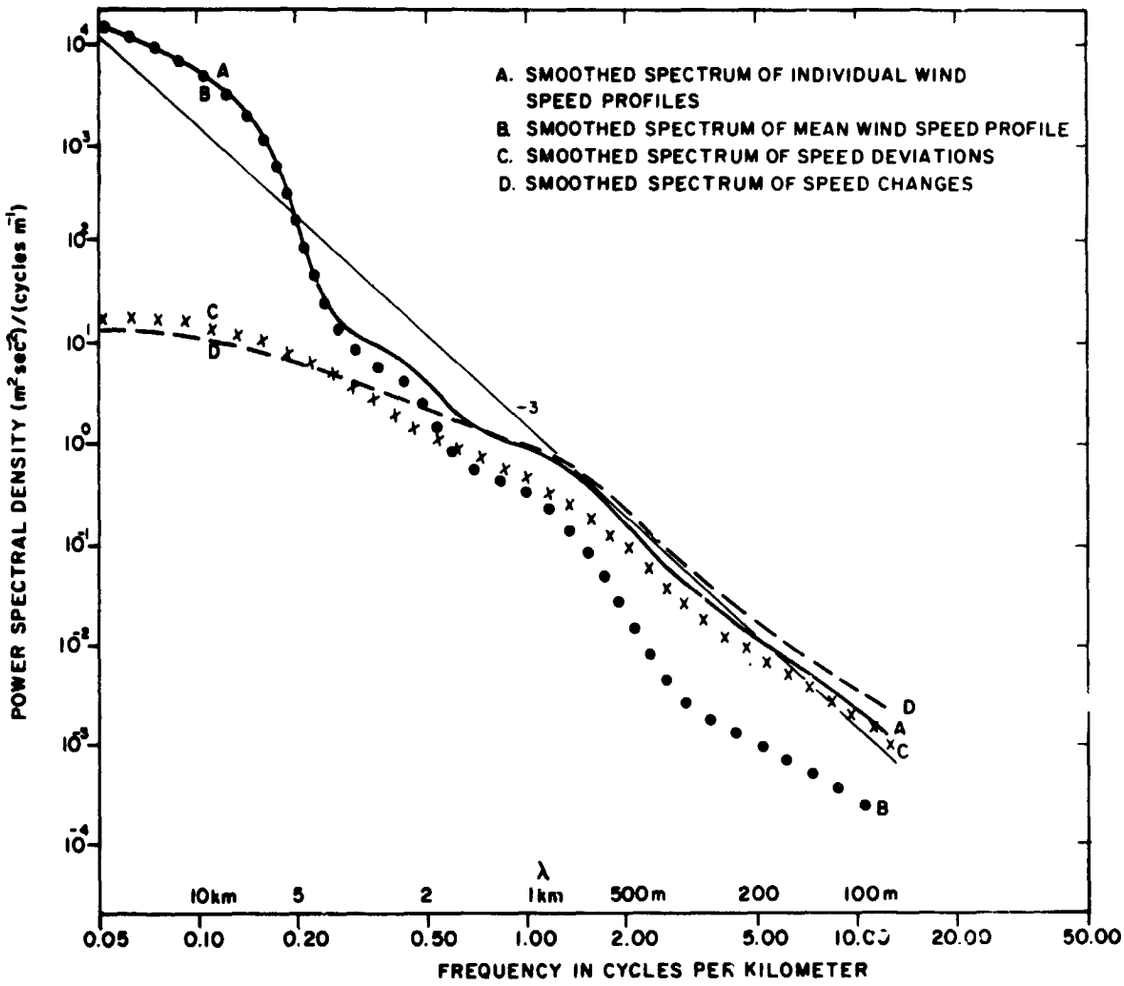

FIG. 9 SUMMARY OF SPECTRA OF WIND SPEED PROFILES ON APRIL 8, 1966

E. Wind Speed Profiles on 5 July 1966

This sequence was selected to represent summer conditions when wind speeds are typically weaker than in winter. Profiles were measured at 2321 GMT on 4 July, and at 0040, 0245, 0516, 0730, and 0930 GMT on the 5th. Thus the measurements were made at intervals of approximately 2 to 2-1/2 hours. The synoptic situation consisted of a weak high-pressure area at sea level over Florida, with westerly winds aloft.

The wind speed profiles are shown in Fig. 10. The first profile of the series is anomalous, in terms of having small, irregular shears throughout. These do not appear in the other profiles of the sequence; perhaps they may be attributed to some equipment difficulty. The speed maximum located at approximately 13 km in curve a of Fig. 10 decreases in magnitude and is found at progressively lower altitudes in later profiles. As in the April profiles discussed in Sec. 4, there are some features that persist from one profile to the next of Fig. 10, especially if altitude changes are permitted, and other features that change erratically.

The spectra of the profiles are shown in Fig. 11(a-f), and a line having a slope of -3 is plotted identically on each as a reference. The spectrum of Fig. 11(a) departs strongly from the -3 line at frequencies above 5 cycles km^{-1}, evidently due to the speed variations mentioned above. On an overall basis, the spectra of Fig. 11(b-f) conform to the -3 line reasonably well, and thus have similar slopes to those found in April; however, the July winds are of lower speeds and the spectra contain less total variance.

The mean speed profile for this series (excluding profile a) is shown as curve g in Fig. 10, along with the cosine connection above approximately 15 km. The spectrum of this mean profile is given in Fig. 11(g). It is similar in shape to its analogue in the April case (Fig. 4), but has less variance at frequencies lower than approximately 1 cycle km^{-1}.

Deviations of the individual profiles from the average are shown in Fig. 12. Below approximately 7.5 km the deviations are relatively small; however, at higher altitudes they are as large as those observed in the April data (Fig. 5). In Fig. 12 a rather marked minimum in speed appears at approximately 14 km in the deviation profile for 0245 GMT. This feature then appears at successively lower altitudes as time proceeds. Most other features have less persistence.

The spectra of the deviations [Fig. 13(a-e)] are very similar to those shown earlier for the April series and contain as much or slightly greater variance than the spectra of Fig. 6. The higher frequencies conform approximately to a slope of -2.5.

The changes in speed between profiles are shown in Fig. 14. These, like Fig. 12, have largest magnitudes in the upper troposphere. Here the patterns tend to persist if one allows for vertical displacements. The spectra of the speed changes are shown in Fig. 15(a-d) and are similar to those of Fig. 8.

A smoothed spectrum representing the individual profiles of Fig. 10 is labeled A in Fig. 16. It was prepared in the same manner as curve A in Fig. 9. Similarly, the other curves in Fig. 16 represent the mean profile (curve B), the deviations from the mean (curve C), and the changes (curve D). In Fig. 16 their relative characteristics can be compared. Crossing points between curves A and D and between B and C are at lower frequencies than in Fig. 9.

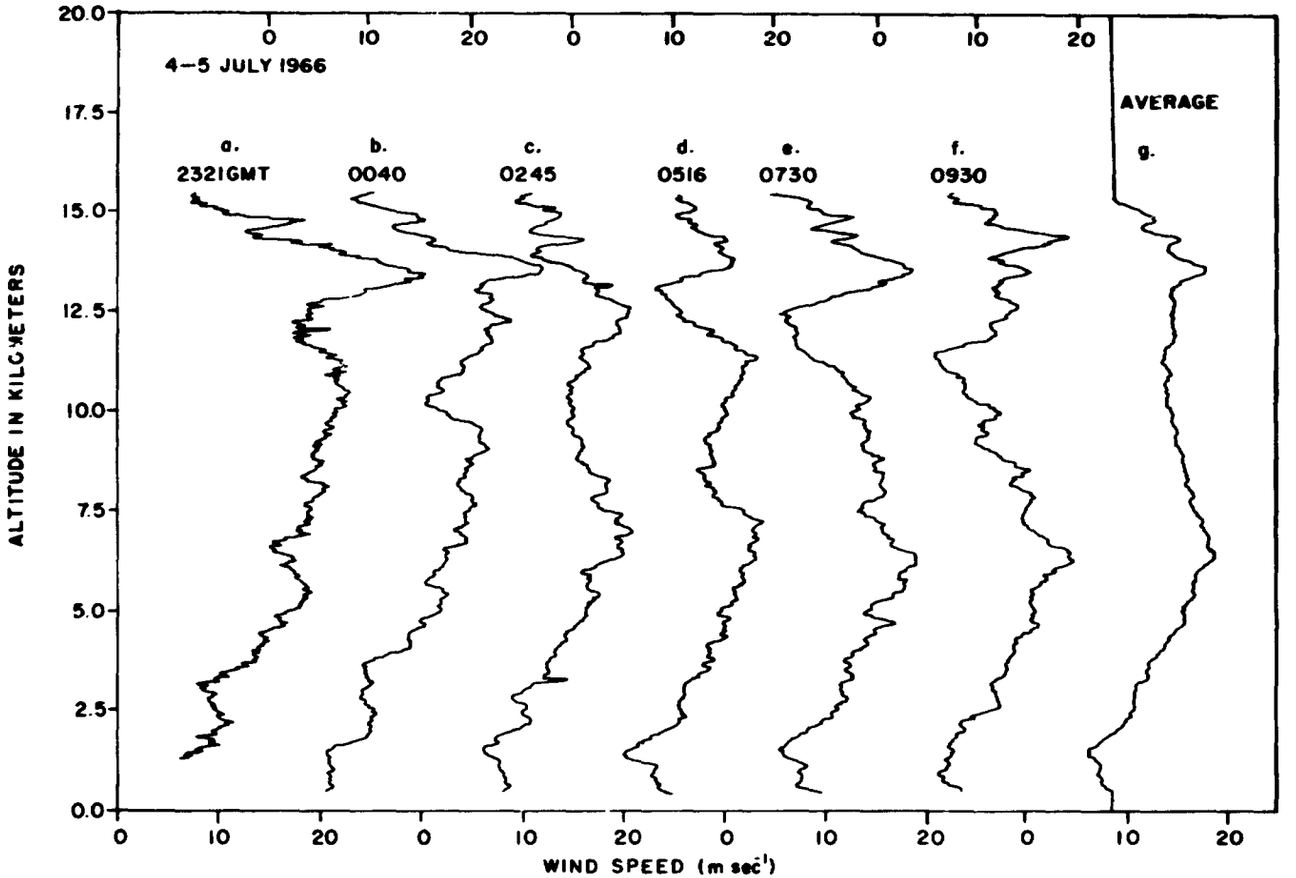

FIG. 10 WIND SPEED PROFILES MEASURED AT CAPE KENNEDY, FLORIDA BY THE FPS-16 JIMSPHERE TECHNIQUE ON JULY 4–5, 1966

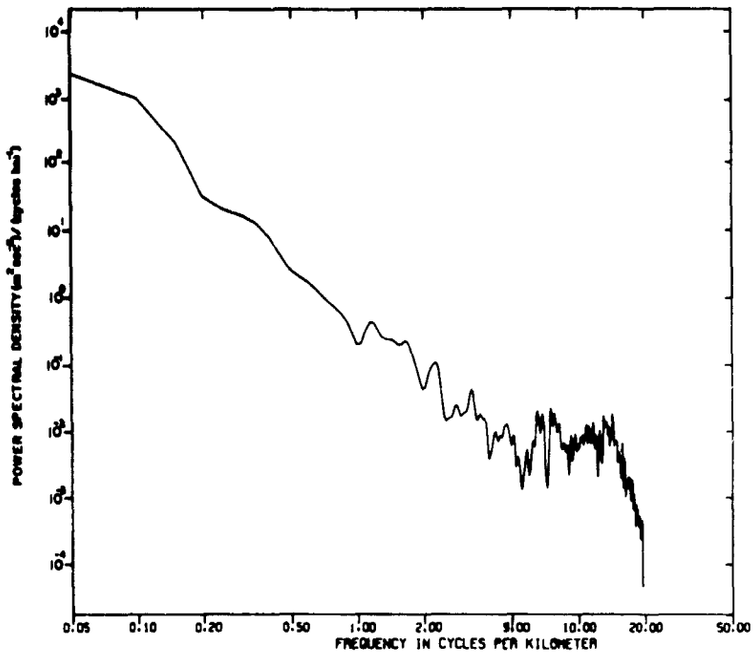

FIG. 11 SPECTRUM OF WIND SPEED PROFILES
(a) At 2321 GMT

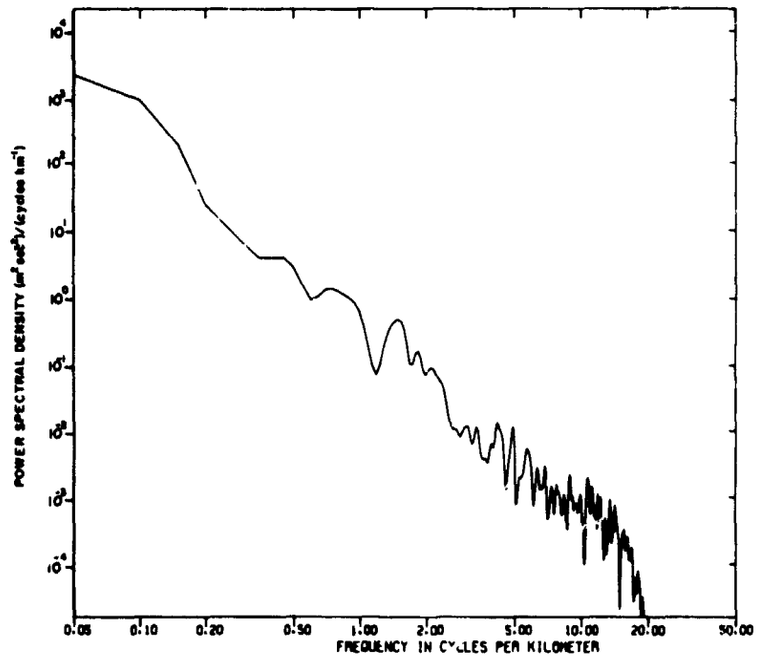

FIG. 11 – (b) At 0040 GMT

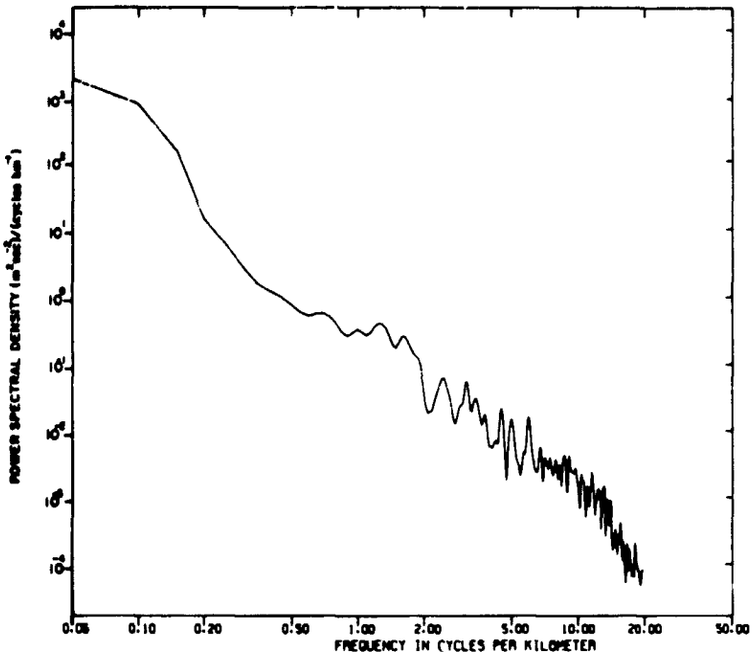

FIG. 11 – (c) At 0245 GMT

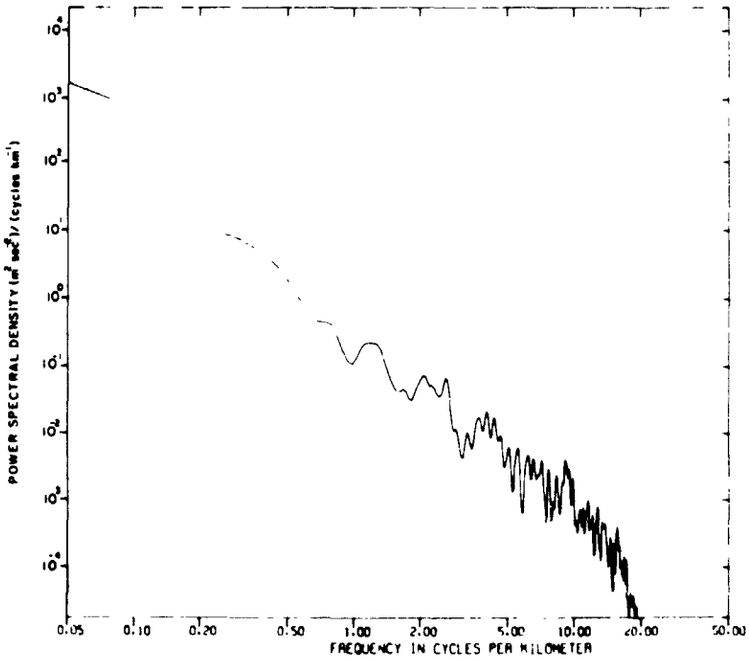

FIG. 11 – (d) At 0516 GMT

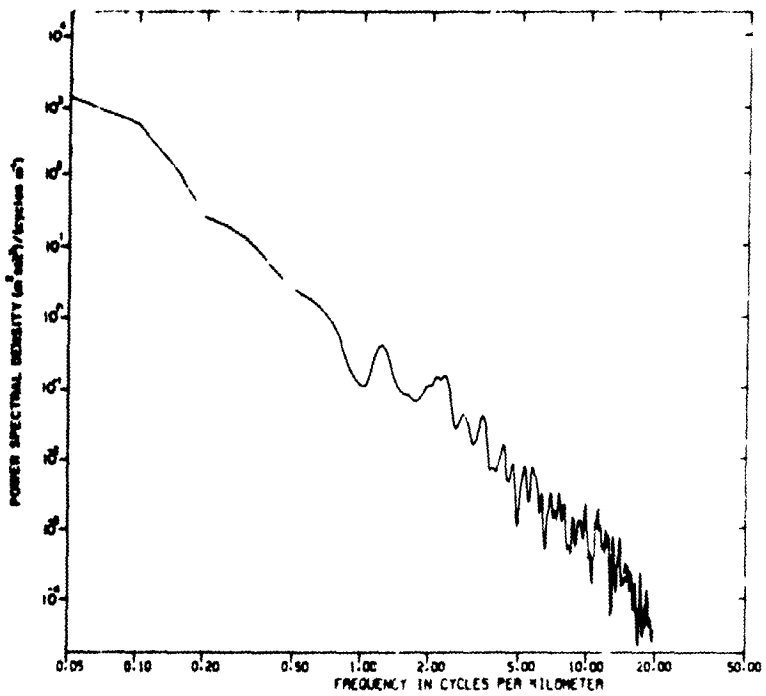

FIG. 11 – (e) At 0730 GMT

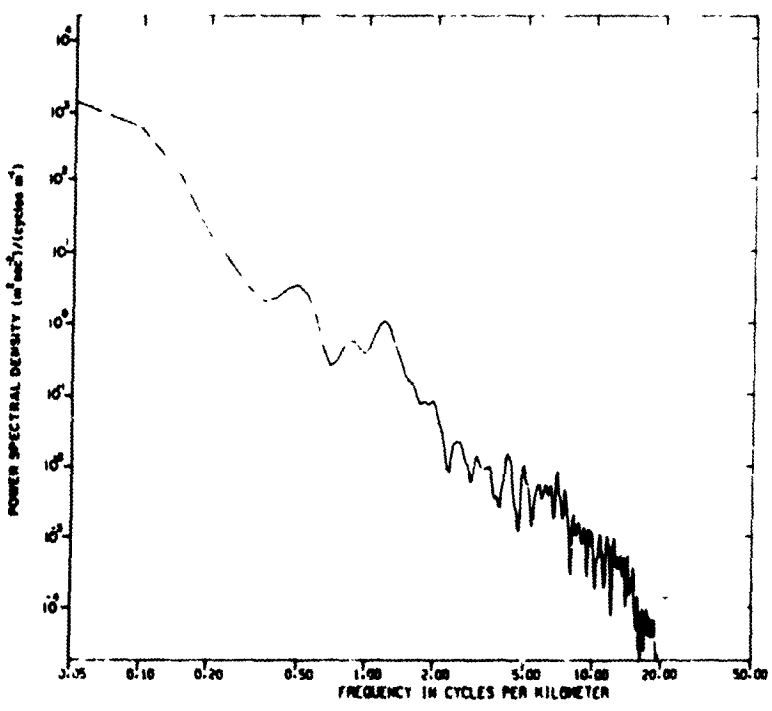

FIG. 11 – (f) At 0930 GMT

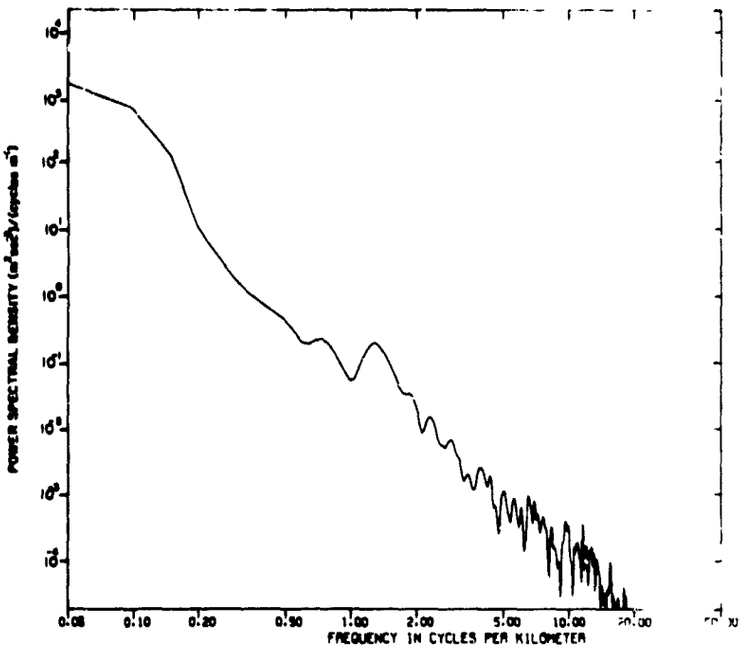

FIG. 11 – (g) Mean speed profile

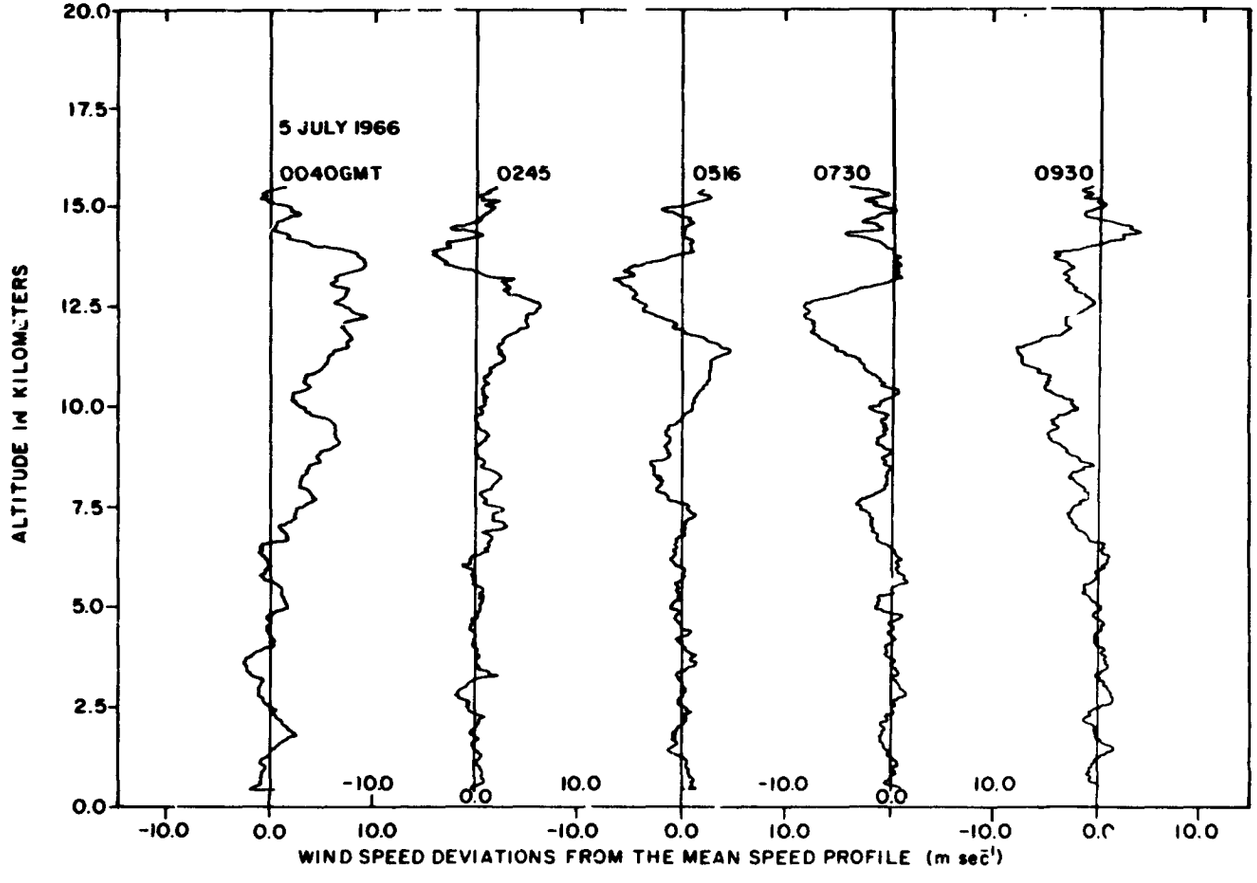

FIG. 12 DEVIATIONS OF INDIVIDUAL WIND SPEED PROFILES FROM THE MEAN PROFILE, JULY 5, 1966

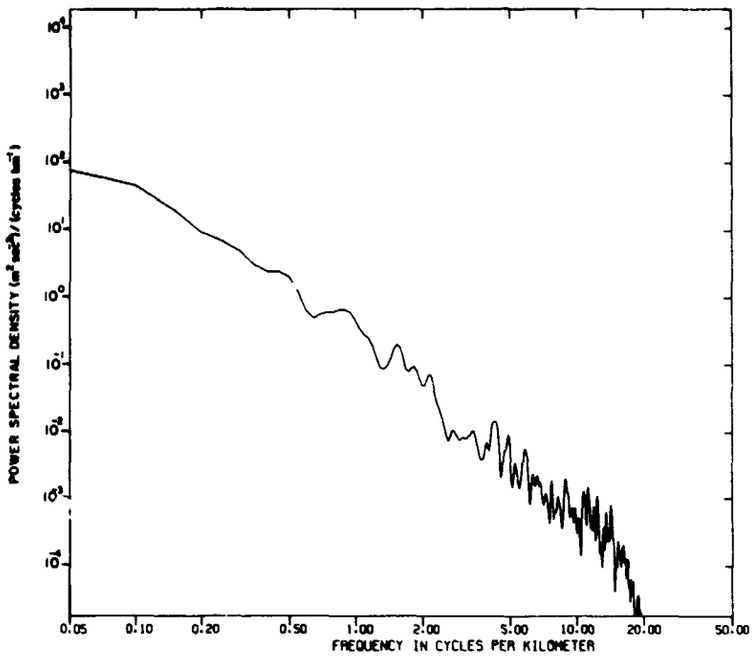

FIG. 13 SPECTRA OF THE PROFILES OF DEVIATIONS FROM THE MEAN SHOWN IN FIG. 12 (a) At 0040 GMT

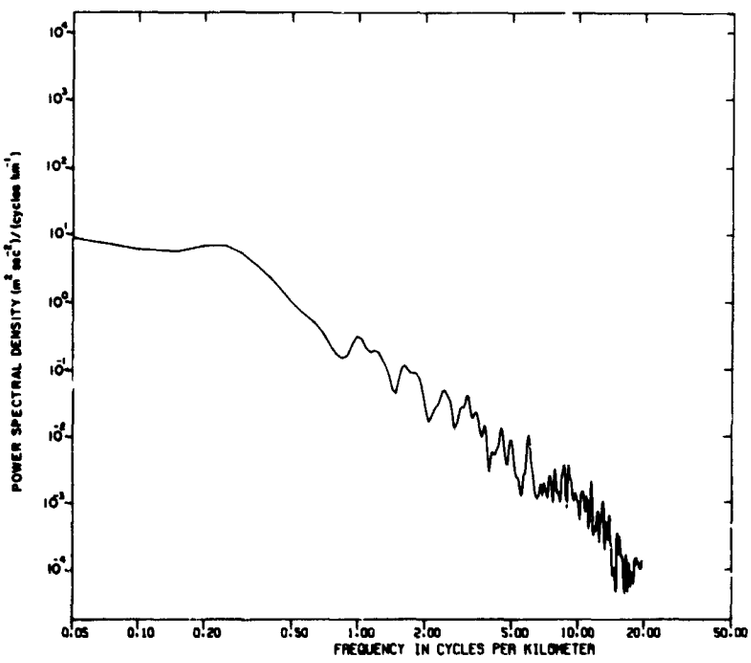

FIG. 13 – (b) At 0245 GMT

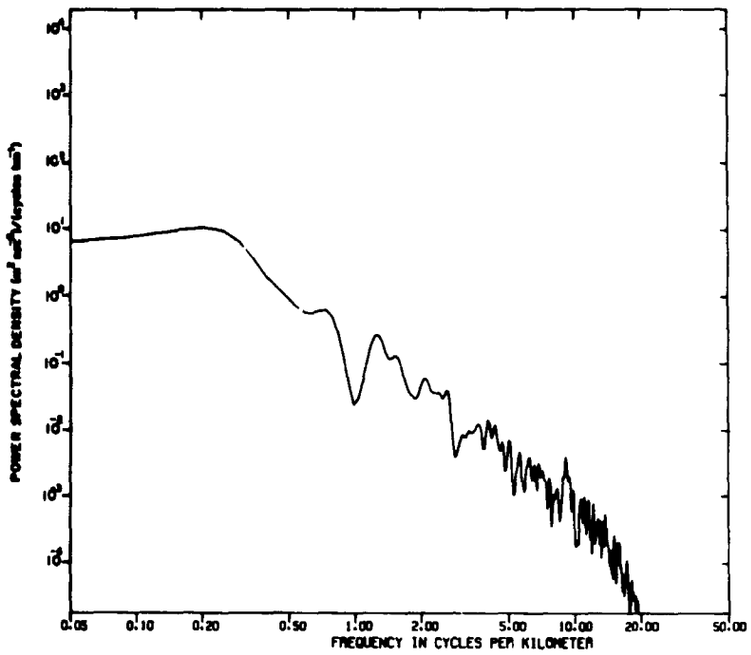

FIG. 13 – (c) At 0516 GMT

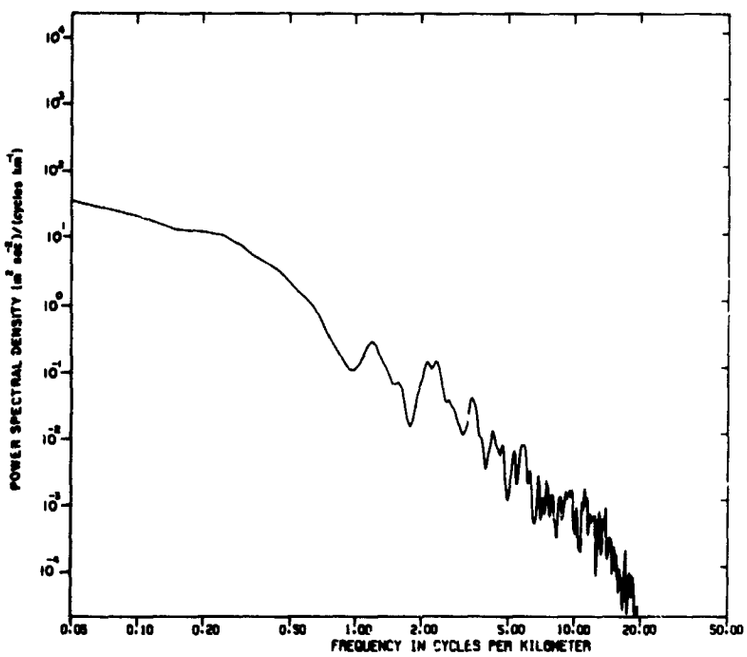

FIG. 13 – (d) At 0730 GMT

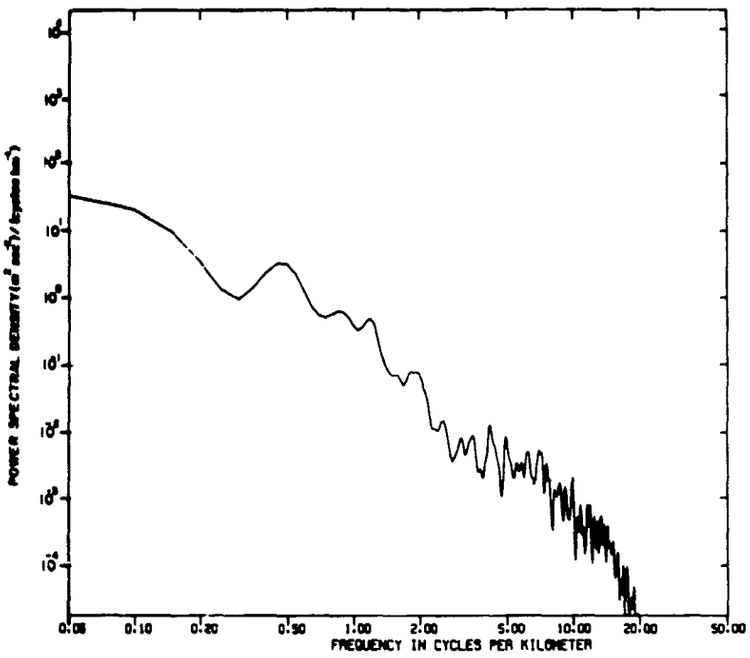

FIG. 13 – (e) At 0930 GMT

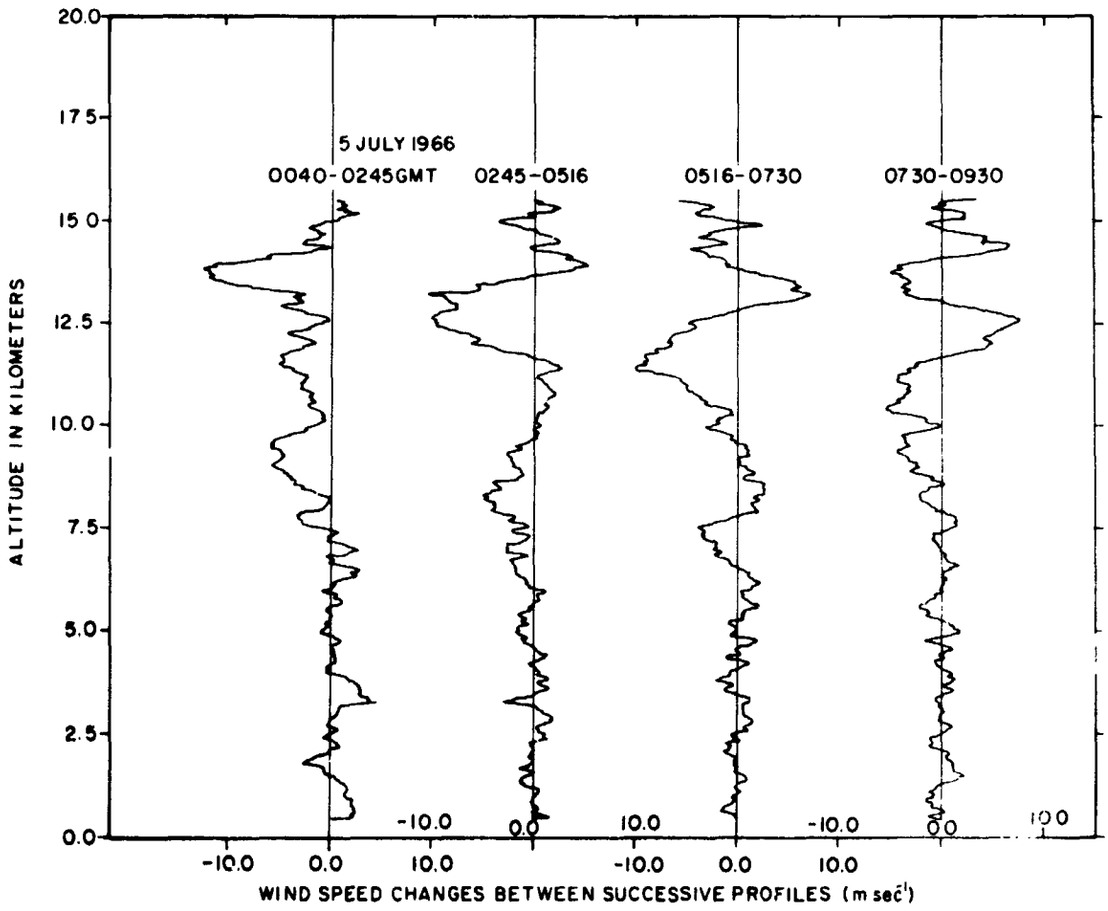

FIG. 14 SPEED CHANGES BETWEEN SUCCESSIVE VERTICAL PROFILES, JULY 5, 1966

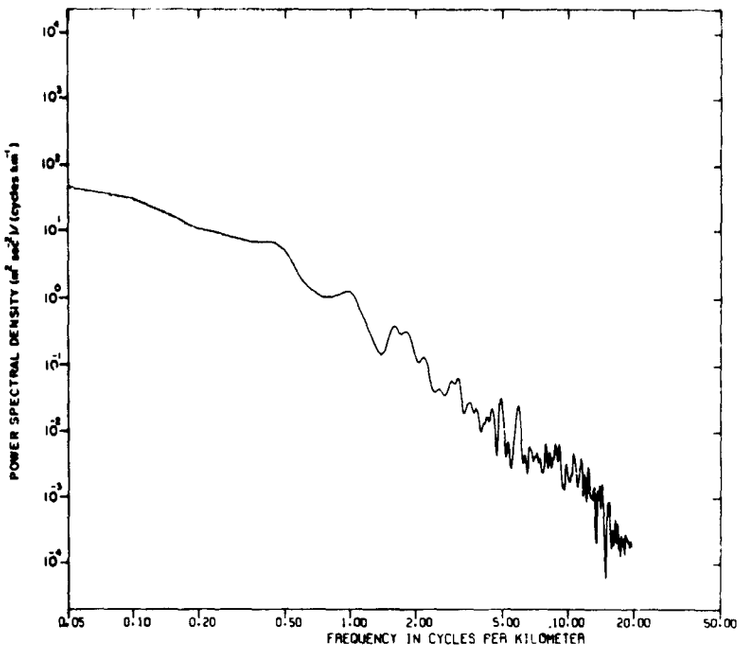

FIG. 15 SPECTRA OF THE SPEED CHANGE PROFILES OF FIG. 14 (a) From 0040 to 0245 GMT

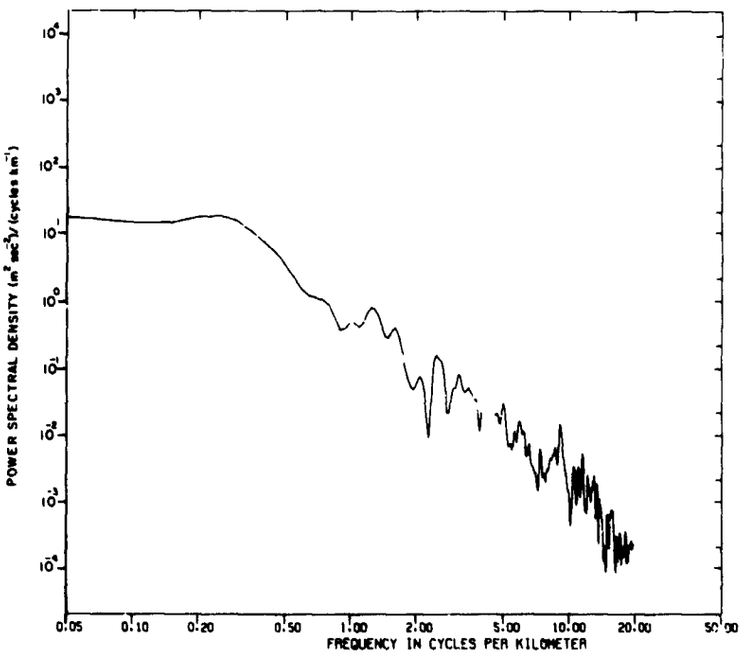

FIG. 15 – (b) From 0245 to 0516 GMT

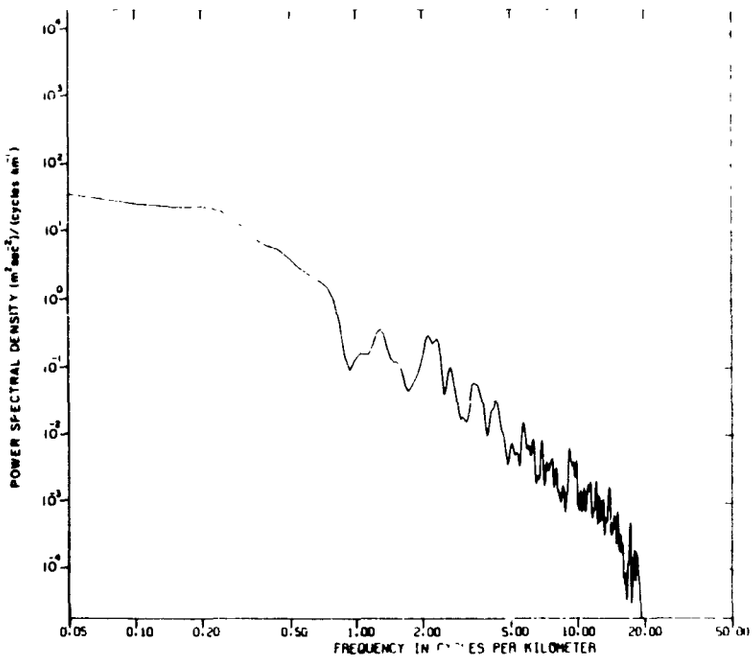

FIG. 15 – (c) From 0516 to 0730 GMT

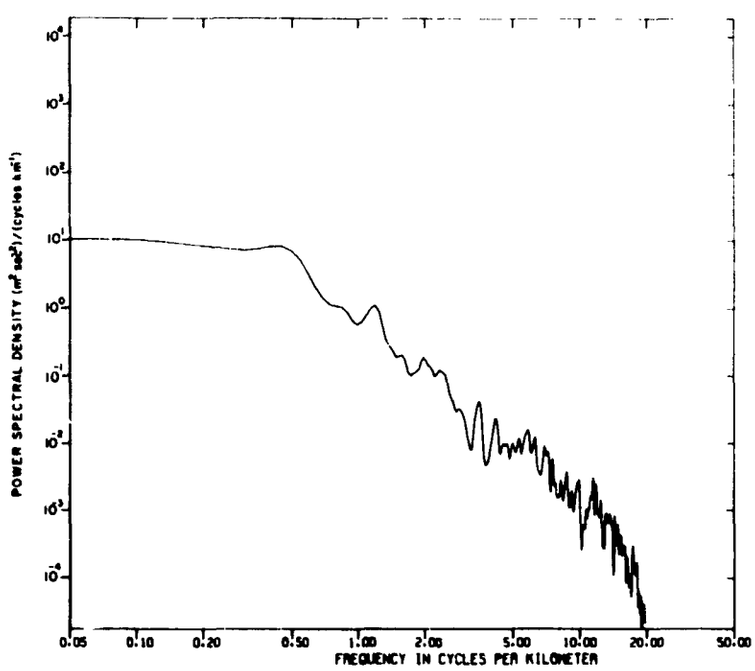

FIG. 15 – (d) From 0730 to 0930 GMT

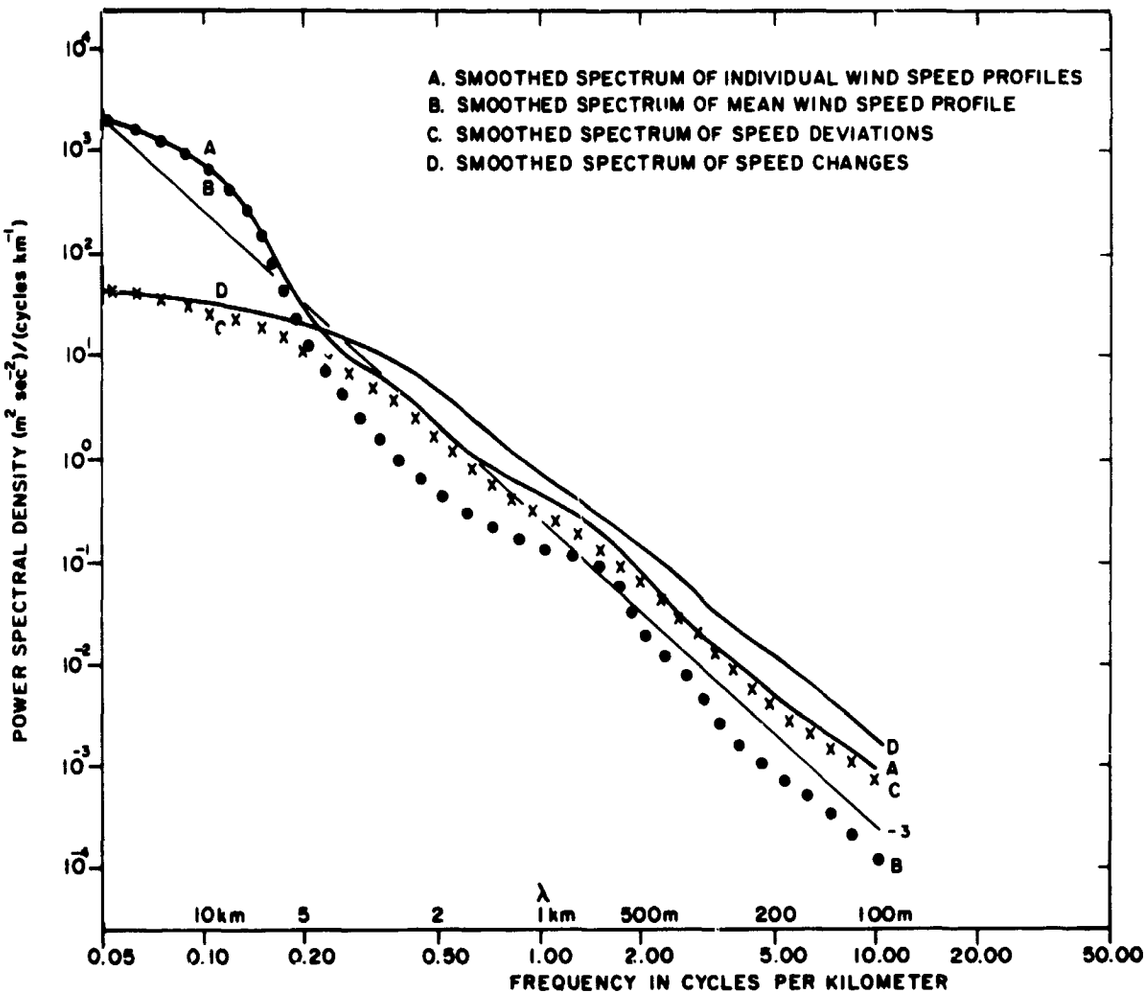

FIG. 16 SUMMARY OF SPECTRA OF WIND SPEED PROFILES ON JULY 5, 1966

F. Wind Speed Profiles on 10 November 1965

On this day, Cape Kennedy was under the influence of a flat surface pressure gradient with no active weather systems over Florida, and winds aloft were of moderate speeds from the west. Detailed wind profiles were measured at 1515, 1630, 1900, and 2130 GMT. Other profiles, measured at 1745 and 2245, terminated prematurely in the troposphere and are therefore not included in the discussion that follows.

The shapes of the four speed profiles designed a to d in Fig. 17 are quite complex, particularly in the upper portions. This is also true of the average profile (curve e in Fig. 17). The spectra of the individual profiles generally conform well to the -3 line, which is plotted identically on Figs. 18(a-d). The spectrum of the mean profile [Fig. 18(e)] falls below the -3 line at higher frequencies, as in the April and July cases. Evidently the jagged nature of the profiles of Fig. 17 does not imply any preferred mesoscale structure, since the spectra do not have pronounced maxima or minima.

The deviations of individual speed profiles from the mean are shown in Fig. 19. These deviation profiles are similar in appearance to those of Figs. 5 and 12. For the most part, resemblances between successive deviations are not very great. Their spectra are given in Fig. 20(a-d), and may be compared with Figs. 6 and 13. The spectra of Fig. 20 all have nearly the same general shape.

The changes in speed between successive profiles are shown in Fig. 21. For the first change profile the time interval is an hour and 15 minutes, while for the latter two profiles it is twice as long. Changes are smallest below an altitude of 5 km. It is difficult to discern any particularly consistent features in these change profiles. Their spectra are shown in Fig. 22(a-c). Figure 22 (a) has a pronounced peak at a frequency of approximately 0.4 cycles km^{-1}, while the other two spectra flatten at about this point.

The spectra of this sequence are summarized in Fig. 23 in a manner analogous to Figs. 9 and 16. The crossing points between curves A and D, and also between B and C, are at a wavelength of approximately 1 km.

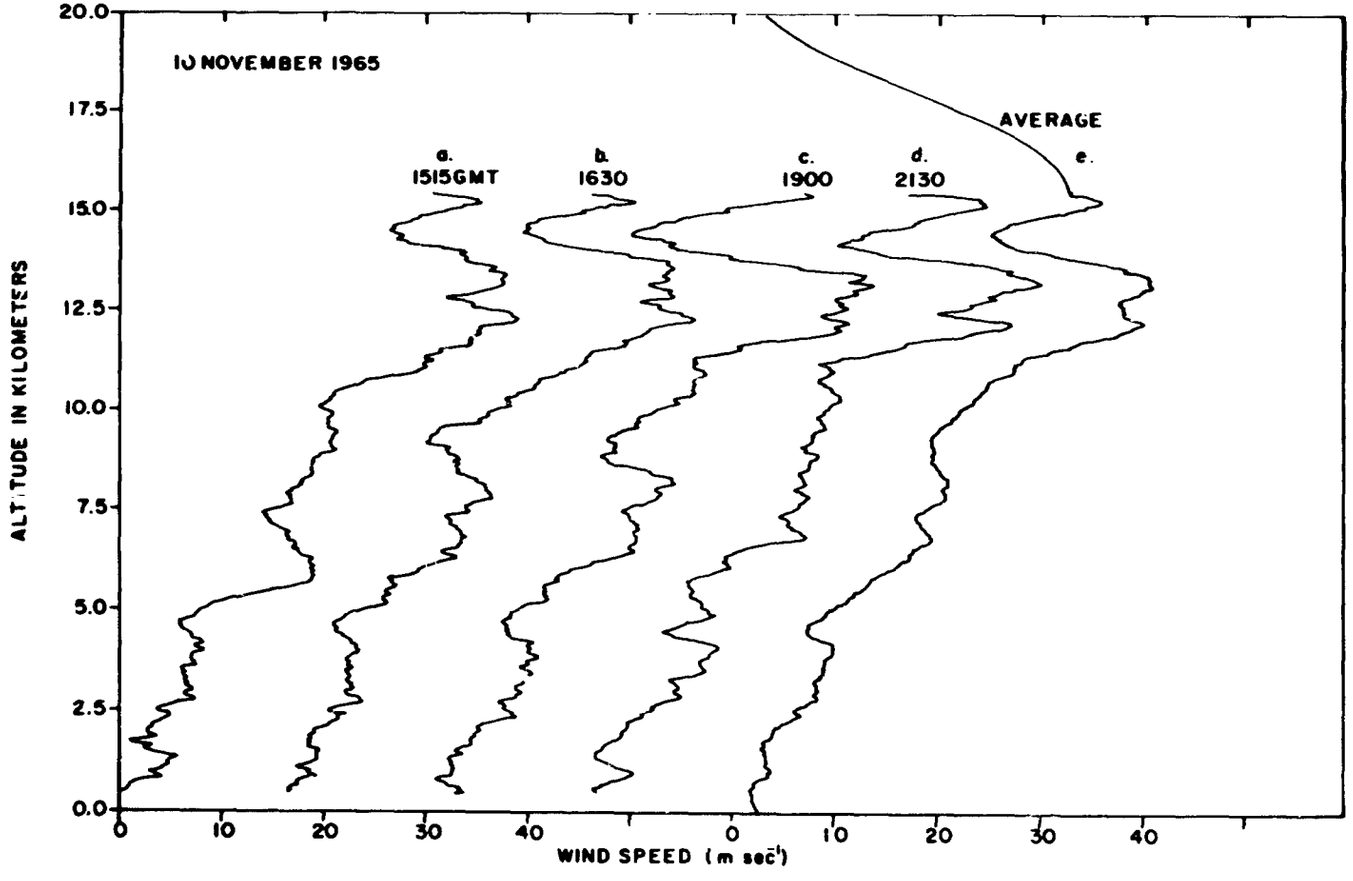

FIG. 17 WIND SPEED PROFILES MEASURED AT CAPE KENNEDY, FLORIDA BY THE FPS-16 JIMSPHERE TECHNIQUE ON NOVEMBER 10, 1965

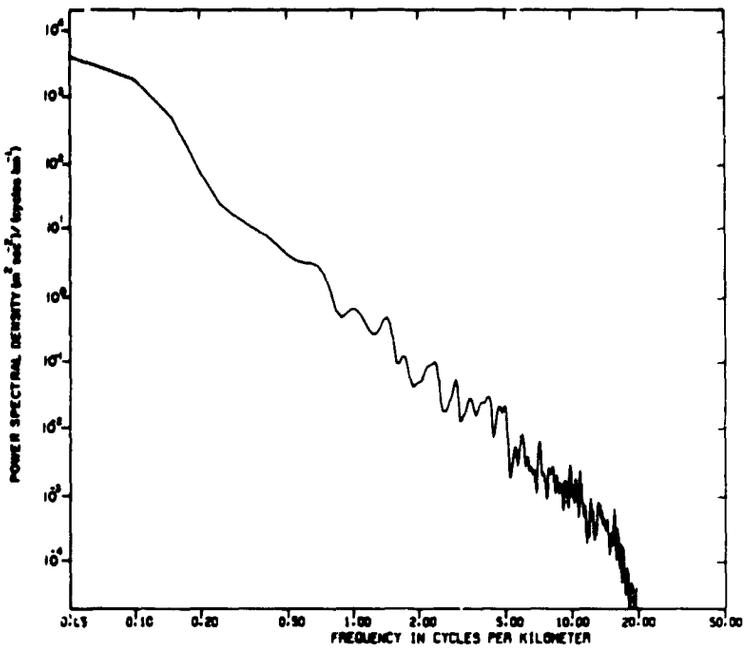

FIG. 18 SPECTRUM OF WIND SPEED PROFILES OF FIG. 17
(a) At 1515 GMT

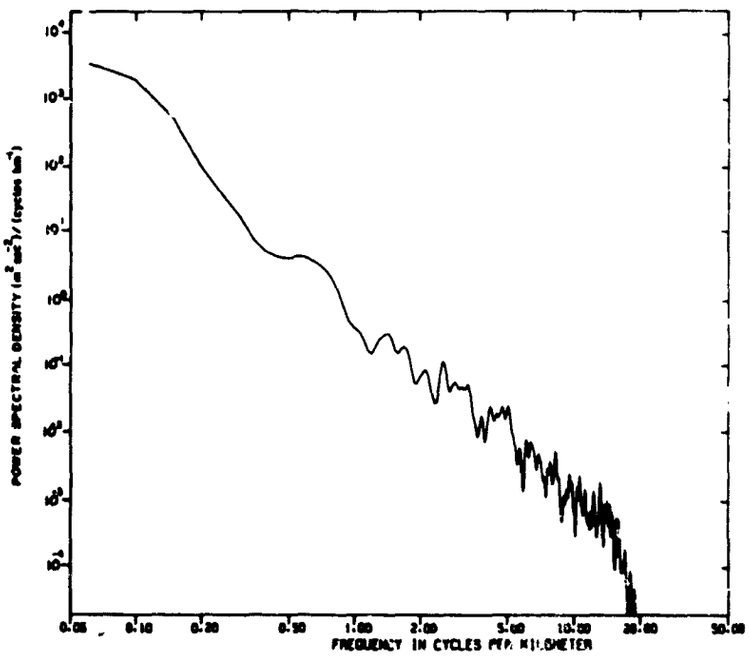

FIG. 18 – (b) At 1630 GMT

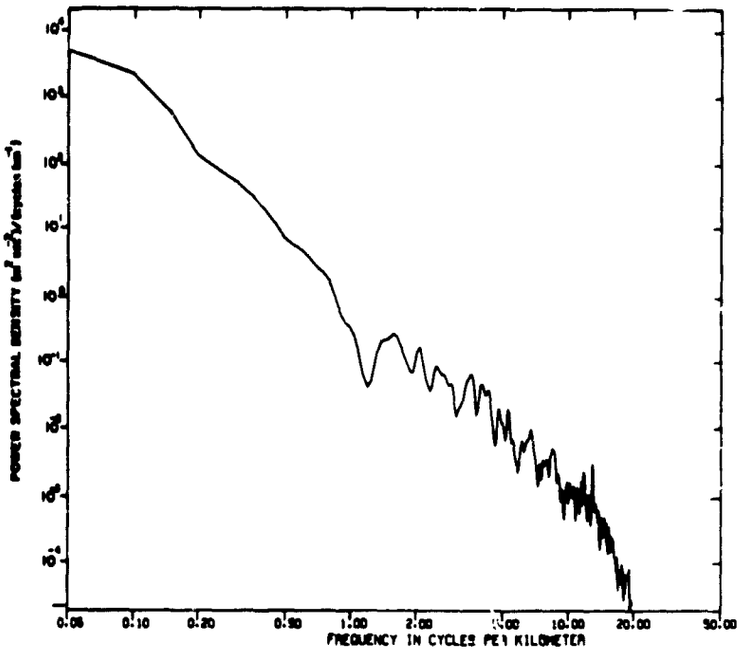

FIG. 18 – (c) At 1900 GMT

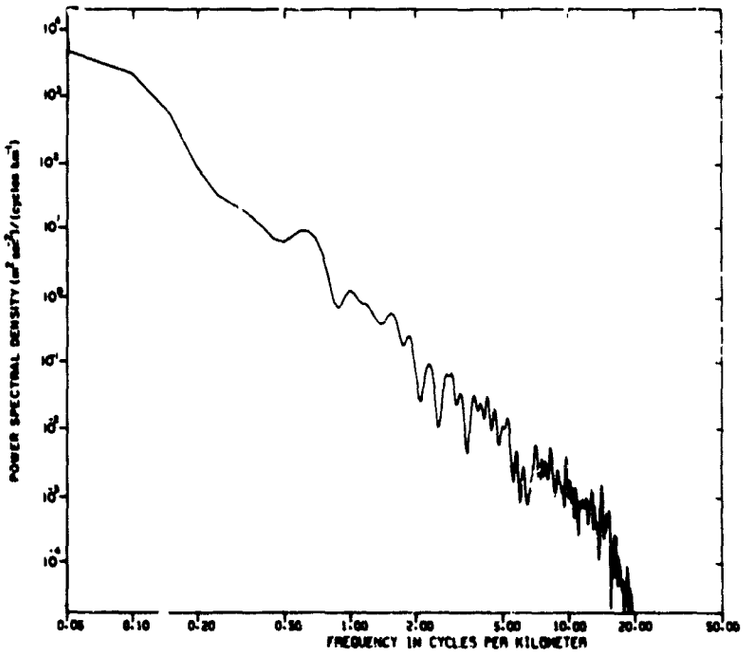

FIG. 18 – (d) At 2130 GMT

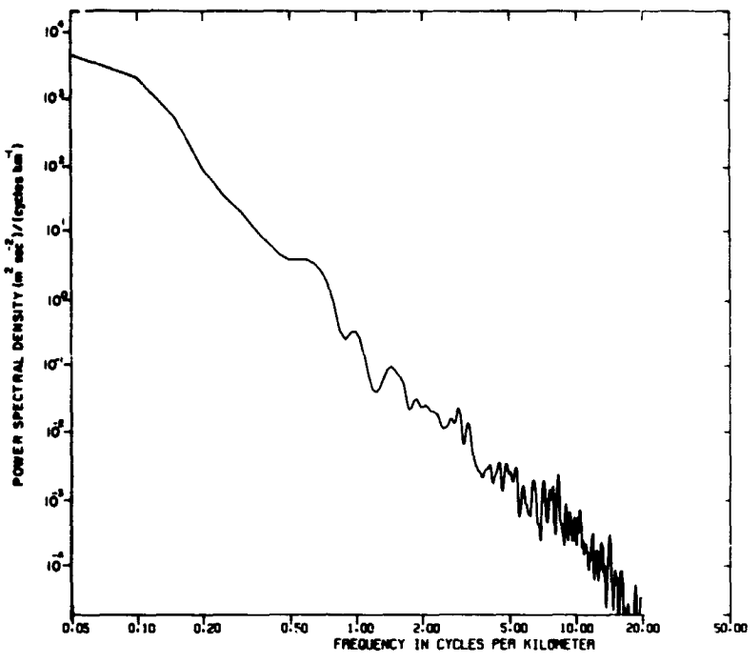

FIG. 18 – (e) Mean speed profile

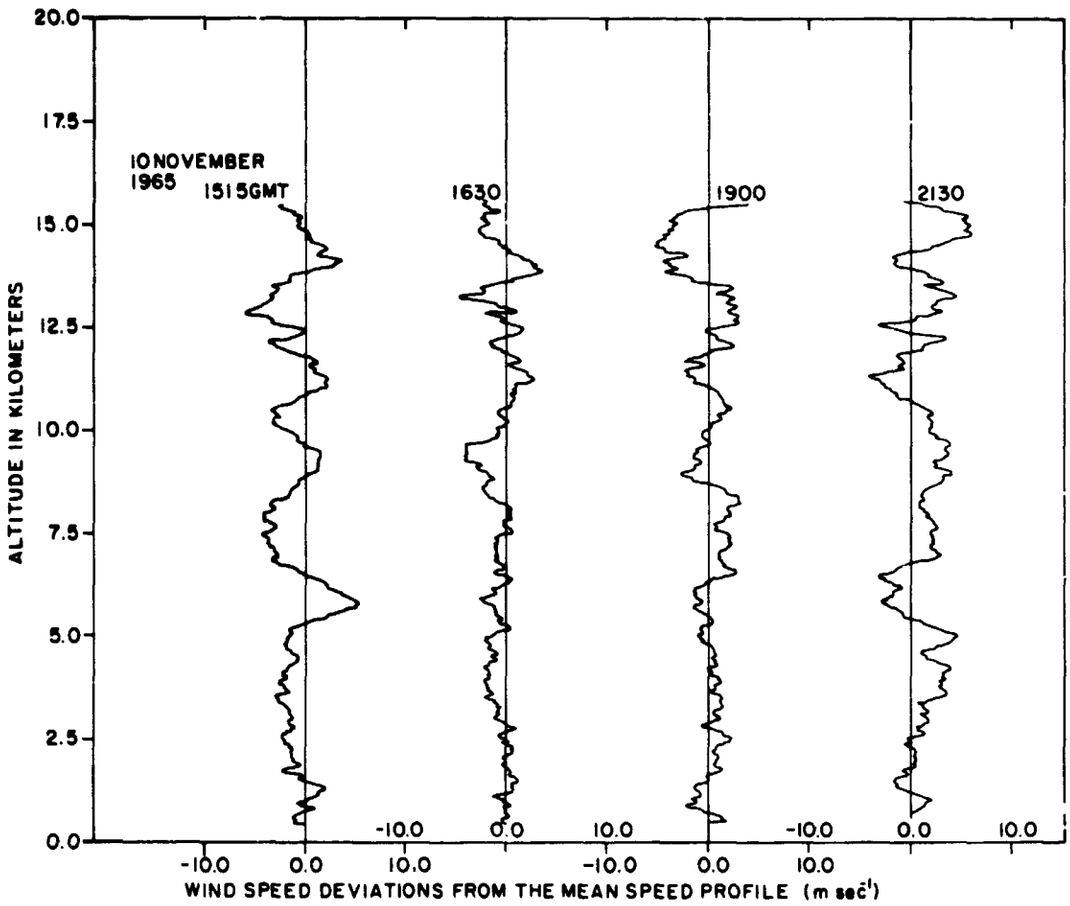

FIG. 19 DEVIATIONS OF INDIVIDUAL WIND SPEED PROFILES FROM THE MEAN PROFILE, NOVEMBER 10, 1965

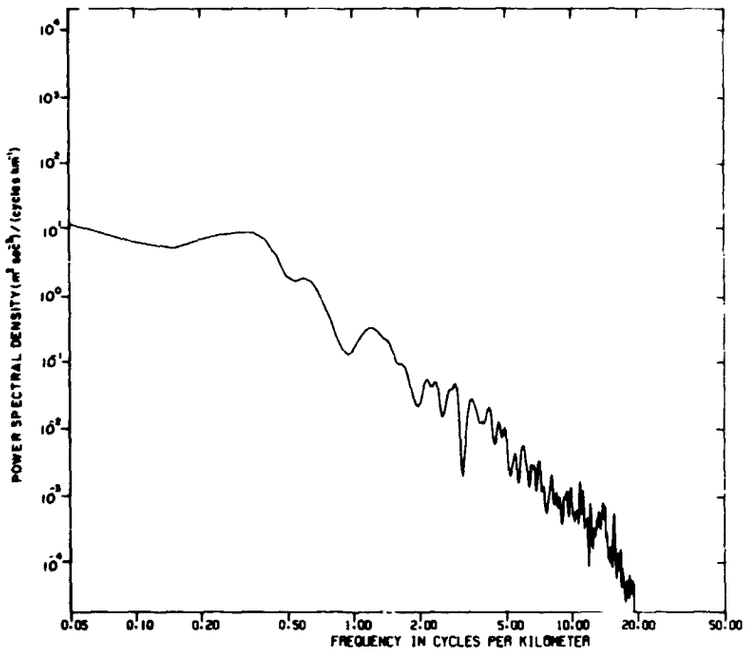

FIG. 20 SPECTRA OF THE PROFILES OF DEVIATIONS FROM THE MEAN SHOWN IN FIG. 19 (a) At 1515 GMT

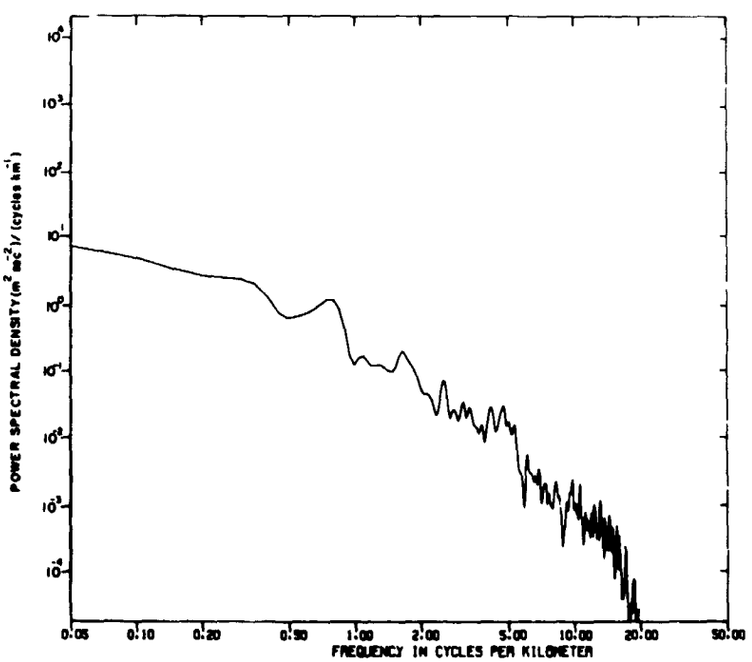

FIG. 20 – (b) At 1630 GMT

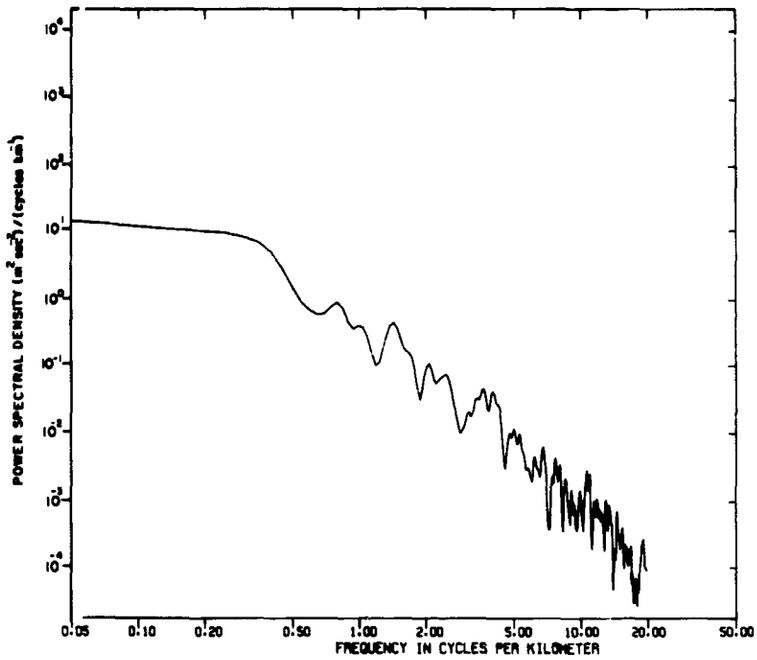

FIG. 20 – (c) At 1900 GMT

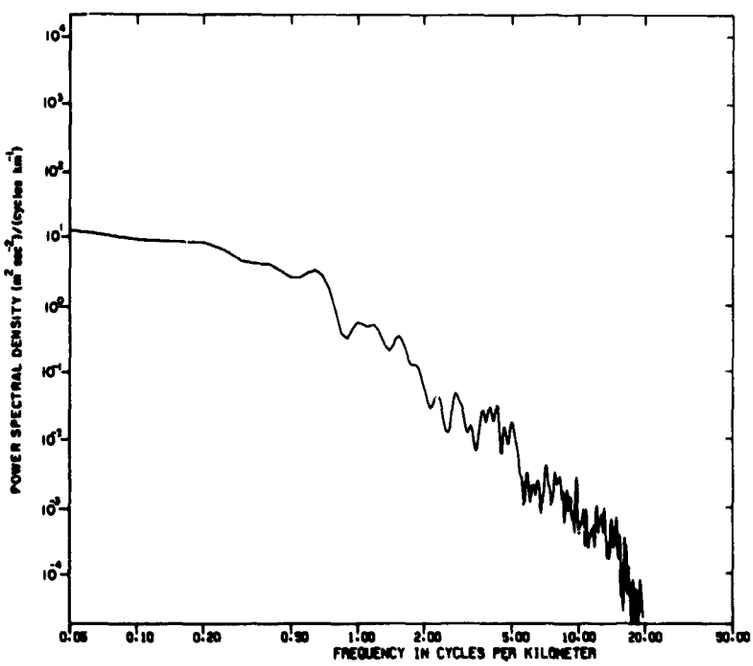

FIG. 20 – (d) At 2130 GMT

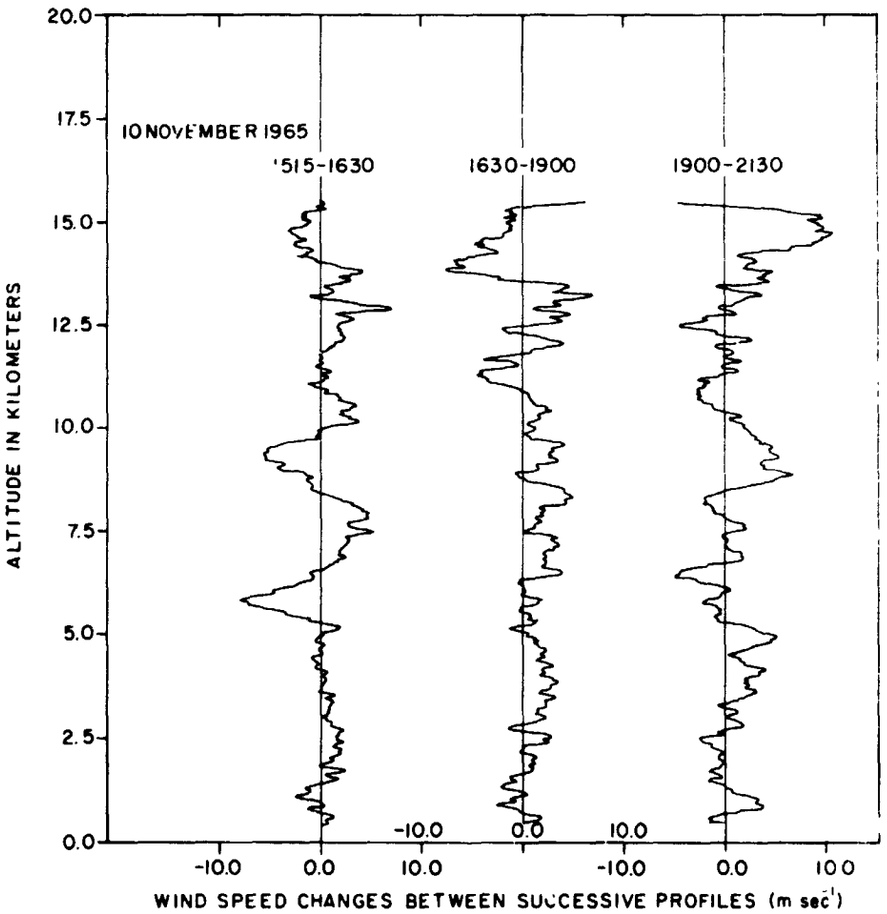

FIG. 21 SPEED CHANGES BETWEEN SUCCESSIVE VERTICAL PROFILES, NOVEMBER 10, 1965

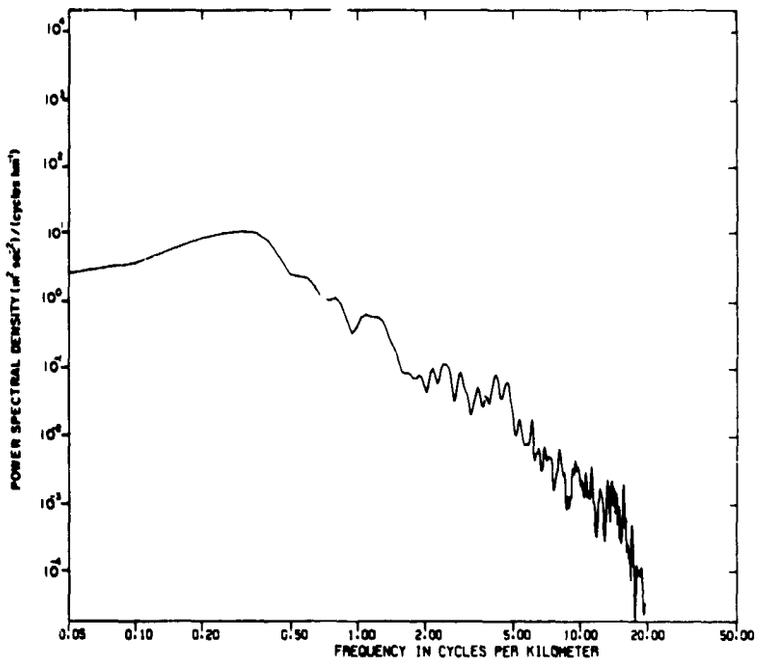

FIG. 22 SPECTRA OF THE SPEED CHANGE PROFILES OF FIG. 21 (a) From 1515 to 1630 GMT

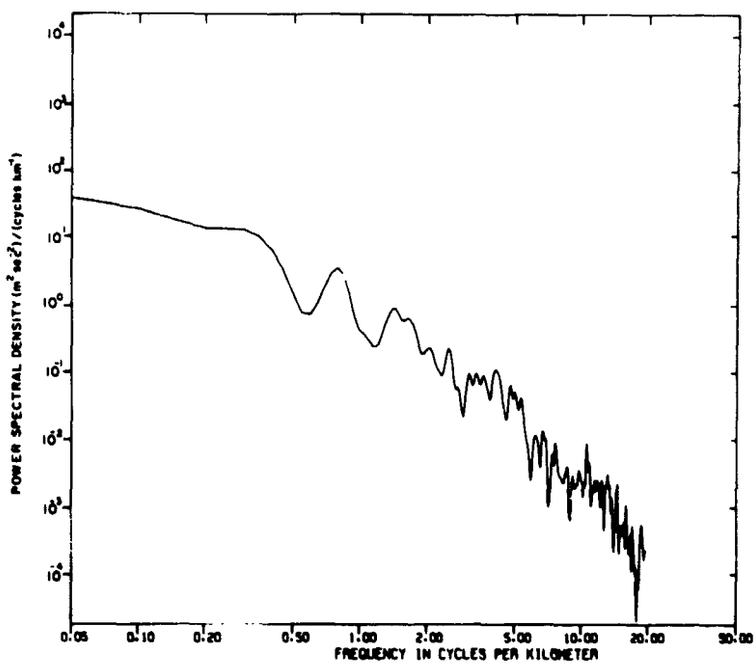

FIG. 22 – (b) From 1630 to 1900 GMT

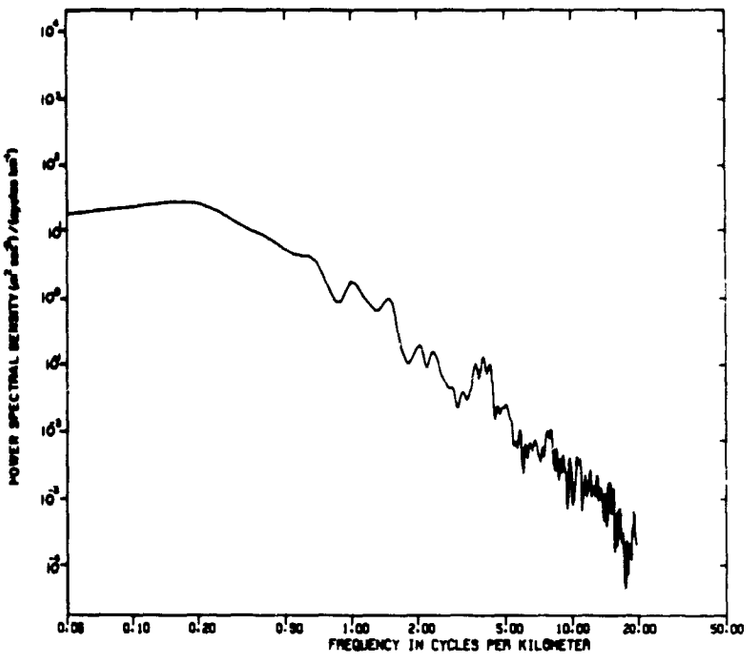

FIG. 22 – (c) From 1900 to 2130 GMT

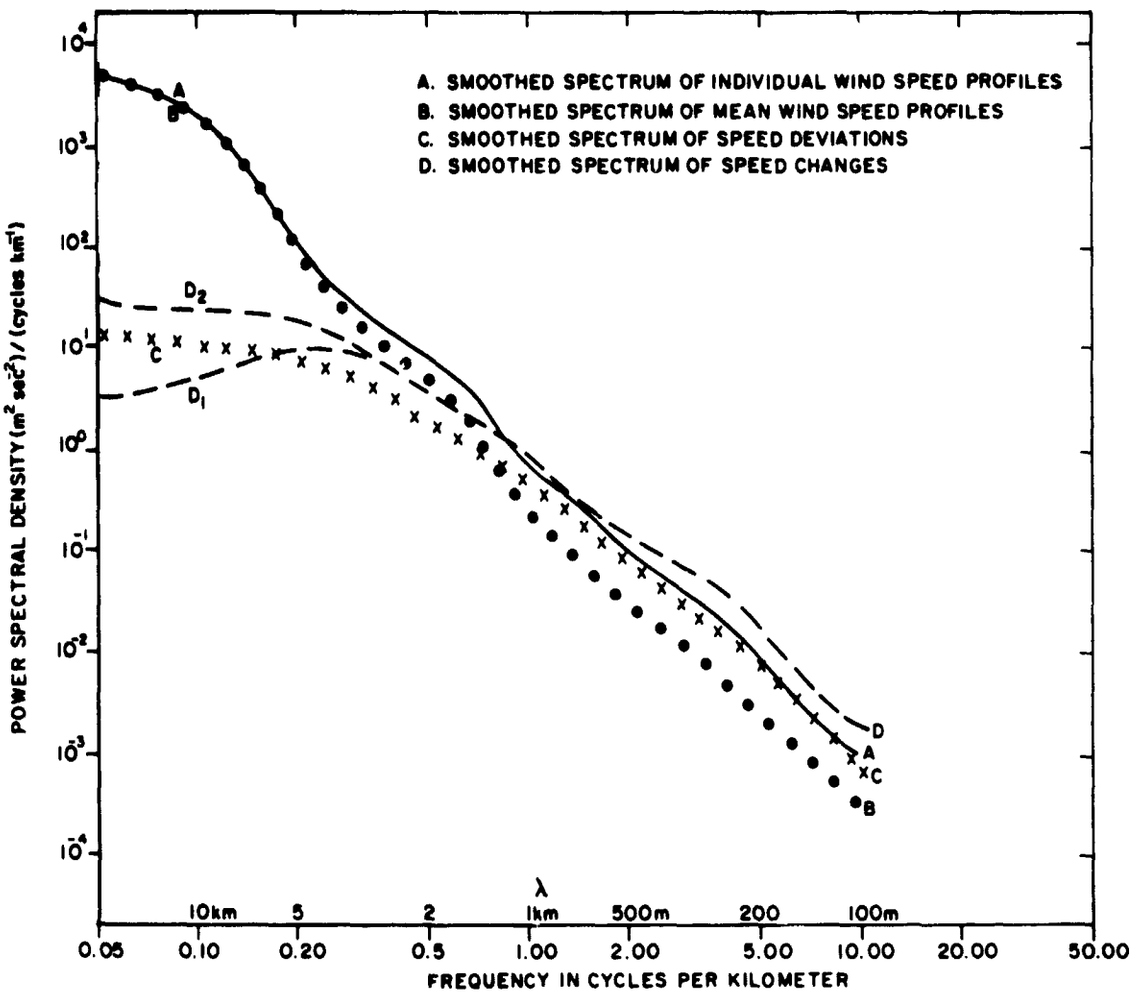

FIG. 23 SUMMARY OF SPECTRA OF WIND SPEED PROFILES ON NOVEMBER 10, 1965

G. Discussion

The properties of the spectra for the three different cases, encompassing strong winds of 8 April 1966, weak winds on 5 July 1966, and moderate winds on 10 November 1965, are summarized in Fig. 24. In Fig. 24(a), the three smoothed spectra of individual profiles have generally similar shapes. The major difference among them is that the power is greater at low frequencies in proportion to the average wind speed of the profile. The minor relative gap in the April spectrum between frequencies of 0.2 and 1.0 cycle km^{-1} may be typical of strong winds but does not appear in the other two cases. In this portion of the spectrum, the jagged profiles of 10 November have the greatest energy. There are apparently no predominant sizes to the speed variations along the vertical, and thus certain terminology, such as mesoscale in reference to vertical variations of 1-3 km extent, should not be understood to imply that this scale is a preferred or typical one. Instead, all scales are mixed in together, with rapidly decreasing energy as frequency increases. An envelope of the three spectrum curves is also shown; spectra for most meteorological situations would probably lie below it.

The smoothed spectra of the mean wind speed profiles for April, July, and November are shown together in Fig. 24(b). The -3 line is placed in the same position as in Fig. 24(a) as a cross reference. The curves of Fig. 24(b) are similar to those of Fig. 24(a) but have less energy at frequencies above approximately 0.3 cycles km^{-1}. An approximate envelope is also shown; this may be taken to represent quasi-steady or averaged vertical profiles.

The smoothed spectra of the deviations from average profiles for the three cases are shown together in Fig. 24(c). They are remarkably similar at frequencies above approximately 0.2 cycles km^{-1}. At the low-frequency end it is somewhat surprising that the case of weakest winds (July) has the largest energy. All deviations of these cases are within five hours of the time of the mean profiles. The individual curves indicate a tendency for increasing power at low frequencies with increasing time interval from the time of the mean profile. An envelope spectrum for the three cases is also given.

The smoothed spectra of speed changes between successive profiles are plotted together in Fig. 24(d). They are very similar at frequencies above approximately 0.5 cycles km^{-1}. At low frequencies, the July case has the greatest power, as in Fig. 24(c). The curves are also labeled with a 1 or 2, to denote whether the time change is approximately over one or two hours. Those labeled 2 clearly have greater variance at low frequencies. If the time interval were longer than two hours, probably the left end of the spectra would gradually rise. An envelope for changes over intervals of two hours or less is shown. It lies somewhat above the envelope of deviations [Fig. 24(c)] at all frequencies higher than approximately 0.1 cycle km^{-1}. To summarize Fig. 24, we note that the general characteristics of each type of spectrum (for measured wind speed profiles, deviations, and changes) are apparently not very dependent on season or synoptic situation.

From Fig. 24, it can be seen that at the higher-frequency end of the spectra, power is approximately proportional to frequency to the -2.5 power, i.e., $E(f) \propto f^{-k}$, where k = 2.5. Tatarski (1961) shows that the structure function

$$D(L) = \overline{(S_1 - S_2)^2} \propto L^{k-1}$$

where S_1 and S_2 are wind speeds separated by the distance L. Therefore, for the mean-squared wind shear we divide D(L) by L^2, thus

$$\overline{SH^2} \propto L^{k-3}$$

This relationship provides a means of relating microscale wind shears to those over larger distances. For the Cape Kennedy data, vector shear magnitudes were computed over two intervals to check this relationship. The two intervals chosen were 25 m and 1 km. All data below 12 km from approximately 250 Jimsphere profiles (January through July 1966) were included. It was found that the mean-squared shears over the two intervals were proportional to $L^{-0.5}$. For our value of k = -2.5, this shows excellent agreement with Tatarski. No seasonal variation

in the exponent of L was noted. It appears that microscale shears for any value of L between 25 m and 1 km are related by

$$\overline{SH_1^2}/\overline{SH_2^2} = (L_2/L_1)^{1/2}$$

As mentioned in the Introduction, it is interesting to compare the spectra of vertical wind speed profiles to spectra of winds measured by aircraft in flying horizontally across jet streams. In the latter case the speed profiles in a south to north direction perpendicular to a westerly jet are similar in shape to the profiles of Fig. 3, except that the total horizontal distance is in the range from 500 to 1000 km. Kao and Woods (1964) have computed spectra from Project Jet Stream flights across strong jet streams (the average speed of the profiles was 62 m sec^{-1}). Their spectra are for mesoscale deviations from a smoothed horizontal profile. Comparing their spectra and those of Fig. 24(a) shows that there is approximately the same power spectral density at a horizontal wavelength of 100 km and vertical wavelength of 5 km. Similarly, power is approximately equal at 40 km and 2.5 km horizontal and vertical wavelengths. The range of mesoscale wavelengths having this property of equal power is shown in Fig. 25. Differences between the computational methods of Kao and Woods and ours may affect the diagram somewhat, but it is believed to be approximately correct. This comparison may have some application in selecting vertical and horizontal eddy exchange coefficients in detailed numerical prediction models. As a final comment we note that for cases of moderate or greater clear-air turbulence, Pinus (1963) shows that the power in horizontal mesoscale wind variations is more than an order of magnitude larger than that given by Kao and Woods (which were for cases of predominantly smooth flight). It seems doubtful that the high energy levels of clear-air turbulence can be attributed to transfer of energy from relatively long, vertical or horizontal waves that have greater power. Therefore, we consider the present analysis consistent with the concept that the energy input to clear-air turbulence probably arises from unstable shear-gravity waves (produced either by internal flow patterns or obstacles such as mountains) and not from large-scale variations in the wind field.

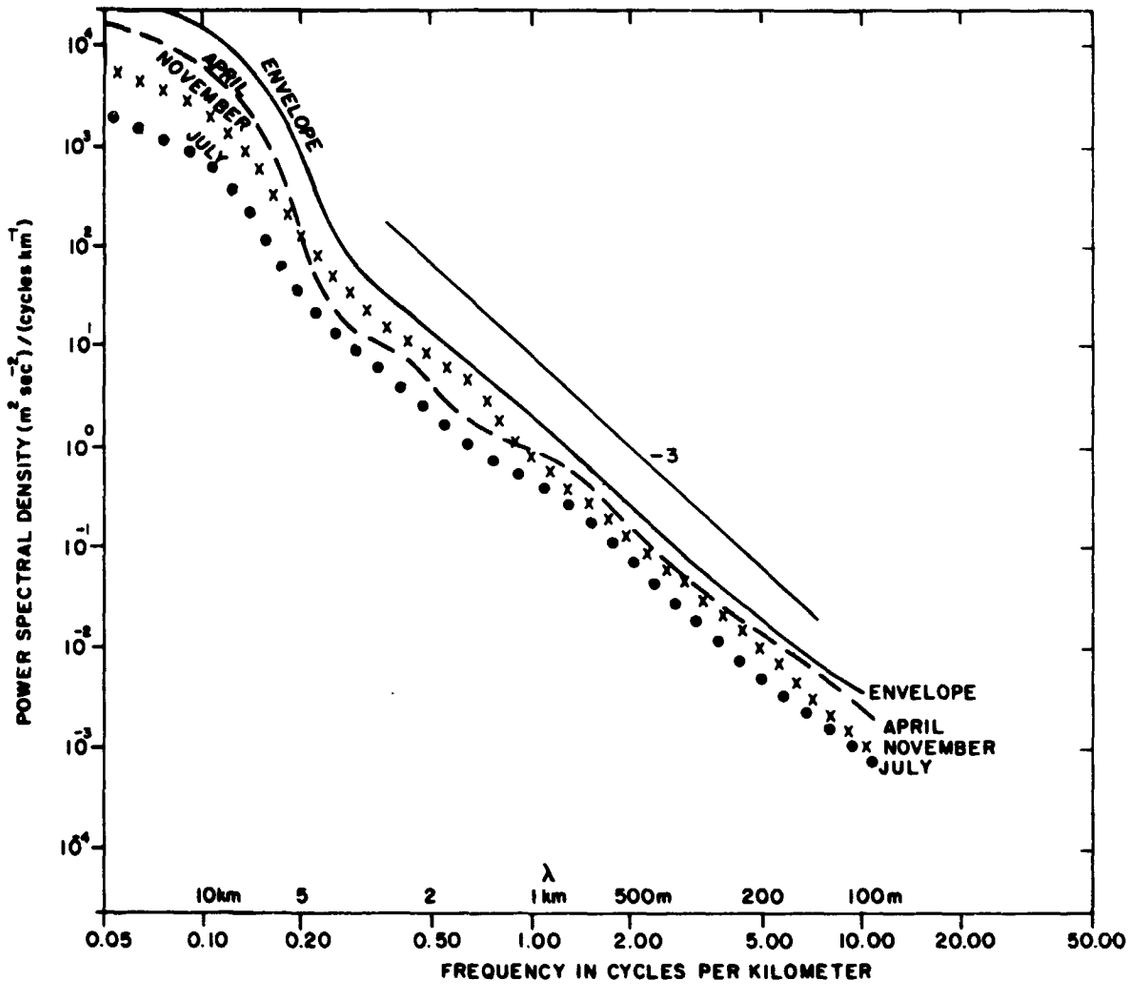

FIG. 24 SMOOTHED SPECTRA FOR THE SEQUENCES OF WIND PROFILES ON APRIL 8, 1966, JULY 5, 1966 AND NOVEMBER 10, 1965
(a) Spectra of individual speed profiles

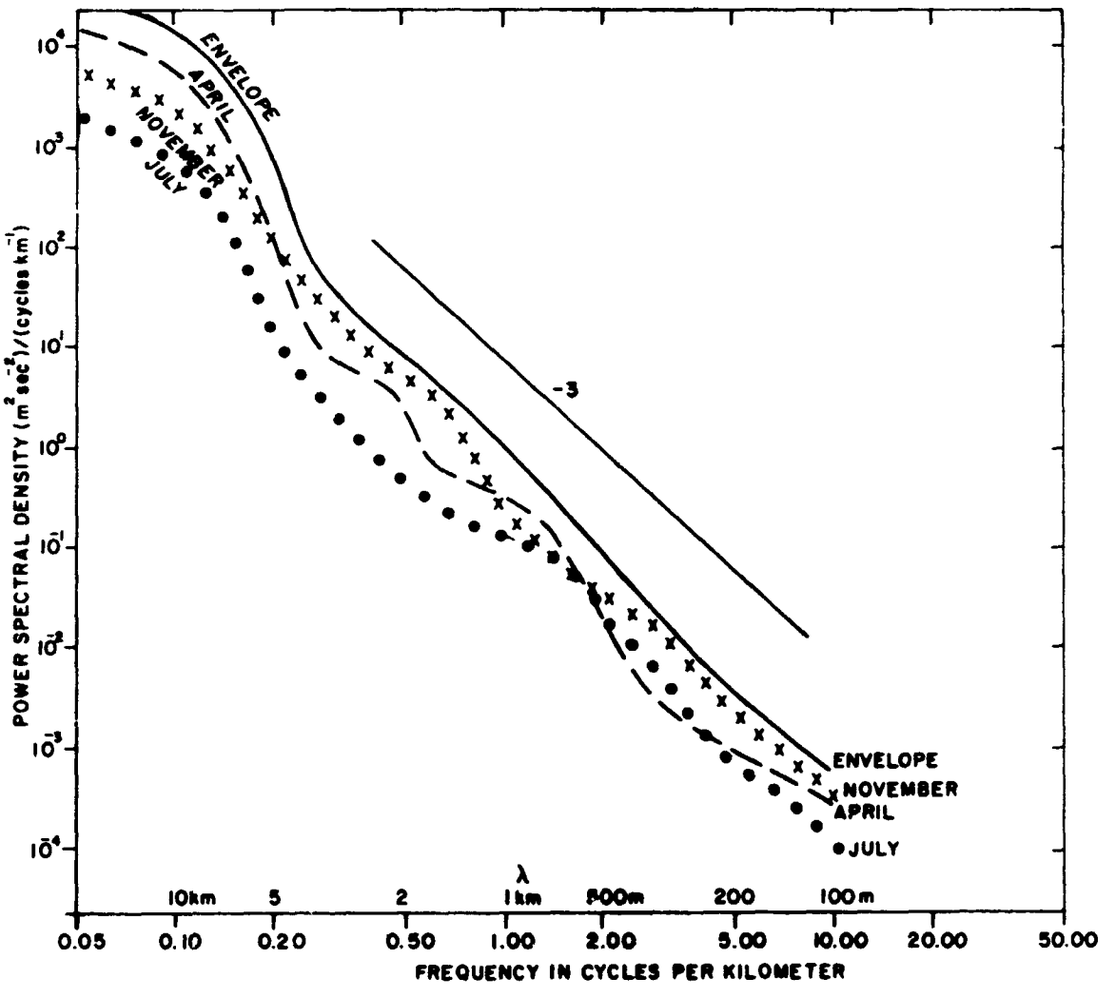

FIG. 24 – (b) Spectra of mean wind profiles

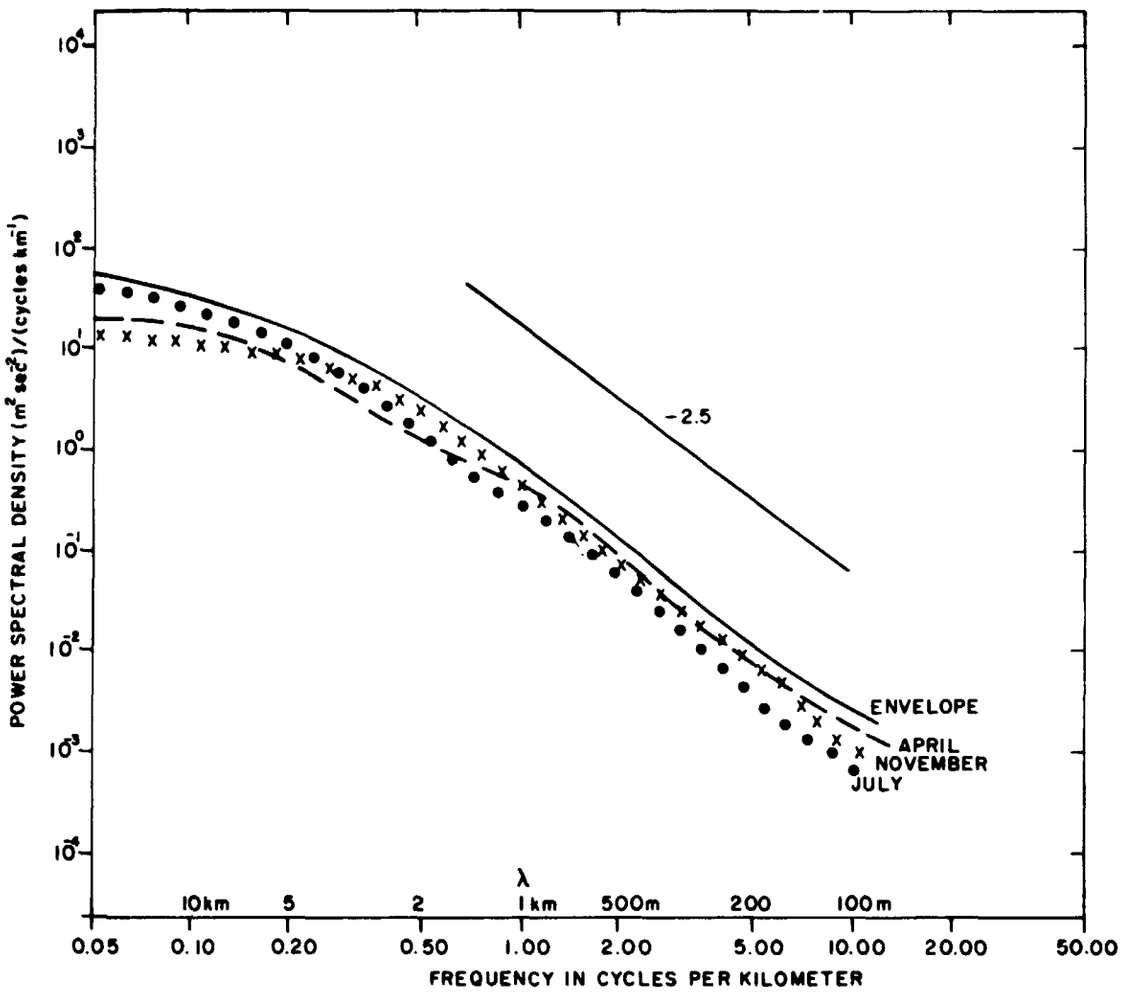

FIG. 24 – (c) Spectra of deviations from mean profiles

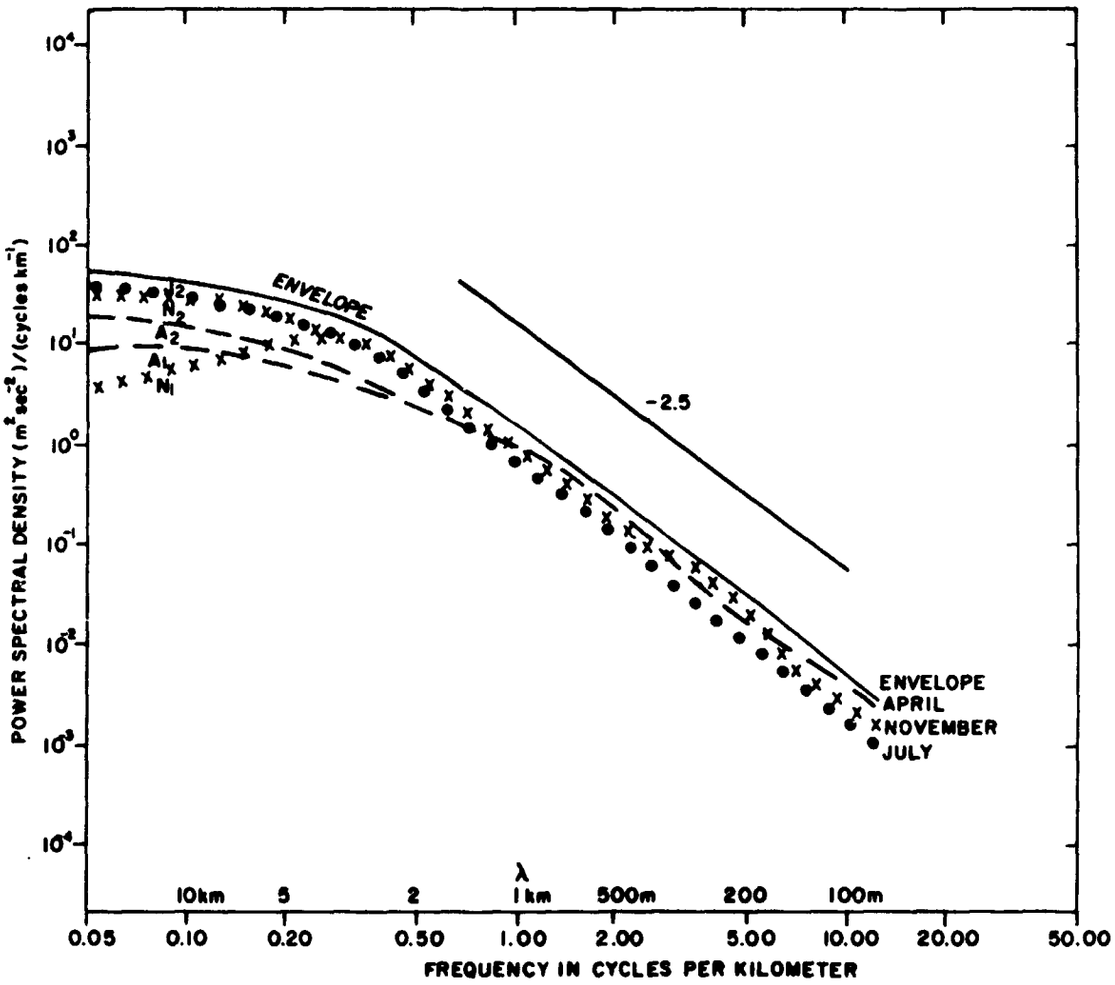

FIG. 24 – (d) Spectra of speed changes

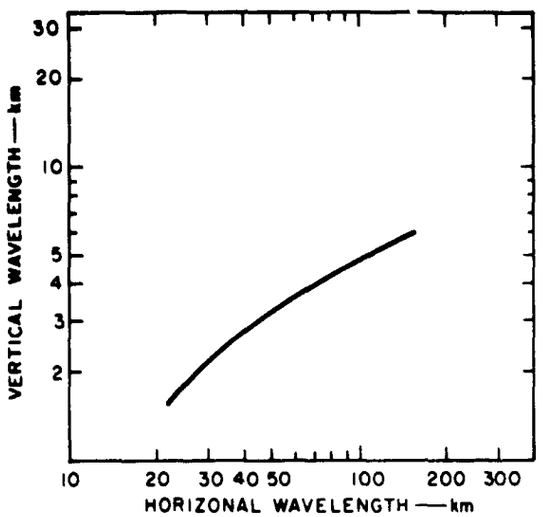

FIG. 25 COMPARISON OF VERTICAL AND HORIZONTAL EDDY SCALES THAT HAVE THE SAME POWER SPECTRAL DENSITY IN THE MESOSCALE REGION

H. Forecasting Implications

Since the profile sequences discussed above were selected without preconceptions, it is reasonable to expect that their characteristics are rather typical. An important result of the analysis is that the spectra do not show any preferred frequencies that correspond to the terminology large-scale, mesoscale, or microscale. Apparently there are no clear-cut, natural separations between different scales of motion. Instead, as far as spectrum shape is concerned, divisions between scales may be selected on an arbitrary basis. This statement applies to problems including both analysis and forecasting.

The present state of the art in forecasting winds in the free atmosphere for periods out to 24 hours in advance, as required by NASA, is limited by several factors. One of these is the sparsity of standard data in space and time. This sparsity limits the accuracy and detail that can be attained in analyses of meteorological conditions upstream from Cape Kennedy. These limitations of analyses are in turn a limitation on predictions. In part, the uncertainties can be lessened in the manner practiced at Cape Kennedy, which consists of monitoring the winds there using the FPS-16 Jimsphere system. However, the sequences of speed deviations and speed changes of this study show patterns with a large degree of variability which appears to be random, for practical purposes. Forecasting future changes or deviations (of the sort shown in previous sections) from those immediately past appears difficult. Further study of the extent to which this can be achieved should be carried out through study of the relationship between vertical air motions (deduced from the ascent rate of the balloon) and the horizontal speed maxima and minima. On the other hand, the spectra of deviations or changes appear to be quite consistent; i.e., there are no major shifts in the energy distribution in the cases studied.

For the immediate future, the writers suggest that the forecasting problem be considered as follows. The smoothed vertical profile, represented for example by average winds over 1- to 2-km layers, can be forecast by numerical methods for periods out to approximately 24 hours and can be used in planning. As the launch approaches (say within

four to six hours), the forecast smoothed vertical profile can be combined (using suitable weighting factors) with a smoothed profile computed from the recent FPS-16 Jimsphere wind profiles. Deviations from this latter profile which the vehicle will encounter will then be considered as noise having the spectrum of Fig. 24(c). Presumably, the vehicle is designed to compensate for or tolerate this noise. In the last hour or two before launch, the forecasting problem is evidently one of estimating whether significant departures from the smoothed measured profile are likely to occur, particularly at critical portions of the trajectory. This judgment could be made partly from a numerical forecast based on the most recent standard data, and also on any trends or other features that can be discerned from the FPS-16 Jimsphere profiles. The ability to make accurate judgments would probably be improved significantly if detailed rawinsonde data over Florida were available on these occasions from additional stations, and at an interval of the order of six hours or less. Also, data of greater density would insure that subsynoptic (or larger) phenomena would not arrive at Cape Kennedy from an upstream location without previous warning.

Further investigation of the material covered in this part of the report can be done by studying additional sequences of FPS-16 Jimsphere profiles in order to insure a representative coverage of weather patterns. Spectrum computations should be made separately for tropospheric and stratospheric portions of profiles, in order to determine whether differences in spectral content exist. The application of cross-spectrum analysis in studying the persistence of wind profiles and in showing momentum transports should also be carried out. Improvement of methods of making short range predictions of details in wind profiles can be undertaken through study of the three-dimensional characteristics of the small, but operationally significant, features. The FPS-16 Jimsphere data give, for the first time, the ability to relate vertical motions to the growth and decay of maxima and minima in speed profiles. In addition, a network of GMD-1 stations near Cape Kennedy, used as a launch approaches, could identify and track phenomena of operational importance, thus giving basic information for use in forecasting.

III NUMERICAL WIND FORECASTS

A space vehicle rising along its launch trajectory is affected by winds, as stated previously, but is little affected by variations in other meteorological features such as temperature, humidity, or pressure. Thus, winds are the meteorological factor of importance. On the other hand, numerical forecasting models that are presently in use place primary emphasis on predicting the heights of constant-pressure surfaces spaced 2-3 km apart in the vertical. Wind vectors are not treated directly; however, they can be computed from the slopes of the pressure surfaces. A disadvantage of this method is that such wind fields tend to be rather smooth in comparison to those directly analyzed by meteorologists from observed wind reports. The human analyst uses mental models and tends to emphasize small features of wind patterns. However, in our opinion it is possible to duplicate hand analyses quite well by computer techniques that have distance-weighting factors and that elongate wind patterns in the direction of flow. Then from such wind analyses, one can step forward in time to produce forecasts of the winds some hours later. If fairly simple prediction equations are used (neglecting terms of secondary importance), such forecasts can be available several hours before those from standard sources, and are of comparable accuracy in regard to winds.

The whole subject of numerical forecasting has undergone rapid growth and is still in a state of experimentation and change. In this part of the report we describe experiments that are intended to lead toward practical, computer wind forecasts. As stated in Sec. II, such forecasts for periods of 12 to 24 hours will deal with the larger features of the flow that can be discerned from standard measurements and that have lifetimes comparable to the forecast period. Thus, the forecasts are intended to answer questions as to how major features, such as jet streams, troughs, etc., are expected to affect Cape Kennedy during the forecast period. The availability of convenient, automatic methods of portraying the wind analyses and forecasts to the meteorologist is also an important topic and will be included in the discussion.

The method of objectively analyzing the wind field will be described briefly. First the wind reports from the radiosonde stations are averaged within layers 1 to 2 km deep. Since forecasts are made for each layer, restricting the number of layers keeps the mathematical problem at a convenient size. The number of layers chosen is not critical when testing techniques; however, in practice, the number is important since it determines the points available to represent the wind profile. It should also be mentioned that the number of layers that should be treated depends on the accuracy of the forecasting methods, with a larger number appropriate to more accurate methods.

After layer-averaged wind components, and also the vertical shear in each layer, are computed, the next step is to represent these data on a regular latitude-longitude mesh. For the density of observations in the area of interest, a 2-1/2-degree mesh is appropriate. Mancuso's analysis technique for representing winds on this grid has been described in a recent paper (Endlich and Mancuso, 1968); therefore, only the general outline will be given here. In each layer, the zonal (u) and meridional (v) wind components are analyzed separately. The value of a wind component at any grid point is an average of the observed values at surrounding stations, with higher weighting given to nearby stations and to those in an upstream or downstream direction from the grid point. The fit is made by a least-squares technique. After the components are analyzed, they may be used in that form or easily converted into wind direction and speed. This analysis process is done by a medium-sized computer in a few seconds.

During the present research, computer programs for automatically presenting data displays on a cathode ray tube were adapted for wind analyses. The CRT is photographed to provide permanent copies. The presentation shows the wind as a vector, plotted to a preselected length scale, in a direction downwind from the grid points. Examples of the observed wind data for six layers are shown in Fig. 26(a-f), and the objective analyses made therefrom are given in Fig. 27(a-f). (Probably a larger length scale should have been chosen to portray the weaker winds of layers one and two.) In our opinion, it is considerably more

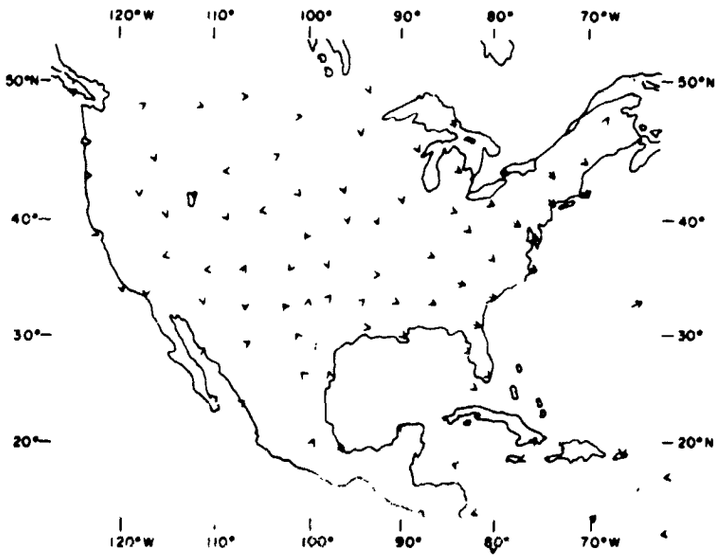

FIG. 26 OBSERVED WINDS IN LAYERS AS PLOTTED ON A COMPUTER-CONTROLLED CATHODE RAY TUBE FOR 0000 GMT, MARCH 28, 1966
(a) Surface to 850 mb

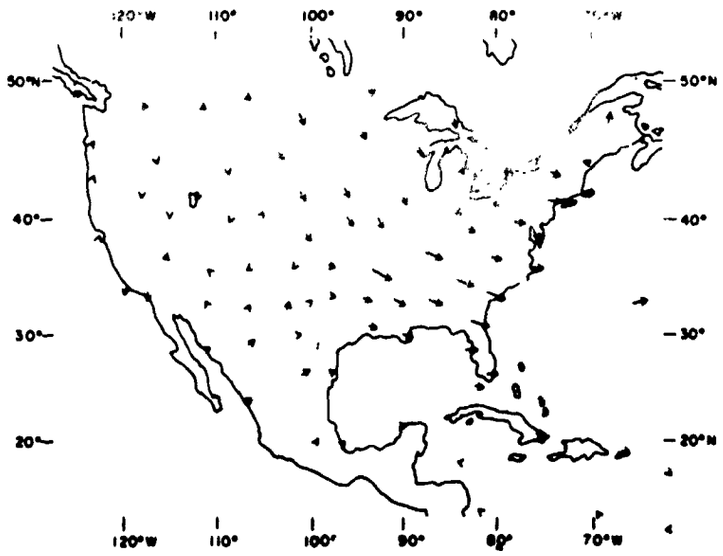

FIG. 26 – (b) 850 to 700 mb

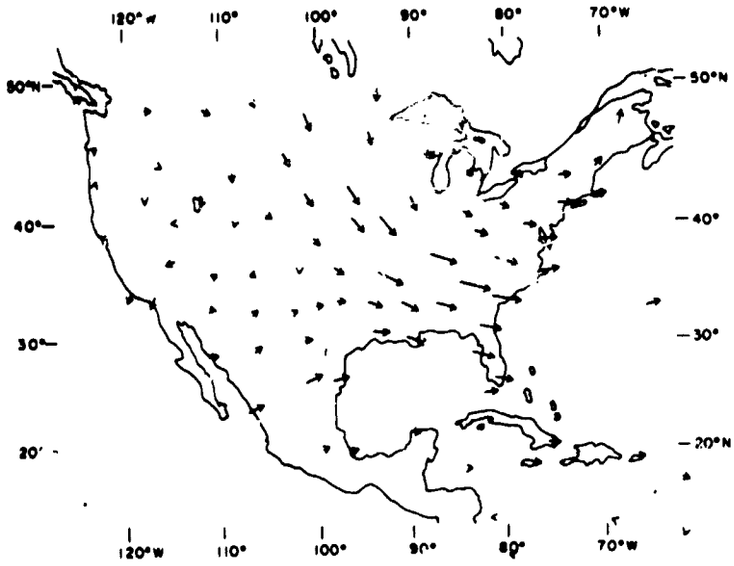

FIG. 26 – (c) 700 to 500 mb

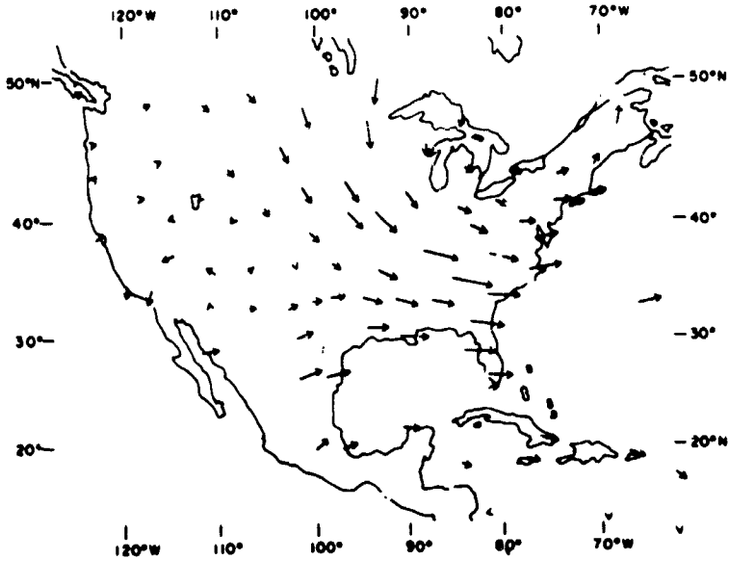

FIG. 26 – (d) 500 to 400 mb

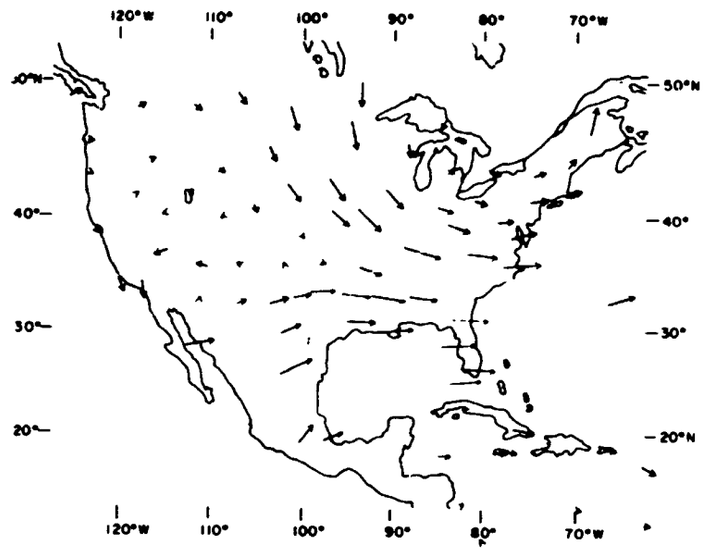

FIG. 26 – (e) 400 to 300 mb

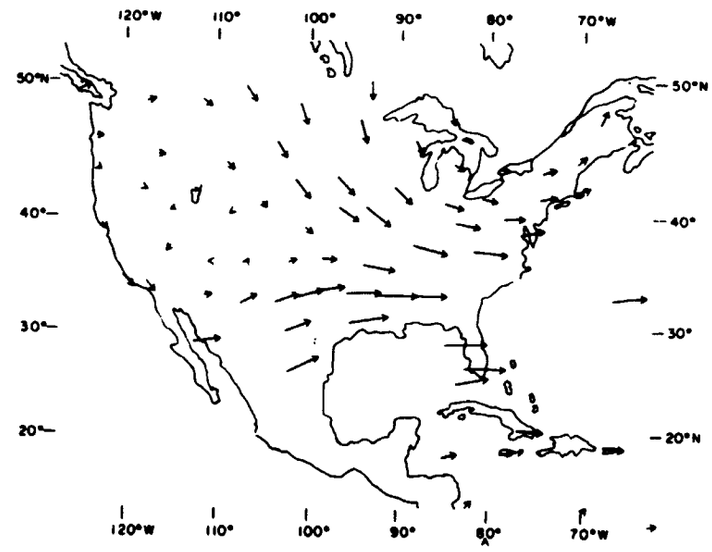

FIG. 26 – (f) 300 to 200 mb

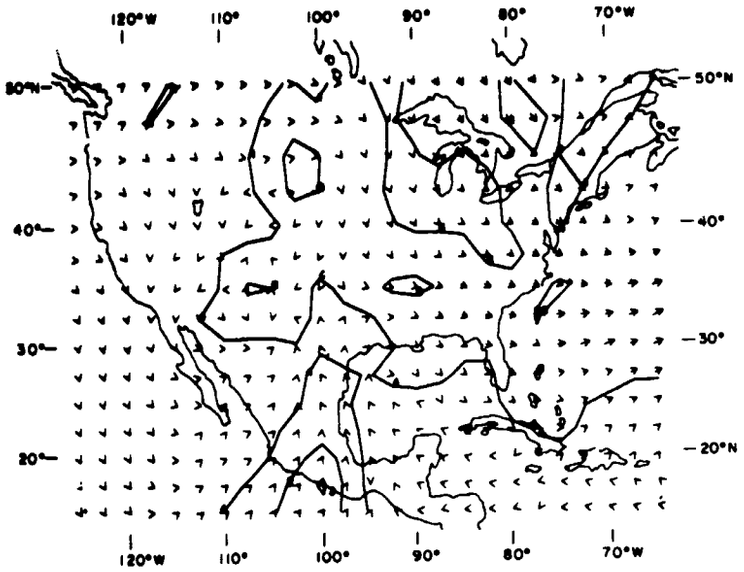

FIG. 27 OBJECTIVE ANALYSES OF THE WINDS OF FIG. 26, AND WIND SHEARS (isolines, units^{-3} sec^{-1}), USING THE CRT DISPLAY
(a) Surface to 850 mb

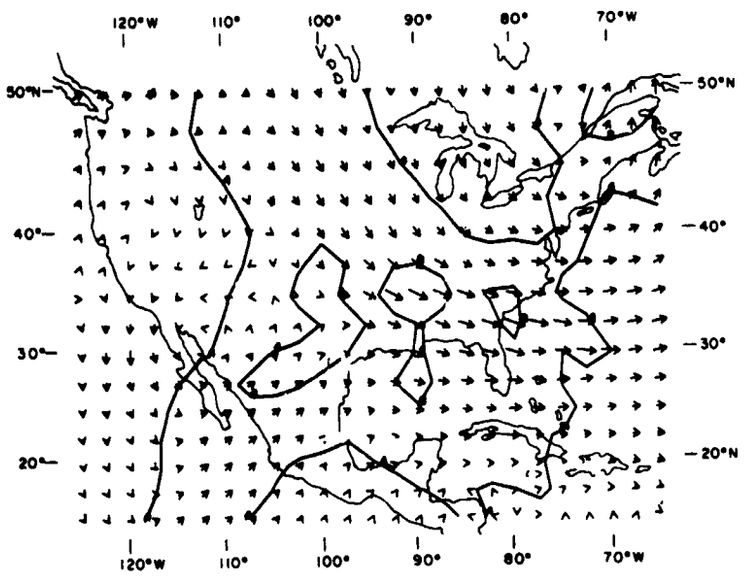

FIG. 27 – (b) 850 to 700 mb

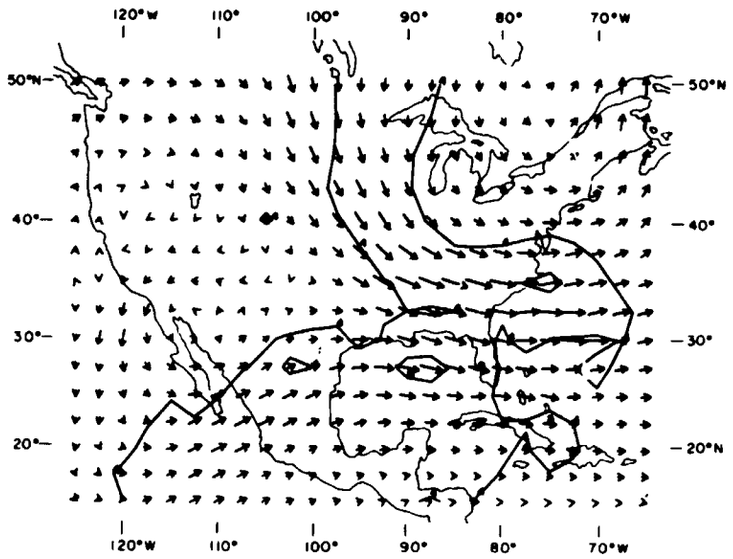

FIG. 27 – (c) 700 to 500 mb

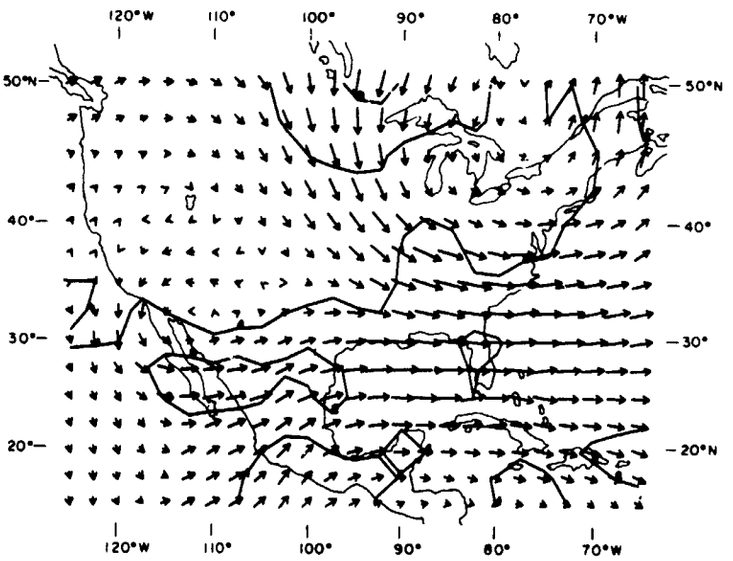

FIG. 27 – (d) 500 to 400 mb

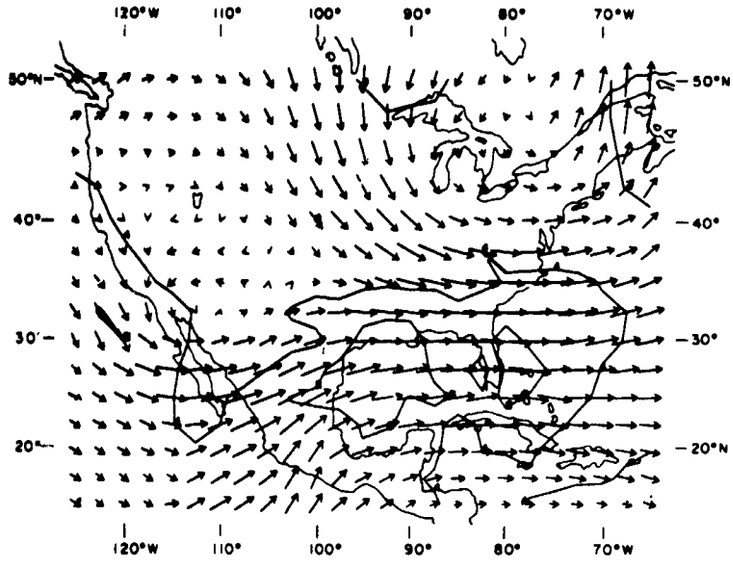

FIG. 27 – (e) 400 to 300 mb

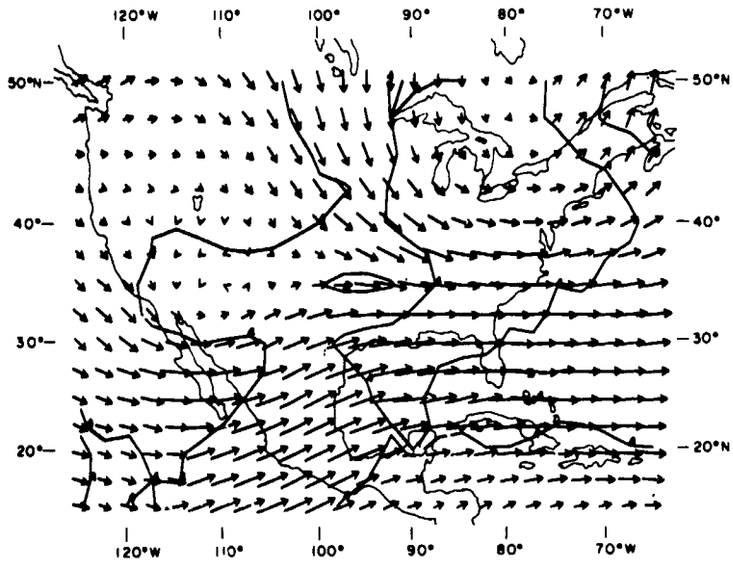

FIG. 27 – (f) 300 to 200

convenient to monitor winds using a presentation of this sort than from standard upper-air charts. Isolines can also be used on the display as shown in Fig. 27. Here they indicate vertical vector wind shear in the units 10^{-3} sec^{-1}.

As mentioned earlier, the forecasting methods used operate primarily on wind data or derived kinematical properties such as vorticity and divergence. Due to the lack of complete knowledge of how to handle three-dimensional air motions in numerical models and the lack of accurate and detailed input data, the process modelled is that of the horizontal movement of the wind patterns. Generally, this is the predominant process which is occurring. In our opinion further refinements based on inclusion of smaller effects are difficult to apply until accurate advection techniques have been worked out by numerical experimentation. Even for advection there are many possible finite-difference formulations, and there is not a great deal of guidance available from existing numerical analysis.

In a recent study of wind forecasting over the United States, we discussed some general aspects of the problem and described the accuracy of some simplified forecasting models (Endlich and Mancuso, 1967). These computer forecasts were based on advection of the patterns of zonal and meridional wind components. Attempts were also made to evaluate and include the effects of geostrophic departures. In general, the forecasts showed skill equivalent to that of human forecasters and that of more complex numerical procedures presently in use. The main advantages of our approach are that winds were treated directly and that the forecasts could be obtained in a matter of minutes after the input data were available in a computer-compatible format.

In this study we attempted to improve these earlier forecasting methods in several ways. (Actually, there are many possible avenues for improvement, and our selection is based partly on personal experience.) One method is akin to that used by human forecasters, who extrapolate past trends. Or stated differently, the forecaster normally assumes that changes that have recently occurred in association with the large-

scale features will continue. To duplicate this process objectively, rates of change of u and v were computed from the two most recent analyses; then the change patterns were advected with the flow for periods of a few hours. Next, a new field of u and v was computed from the original field plus the forecast change at each grid point. This process was repeated to obtain a forecast for the desired period. Verification showed that these forecasts did not give any improvement over previous ones in spite of various alterations in details of the technique.

The next forecasting method tried is based on conservation (i.e., advection) of absolute vorticity; this is one of the oldest numerical forecasting methods. In our treatment, winds are rebalanced to the vorticity at the end of each time step. The rebalancing is done by direct alterations to the wind field (Endlich, 1967). This procedure gave results somewhat more accurate than any achieved previously. The method can also be extended to include effects of divergence, if the additional assumption is made that divergence is conserved ($dD/dt = 0$). Then the vorticity production term (divergence times absolute vorticity) can be included in the numerical integration. However, the experiments showed that the inclusion of the vorticity production term in this manner was not generally beneficial, so it was dropped from the procedure. The reason for this may be the observational uncertainty in the values of divergence at the initial time, and the countervailing effects of the neglected vertical motion terms in areas having large divergence or convergence.

The last experiment carried out during the contractual period used a combination of the advection of u and v fields and the advection of vorticity and divergence, in the following way. During each time step, the fields of u, v, vorticity, and divergence are carried forward; then new fields of each are computed. By direct alterations, the wind field is then balanced to the vorticity and divergence fields, and the cycle is repeated. Of the methods tested, this one gave the best results in forecasting layer-averaged winds, as described below.

In making numerical forecasts there are other decisions involved than those concerning basic equations; for example, one must choose among various techniques of making finite-difference analogues to the equations. We chose to use upstream, one-sided space differences, and forward time differences, due to the simplicity of both. Optimum choices among finite-difference methods in terms of accuracy versus computer time are still under investigation (e.g., Crowley, 1968; Molenkamp, 1968; Young, 1968). The upstream differencing tends to gradually smooth the initial fields, but in practice this effect is not large over the periods of interest. To minimize the number of cycles needed to obtain a forecast, it is desirable to take relatively long time steps. This was done by using the alternating-direction implicit (ADI) method of iteration (see Todd, Chapter 11, 1962), which permitted use of a four-hour iteration cycle.

Test forecasts were made for the United States in the upper troposphere, i.e., at jet stream levels where wind variability is greatest. Test data were chosen in a strong-wind case (speeds up to 90 m sec^{-1}) from 10-15 March 1965 and in moderate speeds from 9-14 June 1965. In the 300-250 mb layer, the RMS errors in the 12-hour wind forecasts by the last method described above were 9.5 m sec^{-1} in the March data and 8.5 m sec^{-1} in the June period. These errors are approximately 20 percent smaller than those of other methods that we tested. Also, these errors may be compared with errors in forecasting winds at the maximum wind level reported by Viegas et al (1966). They gave an RMS error of 12.5 m sec^{-1} for weak winds and 16.7 m sec^{-1} for strong winds. For 24-hour forecasts, our RMS errors are 13.6 m sec^{-1} in March and 12.6 m sec^{-1} in June. Comparable values from Viegas et al are in the range from 14.1 m sec^{-1} for weak winds to 19.5 m sec^{-1} for strong winds. This test, although of limited size, indicates that the forecasting methods reported herein have promise and should be developed further.

An example of a 24-hour forecast from the March series is presented in Figs. 28-30. Fig. 28 shows the initial wind analysis, and Fig. 29 shows the wind changes forecast to occur in the following twenty-four

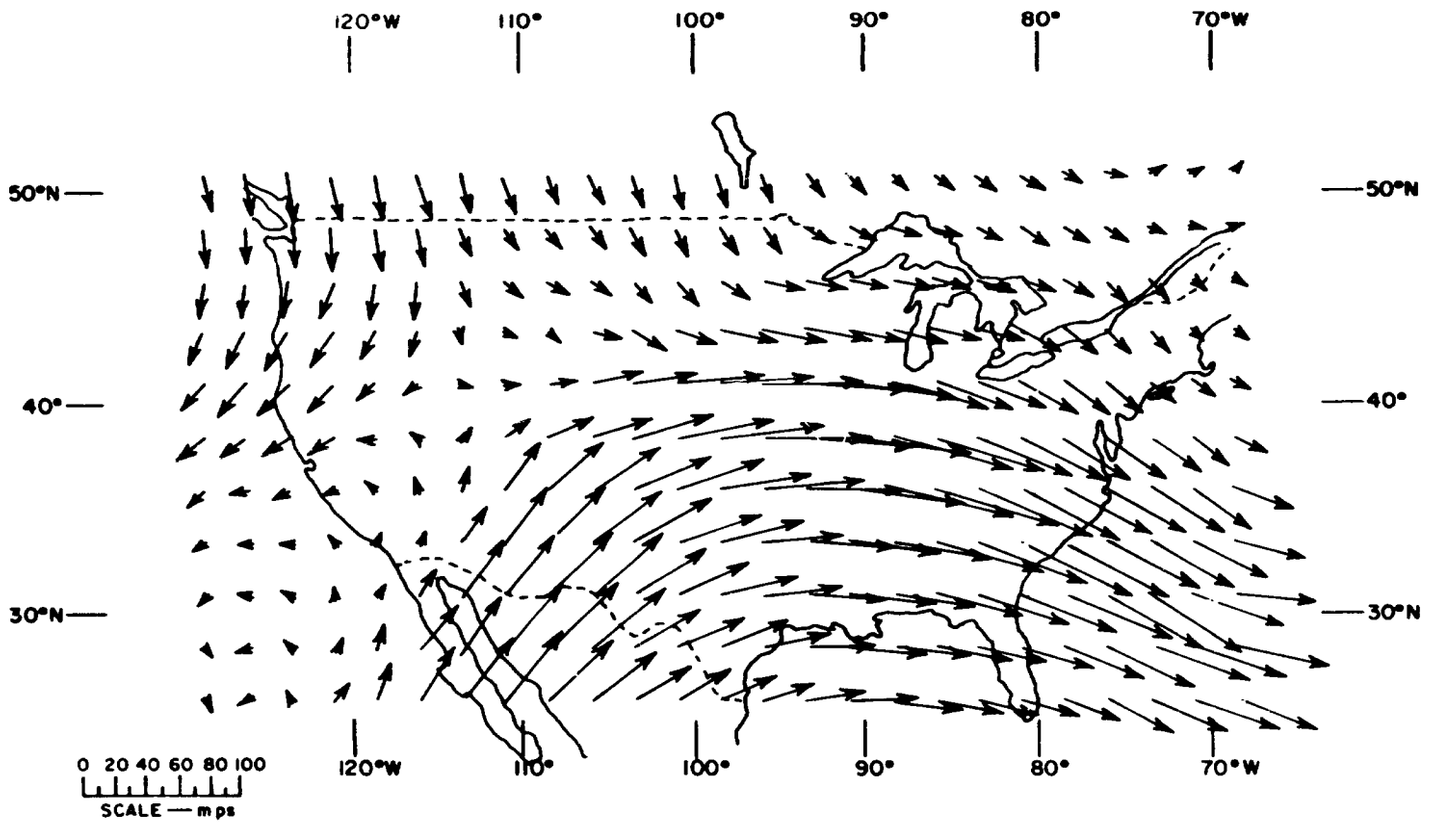

FIG. 28 OBJECTIVE WIND ANALYSIS FOR THE 300–250 mb LAYER AT 1200 GMT, MARCH 11, 1965

hours. If the change vector at a grid point is in the direction of the initial flow, then the wind there is forecast to increase, and conversely. The actual changes that occurred are given in Fig. 30, and are quite similar to those forecast. (Of course, for a perfect forecast Figs. 29 and 30 would agree exactly.) This forecast is one of the better ones of the series. To achieve this degree of accuracy is quite encouraging. In general, the largest errors in the forecasts occurred near the inflow boundaries due to the effects of the unknown conditions outside the region analyzed. In effect, the exterior conditions can propagate unexpected changes into the region of interest during the forecast period.

We summarize the implications of these forecasting experiments as follows. In order to achieve effective wind forecasts that are necessary in highly complex and expensive spacecraft launching operations, it would be desirable for NASA to implement a numerical wind-forecasting method tailored to these particular problems, to carry out studies to improve the technique, and to develop display systems for conveniently portraying the results. An immediate difficulty to be resolved would be in transforming standard rawinsonde data received on teletype to a computer format in real time, or of obtaining transformed data from the appropriate agencies.

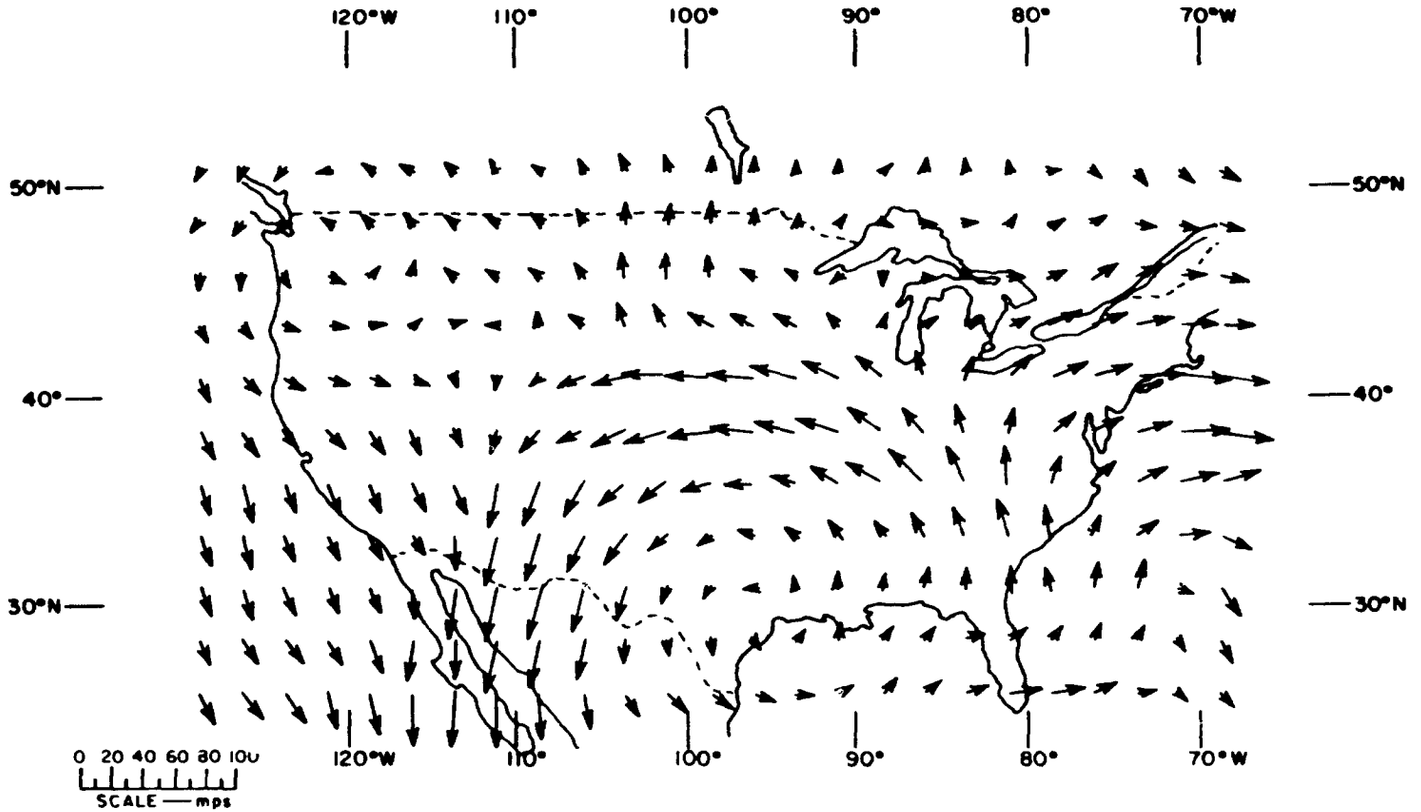

FIG. 29 FORECAST 24-HOUR CHANGES IN WIND VECTORS MADE FROM FIG. 28

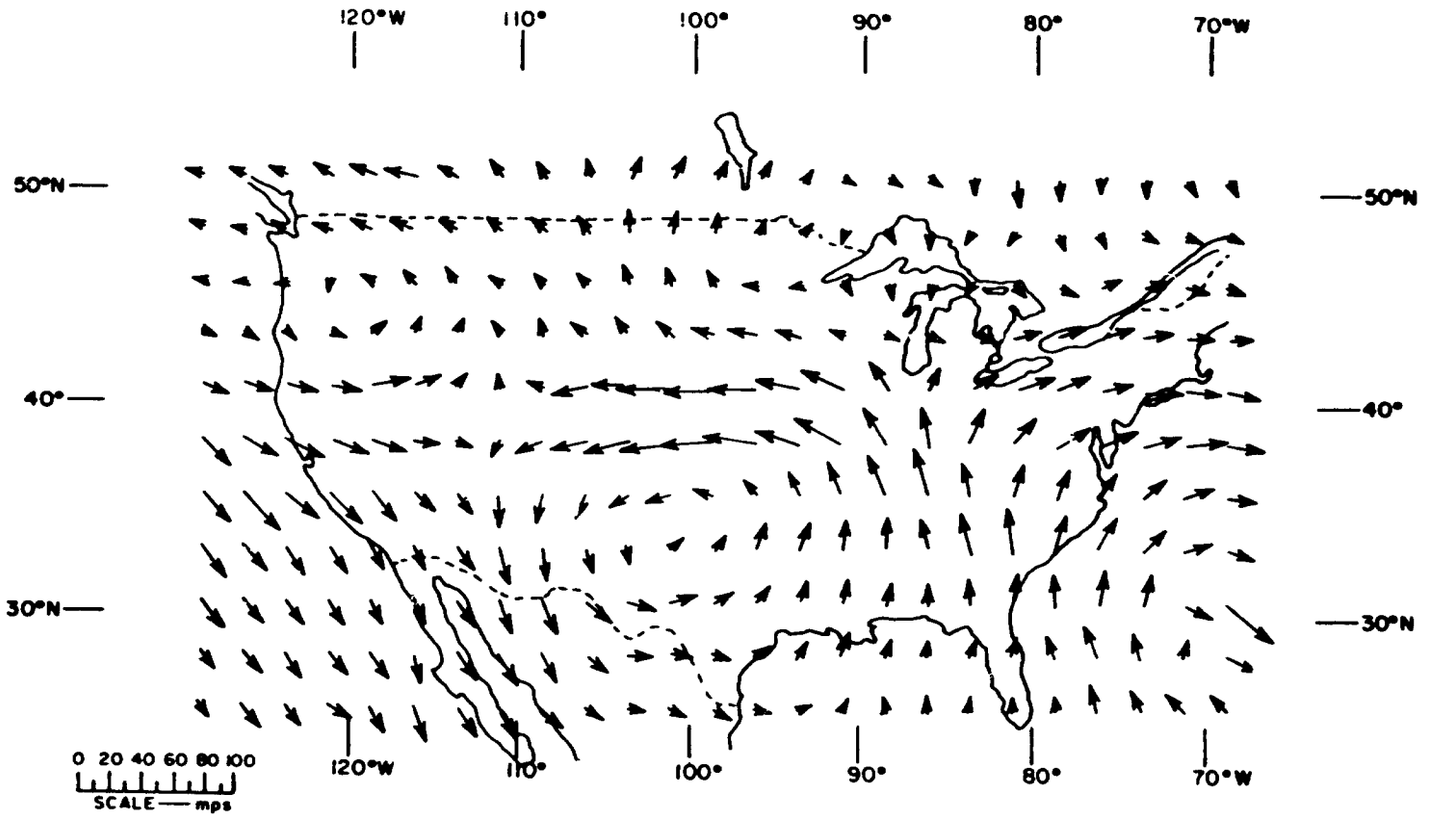

FIG. 30 OBSERVED 24-HOUR CHANGES IN WIND VECTORS. Compare with Fig. 29

PRECEDING PAGE BLANK NOT FILMED.

ACKNOWLEDGMENTS

We are indebted to Mr. John Kaufman, Contract Monitor at MSFC, for informing us concerning operational wind forecasting problems at the NASA test ranges, for helpful advice, and for furnishing data used during the investigation.

PRECEDING PAGE BLANK NOT FILMED.

REFERENCES

Bingham, C., M. D. Godfrey, and J. W. Tukey, 1967: Modern Techniques of Power Spectral Estimation. IEEE Trans. on Audio and Electroacoustics, AU-15, No. 2, pp. 56-66. (This is a special issue on the fast Fourier transform and its application to digital filtering and spectral analysis.)

Blackman, R. B. and J. W. Tukey, 1958: The Measurement of Power Spectra. New York, Dover Publications, Inc., pp. 326.

Cooley, J. W. and J. W. Tukey, 1965: An Algorithm for the Machine Calculation of Complex Fourier Series. Mathematics of Computation, Vol. 19, No. 90, pp. 297-301.

Crowley, W. P., 1968: Numerical Advection Experiments. Mon. Wea. Review, Vol. 96, pp. 1-11.

DeMandel, R. E. and J. R. Scoggins, 1967: Mesoscale Wave Motions as Revealed by Improved Wind Profile Measurements. J. Appl. Meteor., Vol. 6, pp. 617-620.

Endlich, R. M. And J. W. Davies, 1967: The Feasibility of Measuring Turbulence in the Free Atmosphere from Rising Balloons Tracked by FPS-16 Radar. J. Appl. Meteor., Vol. 6, pp. 43-47.

Endlich, R. M. and R. L. Mancuso, 1967: Forecasting Clear-Air Turbulence by Computer Techniques. SRDS Report No. RD-67-65, Final Report, pp. 86, Contract FA66WA-1442, Stanford Research Institute, Menlo Park, California,

Kao, S. K. and H. D. Woods, 1964: Energy Spectra of Mesoscale Turbulence along and across the Jet Stream. J. Atmos. Science, Vol. 21, pp. 513-519.

Larson, A. G. and R. C. Singleton, 1967: Real-Time Spectral Analysis on a Small General-Purpose Computer. AFIPS Conference Proceedings (1967 FJCC), Vol. 31, pp. 665-674 (Thompson Books, Washington, D.C.).

Lumley, J. L. and H. A. Panofsky, 1964: The Structure of Atmospheric Turbulence. New York, John Wiley and Sons, Inc., pp. 239

Molenkamp, C. R., 1968: Accuracy of Finite-Difference Methods Applied to the Advection Equation. J. Appl. Meteor., Vol. 7, pp. 160-167.

Pinus, N. Z., 1963: Statistical Characteristics of the Horizontal Components of the Wind Velocity at Heights of 6-12 km. Bull. Acad. of Sciences, USSR, Geophys. Ser., pp. 105-107.

Reiter, E. R. and P. F. Lester, 1967: The Dependence of the Richardson Number on Scale Length. Atmos. Science Paper No. 111, pp. 43, Contract NASA-N67-34426, Dept. of Atmos. Science, Colorado State University, Fort Collins, Colorado.

Scoggins, J. R., 1964: Aerodynamics of Spherical Balloon Wind Sensors. J. Geophys. Res., Vol. 69, pp. 591-598.

Scoggins, J. R. and M. Susko, 1965: FPS-16 Jimsphere Wind Data Measured at the Eastern Test Range. NASA TM X -53290, pp. 457, G. C. Marshall Space Flight Center, Huntsville, Alabama.

Singleton, R. C. and T. C. Poulter, 1967: Spectral Analysis of the Call of the Male Killer Whale. IEEE Trans. on Audio and Electroacoustics, AU-15, No. 2, pp. 104-113.

Stockham, T. G., 1966: High-Speed Convolution and Correlation. AFIPS Conference Proceedings (1966 SJCC), Vol. 28, pp. 229-233 (Spartan Books, Washington, D.C.)

Tatarski, V. I., 1961: Wave Propagation in a Turbulent Medium. New York, McGraw-Hill Book Co., pp. 285

Todd, J., editor, 1962: Survey of Numerical Analysis. pp. 589, New York, McGraw-Hill Book Co.

Vaughan, W. W., 1962: Wind Profiles at Staging Altitudes. In Air Force Surveys in Geophysics, No. 140, pp. 151-164, Proceedings of the National Symposium on Winds for Aerospace Vehicle Design, AFCRL, Bedford, Massachusetts.

Veigas, K. W., D. B. Spiegler, J. T. Ball, and J. P. Gerrity, Jr., 1966: The Predictability of Winds and Virtual Temperature Profiles for Flight and Static Test Operations. AMS/AIAA Paper, No. 66-378, pp. 28, AMS/AIAA Conference on Aerospace Meteorology, Los Angeles, March 1966.

Young, J. A., 1968: Comparative Properties of some Time Differencing Schemes for Linear and Nonlinear Oscillations. Mon. Wea. Review, Vol. 96, pp. 357-364.

UNCLASSIFIED
Security Classification

DOCUMENT CONTROL DATA - R & D

(Security classification of title, body of abstract and indexing annotation must be entered when the overall report is classified)

1 ORIGINATING ACTIVITY (Corporate author) Stanford Research Institute 333 Ravenswood Menlo Park, California 94025	2a. REPORT SECURITY CLASSIFICATION UNCLASSIFIED 2b GROUP N/A

3 REPORT TITLE

STUDIES OF VERTICAL WIND PROFILES AT CAPE KENNEDY, FLORIDA

4 DESCRIPTIVE NOTES (Type of report and inclusive dates)

Final Report

5 AUTHOR(S) (First name, middle initial, last name)

R. M. Endlich R. C. Singleton K. A. Drexhage R. L. Mancuso

6 REPORT DATE September 1968	7a. TOTAL NO OF PAGES 98	7b NO OF REFS 22
8a CONTRACT OR GRANT NO Contract NAS 8-21148 b PROJECT NO c. d.	9a. ORIGINATOR'S REPORT NUMBER(S) Final Report SRI Project 6645 9b OTHER REPORT NO(S) (Any other numbers that may be assigned this report)	

10 DISTRIBUTION STATEMENT

11 SUPPLEMENTARY NOTES	12 SPONSORING MILITARY ACTIVITY Aero-Astrodynamics Laboratory George C. Marshall Space Flight Center National Aeronautics and Space Admin. Huntsville, Alabama

13 ABSTRACT

This study is concerned with methods of forecasting vertical wind profile for NASA operations in launching missiles and spacecraft. The first subject considered is the structure, persistence, and predictability of details of vertical wind profiles. This portion of the investigation is based on sequences of wind profiles measured at Cape Kennedy, Florida, using the FPS-16 radar/Jimsphere technique. The details of the flow are shown by wind measurements at 25 m intervals between the surface and the lower stratosphere. The main analytical tool used is spectrum analysis. Spectra were computed using the "fast Fourier transform" rather than the more common but less efficient "lagged product" method. The spectra have the general characteristic that power is proportional to frequency to the -3 power. There are no clear minima in them that would indicate natural separations between predominant scales of motion as suggested by terminology such as large scale, mesoscale, and microscale. If these terms are to be used in reference to speed variations along a vertical axis, they must be defined on some other basis than the existence of clearly demarked spectral regions.

Spectra were also computed for deviations from mean speed profiles, and for speed changes between successive wind profiles. These deviations and changes show predominantly the smaller, transitory features of the flow. To a large extent, the behavior of these features appears to be random. At frequencies above approximately 0.3 cycles km^{-1}, their spectra have a slope near -2.5. If short-range forecasts are made from previous profiles, the errors of the forecasts can be expected to have distributions similar to these spectra. The spectra of vertical profiles are compared with previous ones computed from winds measured by aircraft in horizontal flights across jet streams. Horizontal and vertical wavelengths having equal spectral density are shown.

In the second portion of the study, numerical methods of forecasting the general wind profile for periods twelve to twenty-four hours in advance are described. These methods are based on objective analyses of standard wind observations. The forecast is made by advection of fields of wind components, vorticity, and divergence. Winds are matched to the forecast vorticity by a direct method. Test results indicate that the technique can be applied rapidly and is at least as accurate as other methods presently in use.

DD FORM 1 NOV 65 1473 (PAGE 1)

S/N 0101-807-6801

UNCLASSIFIED
Security Classification

UNCLASSIFIED
Security Classification

14 KEY WORDS	LINK A ROLE	LINK A WT	LINK B ROLE	LINK B WT	LINK C ROLE	LINK C WT
Vertical Wind Profiles						
FPS-16 radar/Jimsphere Data						
Wind Shear						
Spectrum Analysis						
Numerical Forecasting						

DD FORM 1 NOV 65 1473 (BACK)
(PAGE 2)

UNCLASSIFIED
Security Classification